UCLouvain

UNIVERSITÉ DE NAMUR

FACULTE DES SCIENCES

Faculté des sciences

On the bioluminescence of Echinodermata in the south-eastern Australian deep-sea

New insights into sacculi and light emission in Comatulida (Crinoidea)

Pablo Martinez Soares

Mémoire présenté en vue de l'obtention du diplôme de Master en Biologie des Organismes et Ecologie

Promoteurs : Dr. Jérôme Mallefet
Dr. Laurent Duchatelet

Lecteurs: Dr. Igor Eeckhaut (UMons)
Dr. Frédéric Silvestre (UNamur)
Dr. Nicolas Pinte (UCLouvain)

Année académique 2019 - 2020

Acknowledgements

During nearly a year of work a lot of difficulties arise. Yet, a lot of solutions are found too and thus, I would like to thank the people who helped find these solutions in a direct or indirect way.

I would like to most sincerely thank Pr. Jérôme Mallefet, my supervisor, for accepting me in his laboratory, trusting me with precious deep-sea tissues and guiding me all this way. Knowing what to look for under the microscope is no easy task at the beginning but luckily, I had one of the best teachers.

I would also especially like to thank Laurent Duchatelet, my second supervisor, for teaching me different techniques but most of all for guiding my work, giving council and reading my drafts.

I thank my lectors, Dr. Igor Eeckhaut, head of the laboratory for Biology of Marine Organisms and Biomimetics from UMons, Dr. Frédéric Silvestre, head of the laboratory for Evolutionary and Adaptive Physiology from UNamur, and Dr. Nicolas Pinte, from the Marine Biology laboratory from UCLouvain, for accepting to be members of my jury and taking their time to read my work.

I thank the laboratory for Biology of Marine Organisms and Biomimetics from UMons and their members for their welcome, Dr. Patrick Flammang and specially Dr. Jérôme Delroisse for recognising sacculi for what they were, teaching me how to do the semi-thin sections and generally all his help and time.

I also want to thank all the actual and former members of the Marine Biology laboratory for their humour, their help whenever needed and generally for this amazing time I got to share with you.
Special thanks to Constance Coubris for helping me with my statistics and reading over my work. And a very special thanks to my “comémorants”, Yannick van den Bossche and particularly Ilona Strammer.

A final thanks to my family and friends, for their unconditional love and support and helping me through these sometimes difficult moments.

Abstract

Bioluminescence is an organism's capacity of emitting cold, visible light thanks to a chemical reaction. It is a very widespread phenomenon specially in marine environments. Utilities vary from luring prey to intraspecific communication. In the phylum Echinodermata bioluminescence seems to be used mainly as a defence mechanism. The capacity of echinoderms to emit light has been known for over a century, yet, research on the topic is limited for echinoderms other than brittle stars. In this work, we used data collected by Pr. Jérôme Mallefet on board of the RV *Investigator* during the *Sampling the Abyss* cruise in 2017. Luminometry measurements were done on board. We note 26 new bioluminescent species with new records in all 4 luminescent classes and even the first record for the order Molpadida (Holothuroidea). We calculated the proportions of samples from bioluminescent genera for two latitudinal (tropical and temperate) and three depth categories (upper bathyal, lower bathyal and abyssal) as well as between the four bioluminescent echinoderm classes. We used this information to compare to current knowledge of general bioluminescence distribution and found that our data differs in that the proportion of bioluminescent echinoderm genera significantly decreases in temperate waters and significantly increases in abyssal depths. Furthermore, we find that Ophiuroidea and Holothuroidea have a smaller proportion of bioluminescent than non-luminescent genera. Also, the ratio of green to blue emitters seems to decrease with depth. Using environmental data from O'Hara et al., 2019, we fitted proportion, species richness and Shannon diversity of bioluminescent genera to carbon flux, oxygen and temperature. Here we find that proportion is explained by an increased oxygen concentration, Shannon diversity by an increase in carbon and species richness increases with carbon but decreases with oxygen. Using a SIMPROF we determine that the Central-eastern bioregion is probably a transition zone for echinoderm communities from tropical and temperate waters. We present some of the luminometry measurements with the highest emission intensities for all four classes as well as data showing that the bioluminescence in *Ophioplinthaca rudis* is probably under cholinergic control and that the bioluminescence of the thalassometrid 69_148 tends to increase along with the added adrenaline concentration. Arm tissue from two crinoid species, *Monachocrinus* cf. *aotearoa* and the thalassometrid 80_120, and caudal skin tissue from holothuroid, *Psychropotes longicauda*, were sectioned and observed under blue light stimulation Observations suggest that the sacculi might be the luminescent organ in some crinoids at least. In the holothuroid we observed epifluorescence of a similar type of granular cells than Herring, 1974. However, in both cases, we are unable to make any conclusion with certainty. Eventually, luciferin and luciferase assays were performed on the thalassometrid 69_148. The results show that it is a coelenterazine-luciferase system. Coelenterazine content and luciferin activity resemble that of *Amphiura filiformis*.

Key-words : deep-sea; Echinodermata; Crinoidea; saccule; bioluminescence; coelenterazine

Abstract (FR)

La bioluminescence est la capacité d'un organisme d'émettre de la lumière froide et visible à partir d'une réaction chimique. Il s'agit d'un phénomène fortement répandu spécialement dans l'environnement marin. Son utilité varie de leurre pour attirer des proies à la communication intraspécifique. Dans le phylum Echinodermata la bioluminescence semble être surtout utilisé à des buts de défense. La capacité des échinodermes d'émettre de la lumière est connu depuis un bon siècle, or, la recherche à ce sujet reste limitée pour les échinodermes autres que les ophiures. Dans ce travail nous utilisons les données collectées par le Pr. Jérôme Mallefet à bord du RV *Investigator* durant l'expédition *Sampling the Abyss* en 2017. Des mesures avec un luminomètre nous permettent de rapporter 26 nouvelles espèces bioluminescentes réparties dans les quatre classes d'échinodermes bioluminescents et le premier rapport d'émission de lumière dans l'ordre Molpadia (Holothuroidea). Nous avons calculé la proportion d'échantillons appartenant à des genres bioluminescents pour deux catégories latitudinales (tropical et tempéré) et trois catégories de profondeur (bathyal supérieur, bathyal inférieur et abyssal) ainsi qu'entre les quatre classes d'échinodermes luminescents. Nous avons utilisé cette information pour la comparer aux connaissances actuelles sur la distribution de la bioluminescence et trouvons que nos données diffèrent dans le fait que la proportion d'échantillons de genres bioluminescents diminue significativement dans les eaux tempérées et augmente significativement dans les eaux abyssales. De plus, nous trouvons que les ophiures et les holothuries possèdent une moindre proportion d'échantillon de genres bioluminescents que non-luminescents. En outre, le ratio entre émetteurs verts et bleu semble diminuer avec la profondeur. En utilisant des données environnementales d'O'Hara et al., 2019, nous avons ajusté la proportion, la diversité Shannon et la richesse spécifique des genres bioluminescents au flux de carbone, la concentration en oxygène et la température. Nous trouvons que la proportion augmente avec l'oxygène, la diversité augmente avec le flux de carbone et la richesse spécifique augmente avec le carbone et diminue avec l'oxygène. A l'aide d'une SIMPROF nous estimons que la bioregion centrale-est est probablement une zone de transition entre les eaux tropicales et tempérées pour les communautés d'échinodermes. Nous présentons quelques-unes des mesures de luminométrie les plus importantes pour les quatres classes de même que des données qui indiquent que la bioluminescence chez *Ophioplinthaca rudis* est probablement sous control cholinergique et que la bioluminescence chez le thalassometridé 69_148 tend à augmenter avec la concentration d'adrénaline ajoutée. Des coupes ont été faites dans des tissus de bras de deux crinoïdes, *Monachocrinus* cf. *aotearoa* et le thalassometridé 80_120, et dans des tissues de la peau caudale chez une holothurie, *Psychropotes longicauda*. Des observations sous épifluorescence suggèrent que chez certains crinoïdes c'est les saccules qui pourraient servir d'organe bioluminescent. Chez l'holothurie nous observons des cellules granuleuses et ressemblantes à celles observées par Herring, 1974, qui fluoresces. Or, dans les deux cas, nous n'avons pas de certitude quant à la vraie nature des cellules émettrices de lumière. Finalement, nous avons effectué des dosages de luciférine et luciférase chez le thalassometridé 69_148. Les résultats montrent qu'il s'agit d'un système coelentérazine - luciférase. Le contenue de coelentérazine et l'activité luciférasique ressemblent beaucoup à celle d'*Amphiura filiformis*.

Mots-clés : eaux-profondes ; échinoderme ; crinoïde ; saccule ; bioluminescence ; coelentérazine

Table of content

1 Introduction

1.1 Sampling the Abyss (IN2017_V03)

This work is done in the framework of the data analysis from the *Sampling the Abyss* cruise. *Sampling the Abyss* was a deep-sea sampling cruise that started in Hobart, Tasmania on May 4th, 2017 and ended in Brisbane on June 16th, 2017. Thirty-five scientists under chief scientist Tim O'Hara (Museum Victoria) and voyage manager Brett Muir (CSIRO[1]/MNF[2]) boarded the research vessel RV *Investigator* on May 15th (O'Hara, 2017).

The scientific objectives were multiple from describing the latitudinal and bathymetric distribution of biodiversity from the lower bathyal (2500 m) to the abyssal (4000 m), surveying and photographing for the first time these ecosystems in 7 Commonwealth marine reserves (CMR) (Freycinet CMR, Flinders CMR, East Gippsland CMR, Jervis CMR, Hunter CMR, Central Eastern CMR, Coral Sea CMR), compare the local ecosystems to similar environments in other places on earth, sequence DNA to find out how gene-flow occurs, help determine the evolutionary history of the local fauna and their boundaries, study 'land-ocean coupling', photograph the captured animals alive in aquaria, try to understand their life history, test for bioluminescence and do science communication for informing and inspiring the general public (O'Hara, 2017).

Eventually, 136 operations on 13 different sampling areas (*Fig.1*) between 42° and 24° South were done, allowing to collect 42 747 specimens which are now preserved for future DNA extraction in four Australian museums (Museum Victoria, Australian Museum, Queensland Museum, Tasmanian Museum and Art Gallery) and the CSIRO National Fish Collection (O'Hara, 2017).

The cruise was financially supported by the Marine Biodiversity Hub, funded through the NERP [3] and administered through the Australian Government's Department of the Environment. Granted ship time and allocations were given by the MNF[2], which is owned and operated by CSIRO[1] on behalf of the Australian Government (O'Hara, 2017).

[1] Commonwealth Scientific and Industrial Research Organisation
[2] Marine National Facility
[3] National Environmental Research Program

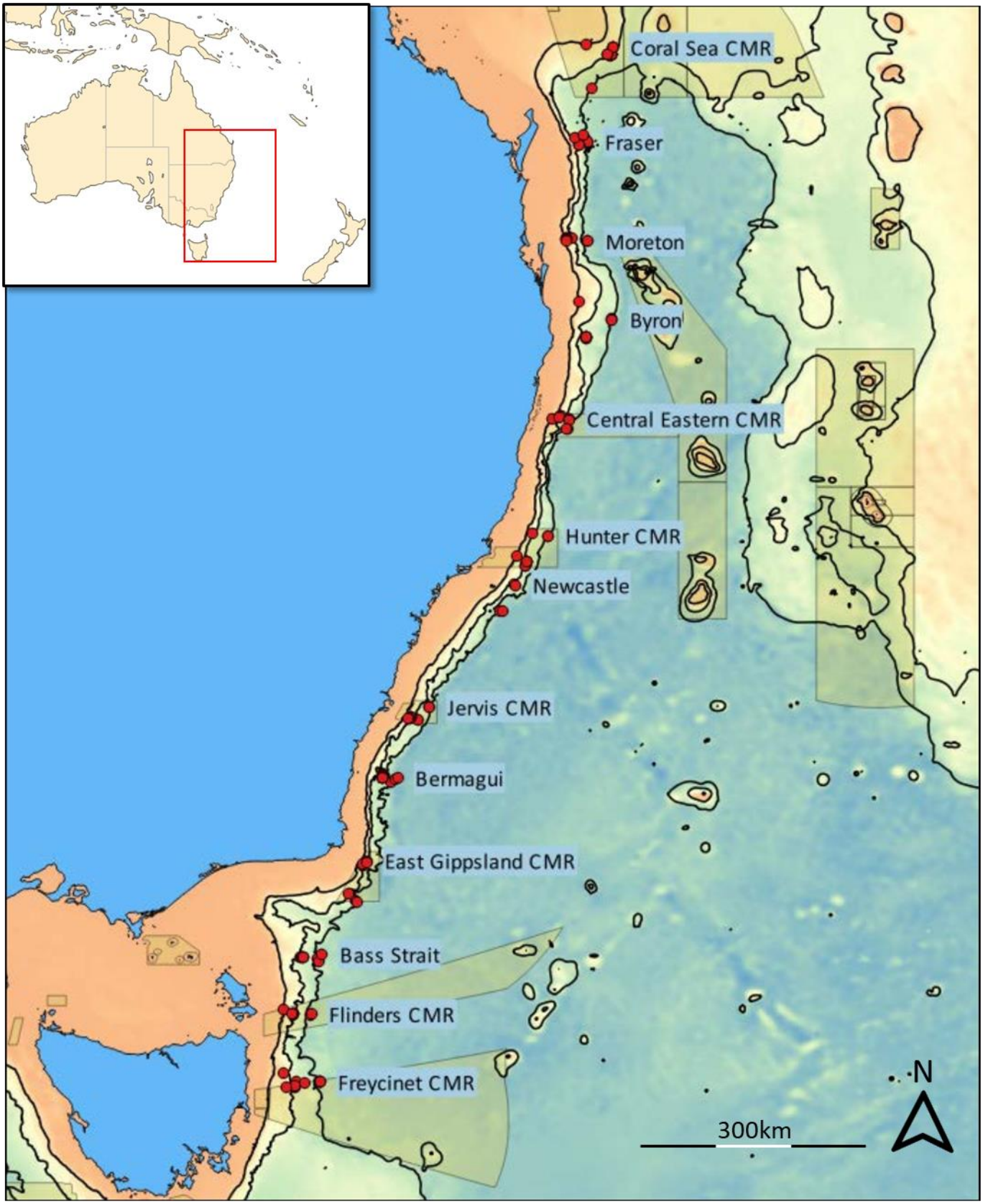

Figure 1. Map of the south-eastern Australian coast. Sampling sites from the *Sampling the Abyss* deep-sea cruise are indicated as red dots and the names are in blue squares. Bathymetry indicates 1000 (orange), 2000 (yellow), 3000 (light green) and 4000 (blue-yellow mix) meters depth. Commonwealth Marine reserves (CMRs) are indicated as translucent yellow polygons. Upper right corner shows a map of Australia and the surrounding Islands. The red rectangle represents the zone mapped in the main map. Adapted from RV *Investigator* voyage summary – Inv2017 V03 – MNF & CSIRO (O'Hara, 2017)

1.2 Echinodermata

1.2.1 Generalities

The phylum Echinodermata encloses five different classes: *(i)* Asteroidea, commonly known as sea stars and sea daisies, *(ii)* Crinoidea, that are the sea lilies and feather stars, *(iii)* Echinoidea, that comprises the sea urchins, heart urchins and sand dollars, *(iv)* Holothuroidea, which are often referred to as sea cucumbers, and *(v)* Ophiuroidea, also commonly called brittle stars, basket stars and snake stars (*Fig.2*) (Byrne and O'Hara, 2017).

In Crinoidea, the most basal class of the five, 664 species are recognized in 183 genera and 32 families (Byrne and O'Hara, 2017). The other four classes can be regrouped in two different clades based on recent phylogenomic approach: Asterozoa and Echinozoa (O'Hara et al., 2014). Asterozoa regroups Asteroidea and Ophiuroidea while Echinozoa is formed by Echinoidea and Holoturoidea. Ophiuroidea is the largest class of echinoderms with about 2091 species ("The World Ophiuroidea Database"). The second largest class, the Asteroidea, has 1897 species described so far ("The World Asteroidea Database"). Echinoidea and Holothuroidea, the two smaller classes, have worldwide around 1000 and 1722 species described respectively (Byrne and O'Hara, 2017).

They are deuterostomes that develop from a ciliated larva with bilateral symmetry to a pentamerous adult. Distinctive echinoderm characteristics are the water vascular system, the mutable connective tissue and a dermal skeleton made from calcareous ossicles. The water vascular system is a major novelty in Metazoans and is a network of tubes and canals filled with liquid (similar in composition to seawater) allowing the movement, respiration and excretion of the animal (Byrne and O'Hara, 2017). The mutable connective tissue (MCT) is, like its name says, connective tissue, but it has the capacity to change its mechanical properties. This means it can soften or harden (pliant-elastic and stiff-inelastic states) and even completely disintegrate allowing autotomy (*i.e.* auto-induced amputation of a body part. Candia Carnevali and Bonasoro, 2001), all through nerve mediation. The last attribute, the calcareous skeleton, lays underneath the epidermis and has a three-dimensional porous structure filled with cells and connective tissue. The interconnected spaces are called stereom. This skeleton defines part of the animal's rigidity, from the fused rigid plates of echinoids to the small ossicles (called spicules) in the soft integument of holothuroids. (Byrne and O'Hara, 2017).

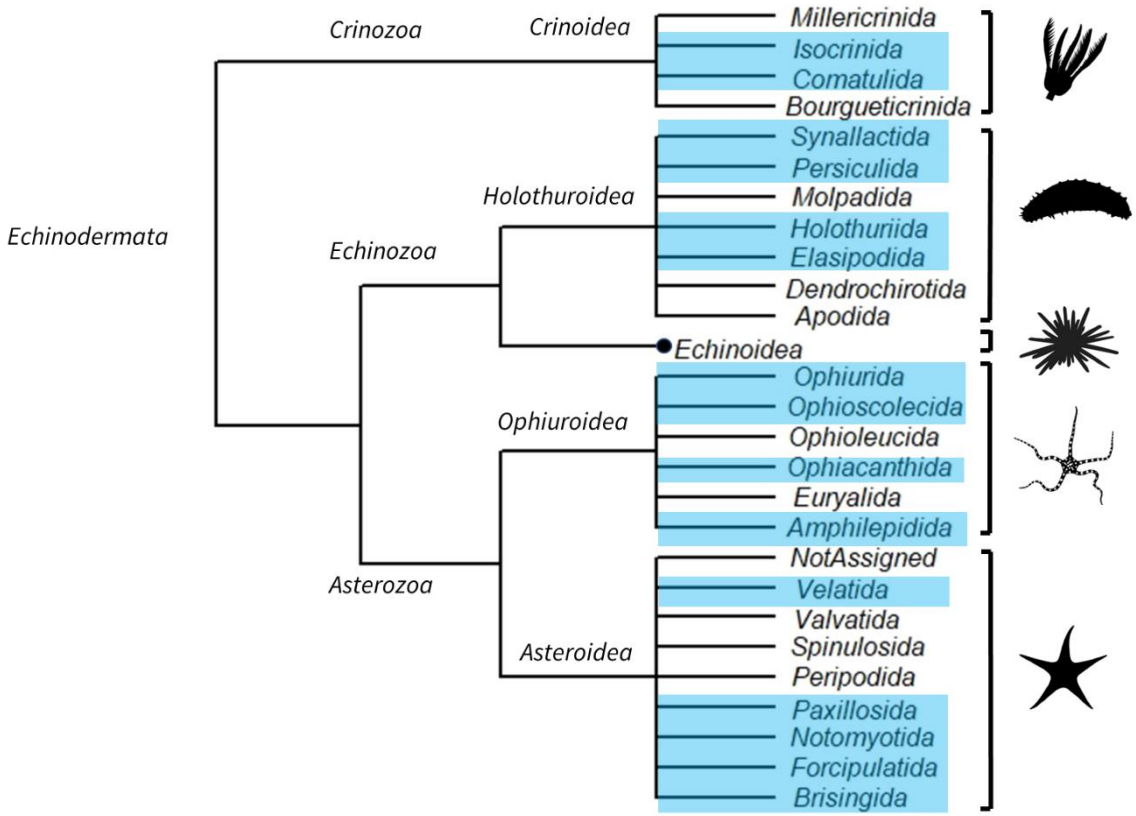

Figure 2. Cladogram representing the phylum Echinodermata, its 3 subphyla and 5 classes. Orders are indicated for all classes except Echinoidea because until today there are no descriptions of bioluminescent sea-urchins. Orders containing bioluminescent species, as of 2017, are indicated in blue. The information for the cladogram structure is taken from the *Catalogue of Life* database. Pictures are taken from *PhyloPic* [credit to Noah Schlottman, photo from Casey Dunn, https://creativecommons.org/licenses/by-sa/3.0/]

1.2.2 Crinoidea

The general structure of crinoids is made out of three major parts (*Fig.3*): (i) a rather small central body build from the calyx, containing the central visceral mass with the digestive system, covered by the tegmen with a mouth opening, hydropores and an anal tube, (ii) a stalk to attach to the substrate and that in most Comatulida is only present during larval stages before falling off and being replaced by stalk-less cirri, (iii) the rays that branch out of the calyx and may continue dichotomising (Heinzeller and Welsch, 1994; Byrne and O'Hara, 2017). Rays have two major purposes namely filtering water for feeding and allowing the animal to move around in its environment through walking or swimming. Free-living Comatulida are of the most mobile echinoderms. Their movement is completely independent from their tube feet (Byrne and O'Hara, 2017; Heinzeller and Welsch, 1994).

Their need for flexibility for moving and, at the same time, rigidity for countering the current while filter-feeding has selected a system of muscles, ligaments and skeletal parts that allows both. Rays are 5 in number and in most genera, they branch to form several arms. These arms form small, alternating side branches, the so-called pinnules who give crinoids their feather-like appearance (Heinzeller and Welsch, 1994; Byrne and O'Hara, 2017). The ciliated

ambulacral grooves radiate from the mouth up to the arms and their pinnules were triplets of ambulacral tube-feet capture food particles out of the water and help transport them through the ambulacral groove back to the mouth. The gonads are also in the rays namely in specialized genital pinnules (Heinzeller and Welsch, 1994; Byrne and O'Hara, 2017). The skeletal calcareous pieces (ossicles) of the rays can be summarized in brachials, the ossicles forming the main axes, pinnulars, the ossicles forming the pinnules, axils, ossicle where the ray branches, and radials, ossicles that are part of the calyx and from which arise the rays (Byrne and O'Hara, 2017). The ossicles are joined by interplays of ligaments and muscles or only ligaments depending on the articulation. The most common articulation on the arms are the muscular synarthries (Byrne and O'Hara, 2017). They contain one or two muscle bundles on the oral side (sometimes in association with MCT) and one large ligament on the aboral side (Byrne and O'Hara, 2017; Carnevali and Saita, 1985). This structure is what allows the crinoids to be flexible and rigid at the same time: when muscles contract the arm curls inwards and when they relax the arm straightens and the MCT can harden thus, allowing the arm to stay in that position, immovable, without wasting energy in muscle contraction (Byrne and O'Hara, 2017). Another articulation type worth mentioning are zyzygies. A zyzygy is an unmovable articulation with only MCT and because of their apposing ridges the suture looks like a series of perforations. They are the autotomy points on crinoid arms. This means that it is here where the arm will break off in a case where auto-amputation would be needed (Carnevali and Saita, 1985; Byrne and O'Hara, 2017).

Positions on the arms are defined as distal when they are far from the calyx and proximal when they are at the base of the arm. Also, for orienting the animals, one speaks of the oral and aboral sides instead of ventral and dorsal. Oral designates the side where the mouth and the ambulacral groove can be found, while aboral designates the opposite side.

1.2.3 Sacculi

Saccules are spherical organs with voluminous granulations found in the oral dermal layers of the arms, pinnules and tegmen in several crinoid species (Prenant, 1928). They can vary in size and numbers and even be completely absent depending on the species (Heinzeller and Welsch, 1994). They are composed of an outer epithelial wall of flat prismatic cells and several inner pyriform cells filled with large granules which are the only organelles left (*Fig.4*) (Heinzeller and Welsch, 1994; Noccart, 1993). These granules have a proteinaceous content with varying electron density (Heinzeller and Welsch, 1994; Holland, 1967; Prenant, 1928).

Their function has been widely debated (Holland et al., 1967; Prenant, 1928; Heinzeller and Welsch, 1994). They have been thought to be used for secreting mucus and defensive substances, the storage of reserve nutrients and zooxanthella, excretion, producing chalk and having a sensory function either for gravitation or light sensitivity as photoreceptive lenses (Holland et al.,1967; Heinzeller and Welsch, 1994). Many of these functions have been refuted

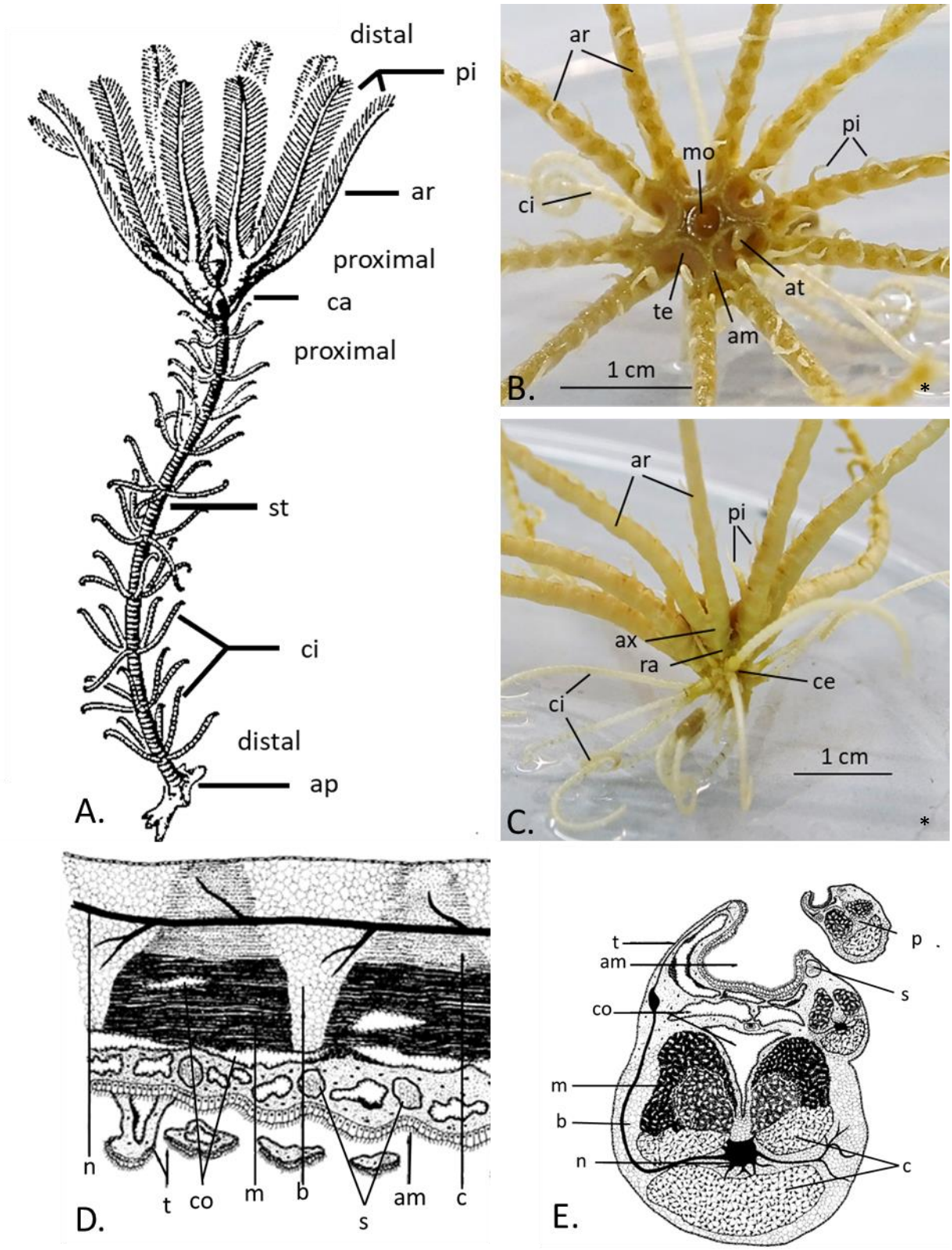

Figure 3. A. Schematic representation of a sea lily. Proximal and distal indicate the relative position on rays and stalk relating to the calyx. Adapted from Heinzeller and Welsch, 1994. B. Oral view of *Stiremetra breviradia*. C. Lateral view of *St. breviradia*. D. Schematic representation of the sagittal section of an arm. Adapted from Carnevali and Saita, 1985. E. Schematic representation of a transversal section of an arm. Adapted from Carnevali and Saita, 1985. am: ambulacral groove, ap: attachment plate, ar: arm, at: anal tube, ax: axial, b: brachial, c: connective tissue, ca: calyx, ce: centrodorsal, ci: cirri, co: coelomic space, m: muscle, mo: mouth opening, n: nerve, p: pinnular, pi: pinnule, ra: radial, s: saccule, st: stalk, t: tentacle, te: tegmen.

like the use as a storage device for nutrients and the presence of symbiotic bacteria (Prenant, 1928; Holland et al.,1967; Heinzeller and Welsch, 1994). It seems *Antedon* can empty its saccule content into the intestinal lumen or its surrounding but this probable holocrine extrusion process' mechanism is unclear, no direct link between saccules and the surface have been found (Heinzeller and Welsch, 1994; Noccart, 1993).

Because of their form and transparency, Holland proposes that the sacculi resemble photoreceptive lenses (Holland et al., 1967). Carpenter stated already in 1876 that saccules were irritable but without saying what stimulus he used (Holland supposes he meant mechanical stimulation) (Holland et al., 1967). Holland hypothesizes that saccules could not only transmit light but also focus it on the underlaying nerve, light would then stimulate electrical activity (Holland et al., 1967).

Holland et al., 1991 describes similar spherical structures in *Calamocrinus diomedae* species in which saccules are absent. These spherical bodies are filled with supposedly symbiotic bacteria (Holland et al., 1991). The benefits from this symbiosis are unknown but Holland et al. present the ideas of chemosynthesis and bioluminescence.

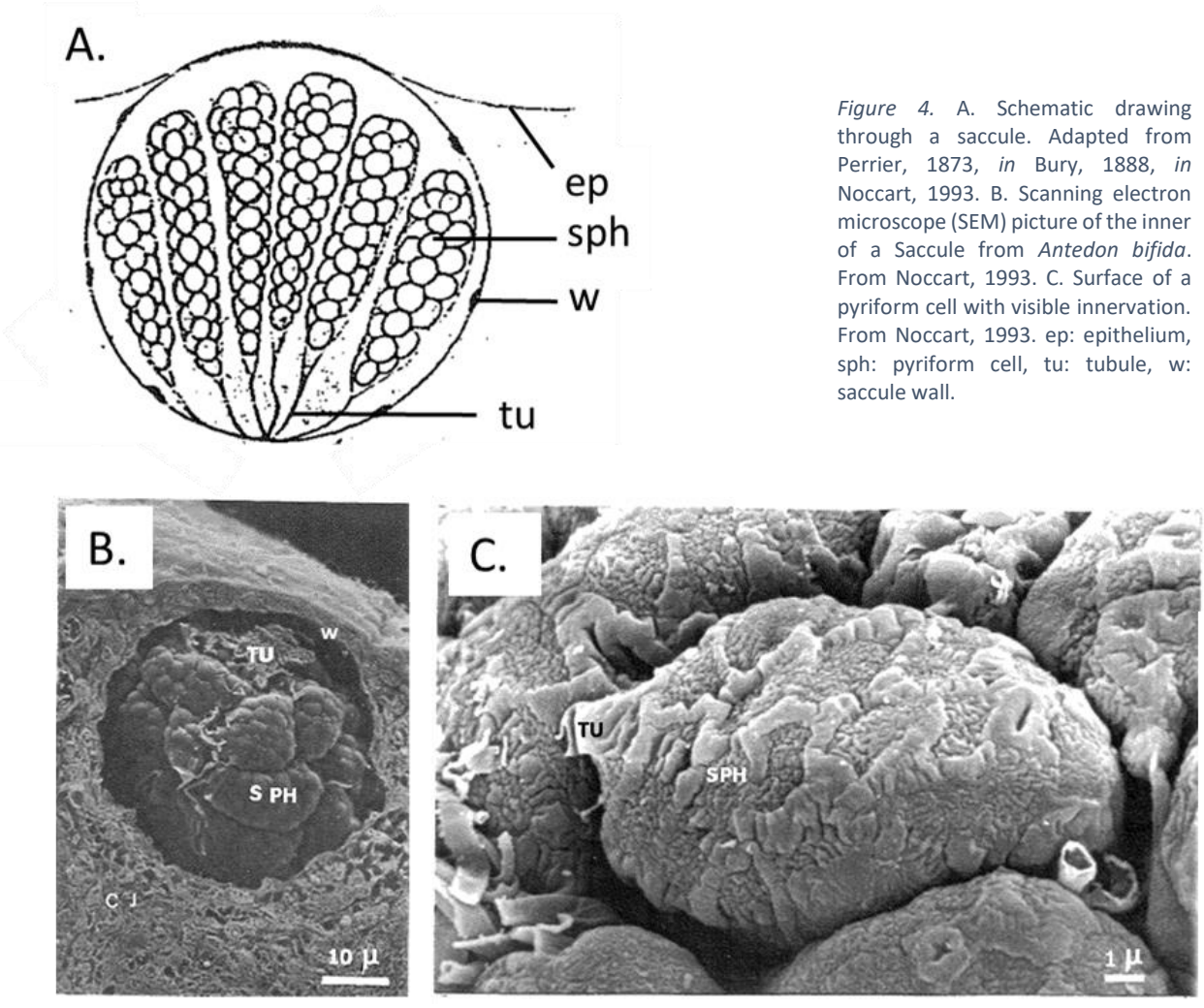

Figure 4. A. Schematic drawing through a saccule. Adapted from Perrier, 1873, *in* Bury, 1888, *in* Noccart, 1993. B. Scanning electron microscope (SEM) picture of the inner of a Saccule from *Antedon bifida*. From Noccart, 1993. C. Surface of a pyriform cell with visible innervation. From Noccart, 1993. ep: epithelium, sph: pyriform cell, tu: tubule, w: saccule wall.

1.3 Bioluminescence

1.3.1 Generalities

This term, probably used for the first time by E. Newton Harvey, 1916, designates the emission of cold visible light ("light emitted by any body whose temperature is below that of incandescence". Merriam-Webster Dictionary) as a result of a natural chemical reaction from living organisms (Haddock et al., 2010; Shimomura, 2006).

Concerning the distribution of bioluminescence in the tree of life, Harvey writes in his book *Bioluminescence*: "[It is] as if the various groups had been written on a blackboard and a handful of damp sand cast over the names, with luminous species appearing wherever a mass of sand stroke". Haddock et al., 2010, estimates that bioluminescence evolved likely more than 50 times which means that it is useful to the organisms and that it is probably an "easy" evolution. Some 820 genera contain light emitting species and these are seemingly erratically distributed (Haddock et al., 2010; Herring, 1987). Light emission capacities are nevertheless more common in marine rather than freshwater and terrestrial environments with 13 marine phyla presenting bioluminescent species (Mallefet, 2009; Shimomura, 2006). Morin, 1983, states that worldwide 1 to 2% of coastal species are bioluminescent contrasting with the pelagic environment where it is estimated that more than 70% of fish species and 90 % of planktonic ctenophores and siphonophores are bioluminescent. Eventual video analysis concluded that 76% of deep-water pelagic observations are bioluminescent animals (Martini and Haddock, 2017) as do about 30 to 40% of deep-water benthos observations (Martini et al., 2019). The main marine bioluminescent groups are bacteria, dinoflagellates, cnidarians, ctenophores, crustaceans, cephalopods, echinoderms and fish (Haddock et al., 2010).

Bioluminescence is chemiluminescence happening inside a living organism (Shimomura, 2006). Two main methods have been discovered so far: Luciferin-luciferase reaction and photoproteins.

Luciferin-luciferase reactions were first reported by Dubois in 1885 using hot- and cold-water extracts from *Pyrophorus* beetles and in 1887 using extracts of the bivalve *Pholas dactylus*. He eventually concluded that it was a substrate (luciferin) – enzyme (luciferase) reaction that emits light. Today's definition of luciferin would be "general term of an organic compound that exists in a luminous organism and provides the energy for light emission by being oxidized, normally in the presence of a specific luciferase" where the latter is the enzyme that "catalyses the oxidative light-emitting reaction of the luciferin" (Shimomura, 2006). One of the most common luciferins is coelenterazine whose reaction path is described in figure 5. So far, nine different types of luciferin have been discovered (*e.g. Fig.6*) (Kaskova et al., 2016). Interestingly, identical molecules can be found in phylogenetically unrelated organisms thus, coelenterazine is present in at least 9 different phyla (Haddock et al., 2010). This can be explained by exogenous acquisition of the molecule through ingestion of luminous prey instead of *de novo* synthesis (Thompson et al., 1988; Haddock et al., 2001; Frank et al., 1984).

In 1961, Shimomura and his team identified in the bioluminescent jellyfish *Aequorea* a protein they named aequorin. It had the property to emit light when Ca^{2+} was added to its aqueous solution even if O_2 was absent (Shimomura et al., 1962). They soon discovered similar proteins

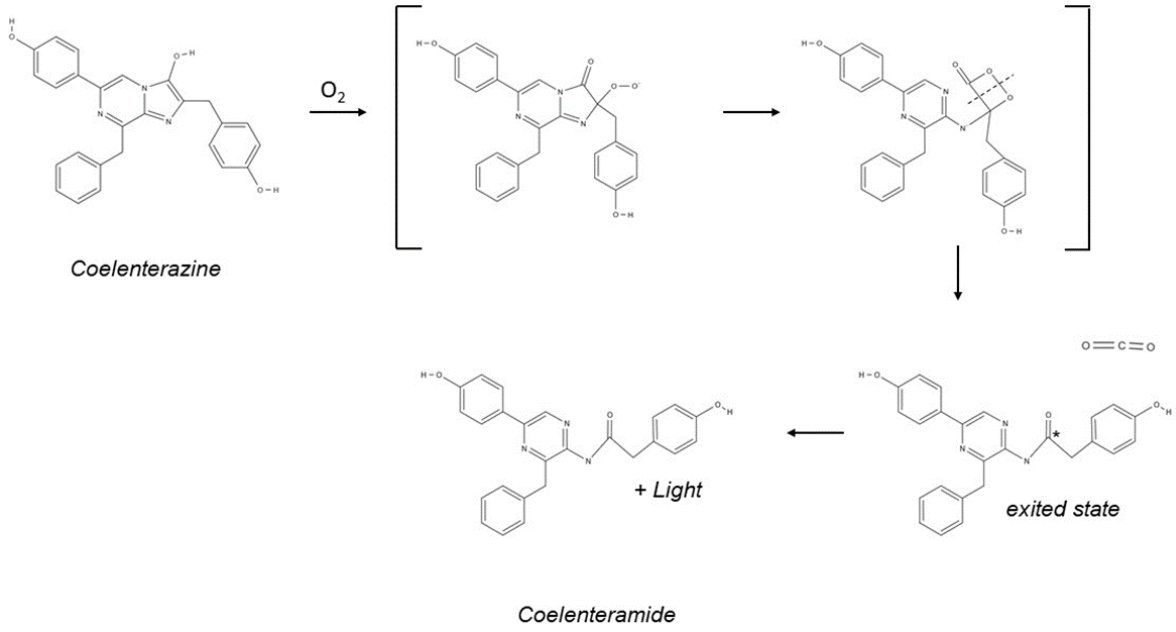

Figure 5. Reaction path of coelenterazine light production. Binding of dioxygen creates a peroxide that creates a "dioxetanone" ring. The latter decomposes rapidly producing CO_2 and the excited state coelenteramide anion. When energy levels drop, blue light is emitted (λ_{max} 450-470 nm). Adapted from Shimomura, 2006. Molecular structures where made with *MolView v2.4*.

in other animals and decided to denominate all these proteins as photoproteins (Shimomura, 2006). Photoproteins are composed from one chromophore (coelenterazine in the case of aequorin) and an apoprotein (apoaequorin for aequorin) (Shimomura, 2006). Numerous types of photoproteins have been described so far, inter alia Ca^{2+}-sensitive types like aequorin, ATP-activation types like in *Motyxia* millipedes and peroxide-activation types that can be found in Polynoid worms, *Pholas dactylus* or even Ophiuroidea (*Table 1*) (Shimomura, 2006).

Eventually Shimomura's work led to the discovery of the Green Fluorescent Protein (GFP) and thereby a Nobel prize. Indeed, aequorin has its emission maximum at 465 nm which is blue and not green like *Aequorea*'s *in vivo* bioluminescence. What happens is that the light energy from the photoprotein or coelenterazine-luciferase reaction uses a radiationless energy transfer mechanism to carry over the energy to the GFP which will then emit with a maximum at 508-509 nm (Shimomura, 2006). It is nowadays regularly used in molecular biology (e.*g.* trace gene expression, protein localisation in living organisms and fluorescence microscopy. Chalfie et al., 1994; Yuste, 2005; Kaskova et al., 2016).

1.3.2 Bioluminescence in Echinodermata

The first description of a with certainty bioluminescent echinoderm is probably Viviani, 1805, where he records the light emission of an ophiuroid nowadays called *Amphipholis squamata* (Harvey, 1952). The first Asteroidea to be assigned as bioluminescent was *Brisinga endecacnemos* (Harvey, 1952). By 1952, Harvey records seven species of luminescent Ophiuroidea and one species of Asteroidea (Harvey, 1952). It took 22 further years before

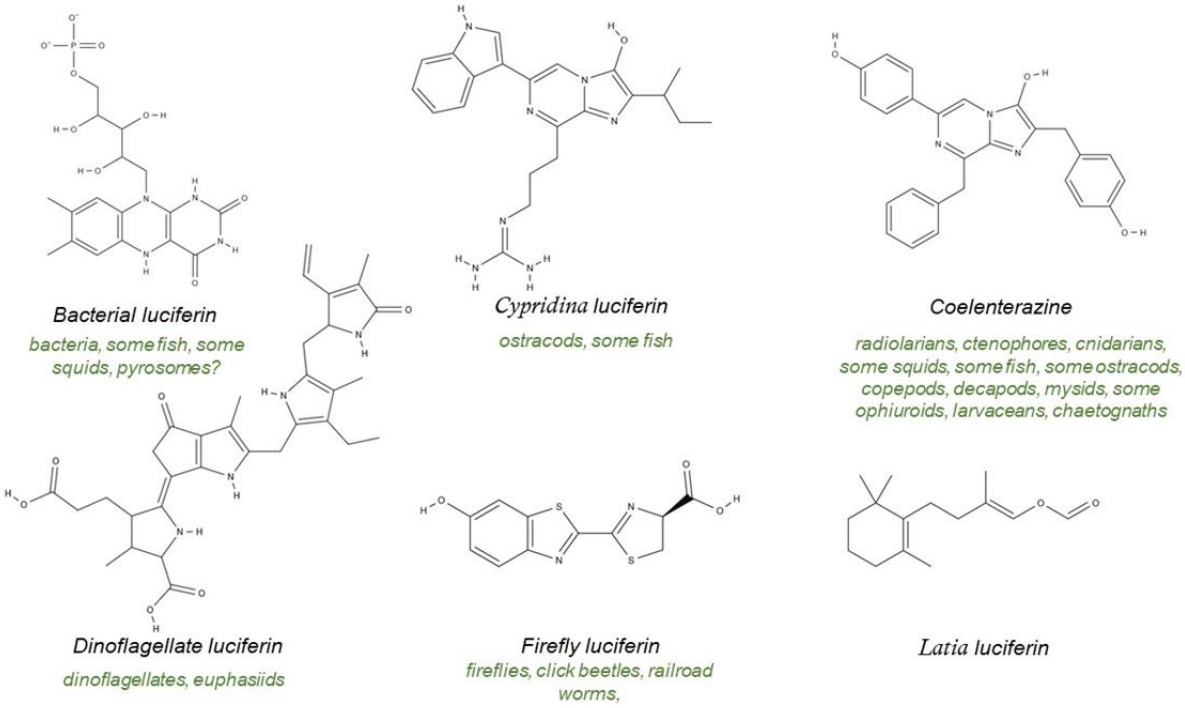

Figure 6. Selection of different types of luciferin indicating name, structure, and animal groups using them (the latter written in green). Adapted from Shimomura, 2006, and Haddock et al., 2010. Molecular structures where made with *MolView v2.4*.

Herring publishes *New Observations on the Bioluminescence of Echinoderms*. It is this article that first publishes descriptions of the bioluminescence in two other classes of Echinoderms namely Holothuroidea and Crinoidea. This article also sets the first verified record of Asteroidea luminescence since the luminescence of *B. endecacnemos* had until that date still not been verified (Herring, 1974).

Since then, the list of bioluminescent Echinodermata keeps increasing. Herring's 1995 list comprises (following current taxonomic status) 34 species of Ophiuroidea in nine families of three orders (Amphilepidida, Ophiocanthida, Ophiurida), 20 species of Asteroidea in seven families in five different orders (Paxillosida, Notomyotida, Velatida, Brisingida, Forcipulatida), 30 species of Holothuroidea in five families and four orders (Elasipodida, Holothuriida, Persiculida, Synallactida) and three species of Crinoidea in three families and two orders (Isocrinida, Comatulida) (*Fig.2*). By 2009, Mallefet registers still 20 bioluminescent Asteroidea but four Crinoidea, 31 Holothuroidea and 66 Ophiuroidea. This tremendous increase in luminous brittle stars is due to a special research interest in this clade because of its accessibility.

Light emissions of the species presented in Harvey, 1952, has thoroughly been described by their respective authors. For example, Panceri, 1878, describes the luminous oval points present on the arm segments of *A. squamata* and the repeated flashes they emit when stimulated before escaping. During the first decade of the 20th century the light emission of respectively spines and/or arm plates was recorded by Mangold, Trojan, Reichensperger and Sokolov in *A. squamata*, *Amphiura filiformis*, *Ophiopsila annulosa* and *Ophiacantha bidentata* (Harvey, 1952). In general, all ophiuroid parts can glow, from the ovaries (not the testes

though. Herring, 1983), to the disk, to the arm plates, spines and tentacular plates depending on the species (Herring, 1995). The emitted pattern may vary with the stimuli like in *Ophiopsila riisei* that shows a faint flash following a small disturbance and a bright flash, travelling along the arm if the disturbance is bigger, associated with arm withdrawal (Grobber, 1988a). *Ophiocomina nigra* has been observed secreting slightly luminous mucus which increases his very weak regular bioluminescence (Jones and Mallefet, 2012).

In Crinoidea light emission has been described from the disk, arms and cirri by Herring, 1974. A "general pale greenish-blue glow, brightest at the disk" was reported for *Thaumatocrinus jungerseni* (Herring, 1974). Furthermore, light points were also visible in the internode regions of the arm segments and the glow spread along the arms when the animal was handled (Herring, 1974). In contrast *Thalassometra lusitanica* does not show light from the main arms but emits from single regions in each cirrus segments (Herring, 1995).

Holothuroid luminescence has also been described by Herring, 1974. Most species seem to have general body luminescence coming from minute points all over the dorsal and ventral regions of the animal (usually more on the back) as in *Enypniastes eximia, Benthogone rosea* or *Kolga hyaline*. Sometimes patterns of brighter lines in the length of the body appear as in *Peniagone théeli* and *Laetmogone violacea* that also shows brighter tips of the dorsal papillae (Herring, 1974; Robison, 1992).

Table 1. List of photoproteins presented in Shimomura, 2006. The organism column contains the names as in Shimomura, 2006. The WoRMS (World Register of Marine Species) column corrects the names to current taxonomic status if necessary. "Name" includes the name of the photoprotein if existent. "Requirements" indicates what the photoprotein needs in order to produce light. "λ_{max}" is the emission spectrum maximum. Adapted from Shimomura, 2006.

		World Register of Marine Species			
PROTOZOA	*Thalassicolla sp.*[1]		Thalassicollin	Ca^{2}+	440 nm
COELENTERATA	*Aequorea aequorea*[1]	*Aequorea forskalea*	Aequorin	Ca^{2+}	465 nm
	Halistaura cellularia[1]	*Mitrocoma cellularia*	Halistaurin	Ca^{2+}	470 nm
	Mitracoma cellularia[1]	*Mitrocoma cellularia*	Mitrocomin	Ca^{2+}	470 nm
	Phialidium gregarium[1]	*Clytia gregaria*	Phialidin	Ca^{2+}	474 nm
			Clytin	Ca^{2+}	
	Obelia geniculata[1]		Obelin	Ca^{2+}	475 nm, 485nm
	Obelia longissima[1]		Obelin	Ca^{2+}	495 nm
CTENOPHORA	*Mnemiopsis sp.* [1]		Mnemiopsin-1	Ca^{2+}	485 nm
			Mnemiopsin-2	Ca^{2+}	485 nm
	Beroe ovata[1]		Berovin	Ca^{2+}	485 nm
ANNELLIDA	*Chaetopterus variopedatus*[1]			Fe^{2+}, hydroperoxide, O_2	455 nm
	Harmothoë lunulata[1]	*Malmgrenia lunulata*	Polynoidin	Fe^{2+}, H_2O_2, O_2	510 nm
MOLLUSCA	*Pholas dactylus*[1]		Pholasin	Fe^{2+} or peroxidase, O_2	490 nm
	Symplectoteuthis oualaniensis[1]	*Stenotheuthis oualaniensis*	Symplectin	alkaline pH?, O_2	470 - 480 nm
	Symplectoteuthis luminosa[1]	*Eucleotheuthis oualaniensis*		catalase, H_2O_2, O_2	
DIPLOPODA	*Luminodesmus sequoiae*[1]	*Motyxia sequoiae*[2]		ATP, Mg^{2+}, O_2	495 nm
ECHINODERMATA	*Ophiopsila californica*[1]		Ophiopsilin[3]	H_2O_2	482 nm

[1] Shimomura 2006
[2] MilliBase http://www.millibase.org/
[3] Mallefet 2009

Herring, 1974, notes for Asteroidea, the luminescence is more of a "general glow" rather than the scintillant points found in Holothuroidea. From all the species he tests, only *Pectinaster filholi* (*P. forcipatus* in the article) presents specific, delimited light emitting sites associated to oval papullaria at the base of the arms (Herring, 1974).

The long-spined sea urchin *Diadema setosum* was described as bioluminescent by Donderlein in 1885 (Harvey, 1952) but it has been shown that it is iridescence from spots on interambulacral plates and genitals (Harvey, 1952) thus, Echinoidea is the only class of echinoderms that has no bioluminescent species described so far.

Let's note that intraspecific variation exists. Different colour variations of *A. squamata* have been shown to produce different intensities of light (Deheyn et al., 1997). There is also evidence for seasonal variability in *A. squamata* (Deheyn et al., 2000).

1.3.3 Photocytes in echinoderms

There are two ways in which an animal can be bioluminescent: *(i)* intrinsic bioluminescence, where the organism itself produces the light, and *(ii)* extrinsic bioluminescence, where symbiotic bacteria are the actual light-emitters (Haddock et al., 2010). Both can coexist in the same individual like in the female anglerfish *Linophryne coronate* (Widder, 2010). Until now, the norm in echinoderms seems to be intrinsic bioluminescence (Herring, 1974; Mallefet, 2009; Delroisse et al., 2017a).

In intrinsic bioluminescence, animals can either produce intracellular or extracellular luminescence (Herring, 1985; Haddock et al., 2010). The latter means that the chemicals producing light are secreted and react outside the organism, one example for this is the scyphozoan *Pelagia noctiluca* (Shimomura, 2006).

Intracellular bioluminescence is done in specialised light-emitting cells called photocytes (Renwart et al., 2015). These can be either dispersed as single cells like in cnidaria (Herring and Widder, 2004) or be part of more complex organs: the photophores (Denton et al., 1985). Photophores differ in size, number and location depending on the species. They are composed of a photogenic mass made from photocytes (or tubules with symbiotic bacteria) associated to pigmented layers, reflectors, selective filters and lenses (*Fig.7*) (Denton et al., 1985; Renwart et al., 2014).

No real photophores have been found in echinoderms yet (Delroisse et al., 2017a). Only photocytes have been described so far and still little is known about these, especially in echinoderms other than Ophiuroidea. In fact, no other paper than Herring, 1974, and Robison, 1992, describe the morphology of the luminescent cells (or rather what is expected to be the luminescent cells) in Asteroidea, Holothuroidea and Crinoidea.

At the beginning of the 20th century a lot of effort was put into describing the light emitting cells of ophiuroids. Mangold, 1910, summarizes the work of his fellows showing a consensus for the statement that the photocytes are unicellular gland cells (or groups of them) in the connective tissues under the plates with a long projection stretching until the epithelium

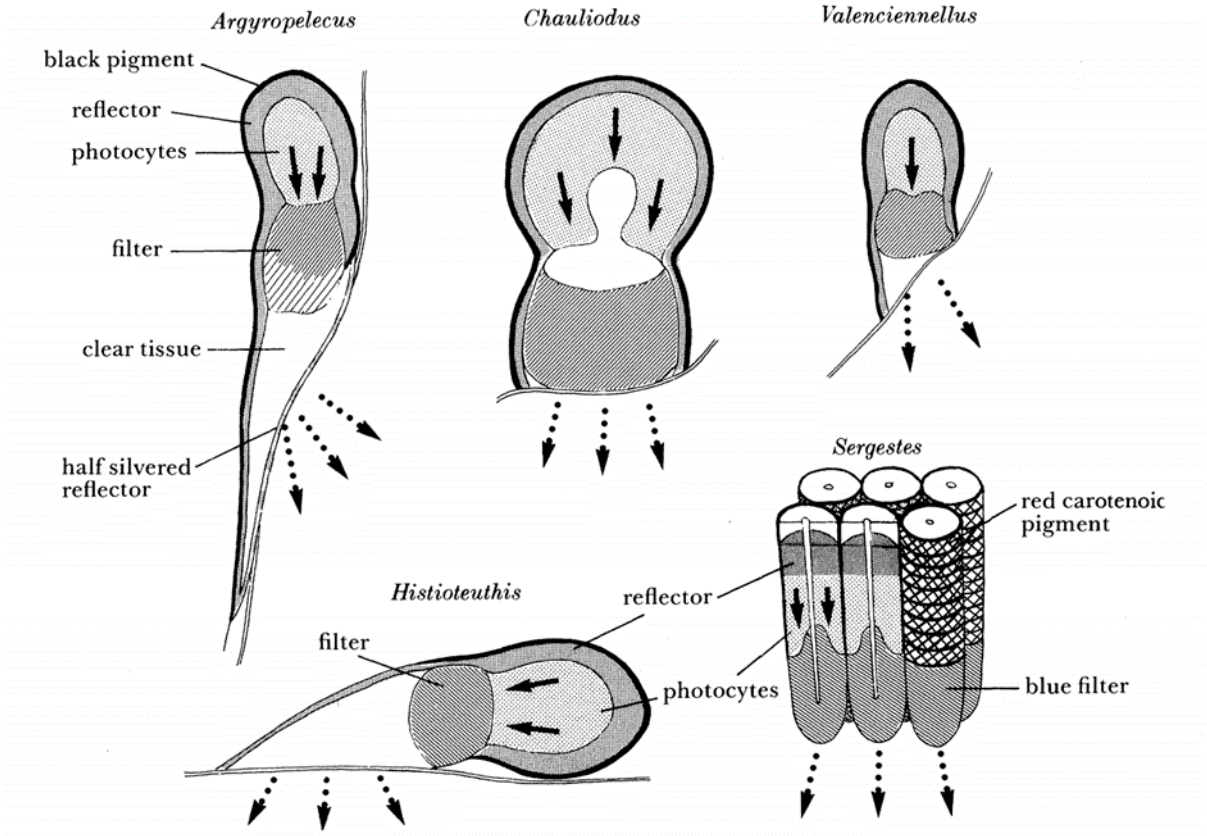

Figure 7. Diagrams of photocytes from fish (*Argyropelecus*, *Chauliodus*, *Valenciennellus*), squid (*Histioteuthis*) and shrimp (*Sergestes*). Arrows represent light emission direction. Arrows with continuous and discontinuous lines help represent different wavelengths to demonstrate the effect of the filter. From Denton et al., 1985.

(Harvey, 1952). They also agreed on the fact that these cells are filled with granular material that can be stained with thionin and mucicarmine and that they are associated to nerve fibres (Harvey, 1952).

Buchanan, 1963, describes the glandular cells and photocytes of *A. filiformis* in a rigorous manner. He makes a description comparable to Mangold's reporting that the photocytes have the same appearance than individual glandular cell and are in the surrounding of the gland cell masses at the spine's base (Buchanan, 1963). Their pyriform body is filled with granules and their long neck follows the gland cell neck column all along the spine (Buchanan, 1963). However, they don't have an opening to the exterior but end under the cuticle with a swelling (Buchanan, 1963). He also gives his opinion on *A. squamata*'s photocytes and agrees with Reichenbacher, 1908, on them being situated around the spine's base articulation based on their granular content resembling *A. filiformis* photocytes (Buchanan, 1963). However, this position (in both *A. filiformis* and *A. squamata*) does not seem to be congruent with the light spots on the spine tips of the animals (Brehm and Morin, 1977).

Herring, 1974, was unable to find probable photocytes in the luminescent areas of the ophiuroids he tested. Hence, Brehm and Morin, 1977, studied *O. californica* and *A. squamata* with fluorescence. The use of fluorescence to study the distribution of luminescence is in many cases an easy and effective approach. It often holds as long as the stimulation persists allowing longer observation time than luminescence and it is maintained even after fixation

(Brehm and Morin, 1977). It has been shown that sites of fluorescence are often equivalent to luminescence (Brehm and Morin, 1977). In *O. californica* they define two components of the photocytes in the spines: "varicosities" which are swellings of the second component called "processes" which are long and narrow cords. The outlines of single photocytes were impossible to determine thus, the number of varicosities and processes that compose one photocyte was not possible to set (Brehm and Morin, 1977). Usually spherical and with an average diameter of 3 µm, the varicosities are most abundant around the ganglion at the base of the spine (Brehm and Morin, 1977). The processes, on their side, are undistinguishable from the nerve cords except for their fluorescence (Brehm and Morin, 1977). They have a diameter of 0.4 µm and seem to originate in the lateral edges of the radial nerve (Brehm and Morin, 1977). Processes and varicosities are present in every light emitting part of the animal and absent where no light is emitted (Brehm and Morin, 1977). They do not stain with thionin like those described by Mangold and Buchanan do. Unfortunately, they were not able to study *A. squamata* in the same way because the fluorescence in this species fades away way to quickly (Brehm and Morin, 1977). Besides, the photocytes described by Brehm and Morin do not resemble those described by Buchanan and previous authors: even though the gland cells described are present in *O.californica*, they do not match with fluorescence and the photocytes morphology. Moreover, their distribution also does not resemble the form and placement of the pyriform cells described in older articles (Brehm and Morin, 1977; Buchanan, 1963; Harvey, 1952). Thus, Brehm and Morin suppose that they are describing a new kind of photocyte that they also expect to be the type present in *A*. *squamata*. They also emit two hypotheses: *(i)* the photocyte processes being undistinguishable from the nervous cord and their probable direct control through the radial nerve cord lets conceive that the processes are extensions of effector cells passing to the axon for innervation as seen sometimes for muscles in echinoderms (Brehm and Morin, 1977); *(ii)* the form and the similar staining allows to theorise that the photocytes are from neural origin (Brehm and Morin, 1977).

The study of the fine structure of the photogenous area around the spinal ganglia in *A. squamata* led to the discovery of cells with a well-developed rough endoplasmic reticulum, a widespread Golgi apparatus and, specially, several irregularly shaped vacuoles (Deheyn et al., 1996). The important ultrastructure change they exhibited after luminescence is indicative of their photogenic activity and they were therefor deemed to be photocytes (Deheyn et al., 1996).

Like in Brehm and Morin (1977), epi-fluorescence microscopy was used to study the photocytes of *Ophionereis schayeri* and *O. fasciata* (Mallefet, 2009). The photocytes are principally located under the ventral arm plates, but also under the dorsal and lateral plates and in the spines but not in the radial nerve cord like in *O. californica* (Mallefet, 2009).

Recently, through immunodetection with polyclonal antibodies directed against *RLuc* (*Renilla* luciferase) which is highly homologous to the brittle star luciferase, presumable photocyte clusters were detected in the spine stroma of *A. filiformis* but also in the arm's terminal segment (Delroisse et al., 2017a, 2017b). Transmission electron microscopy then allowed to identify various pyriform cell types surrounding the spine nerve and projecting processes to the distal parts of the spine as described by Buchanan, 1963 (Delroisse et al., 2017a). Two types of granular cells were apparent from which type II granular cells, that presented smaller granules (1 µm in diameter) compared to the (up to 3 µm) large granules of type I cells, were absent in the non-luminescent species *Amphiura chiajei*. After induction of bioluminescence

through KCl and acetylcholine, these type I granular cells underwent ultrastructure modifications with the almost disappearance of the electron-dense granules (Delroisse et al., 2017a). Delroisse et al. hypothesise that the spine skeleton and specially the longitudinal trabeculae are responsible for the light transmission to the tip of the spine where the light emission is actually visible. They also suggest that the type I granular cells, which are also present in the non-luminescent *A. chiajei* and do not release their granular content, are possible pigment cells and their close association to type II granular cells (the photocytes) could be interpreted as part of a simplified photophore that would be the spine (*Fig.8*) (Delroisse et al. 2017a). Effectively, chromatophores are pigment cells and essential parts of photophores that absorb the light emitted in the undesirable direction by the centrally positioned photocytes (Young and Arnold, 1982). In addition, photophores often contain so-called light guides that control the direction of the emitted light (Young and Arnold, 1982) which is probably what the longitudinal trabeculae do (Delroisse et al., 2017a).

In Herring, 1974, we get the first description of photocytes in echinoderms other than Ophiuroids. He suspects some with large spherical and subspherical granules filled cells, that are always present in (or directly below) the epidermis of the bioluminescent sites, to be the light emitting cells of *Kolga hyalina*, *Ellipinion sp.*, *Laetmogone violacea, Benthogone rosea* and *Galatheathuria sp.* (*Fig.9*). He finds them specially on the ventral podia of *K. hyalina* and the distal tips of the dorsal papillae of *L. violacea.* In the latter, these granular cells are close

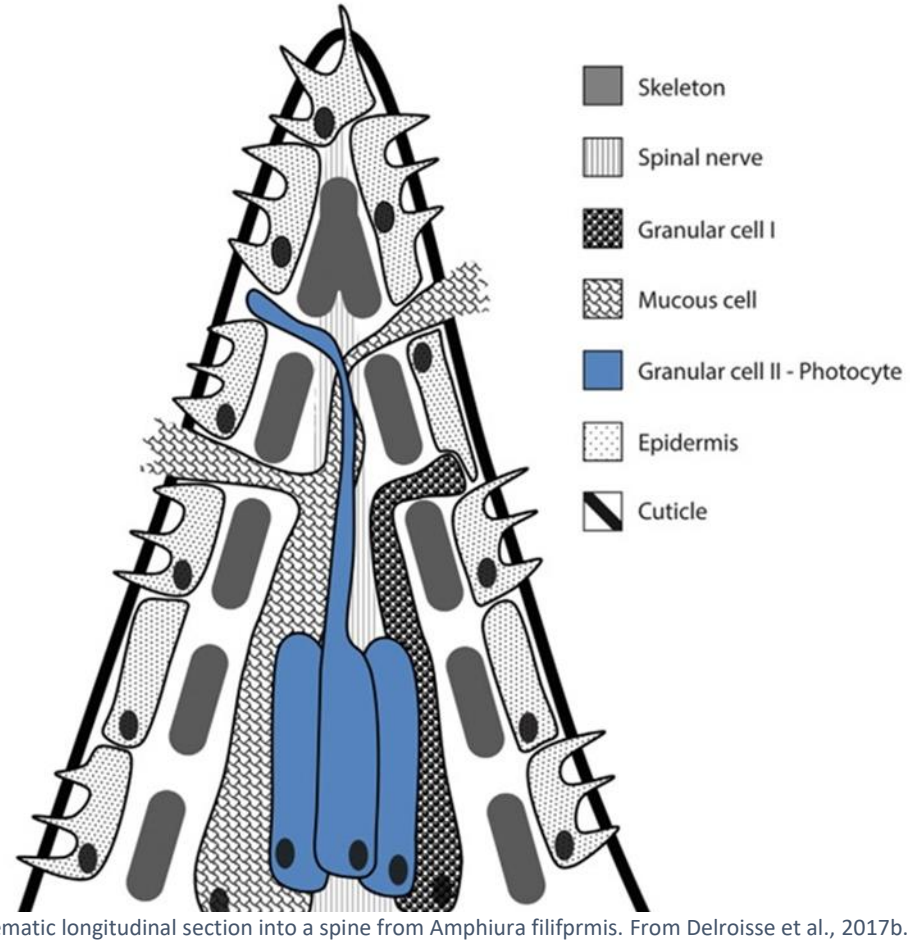

Figure 8. Schematic longitudinal section into a spine from Amphiura filifprmis. From Delroisse et al., 2017b.

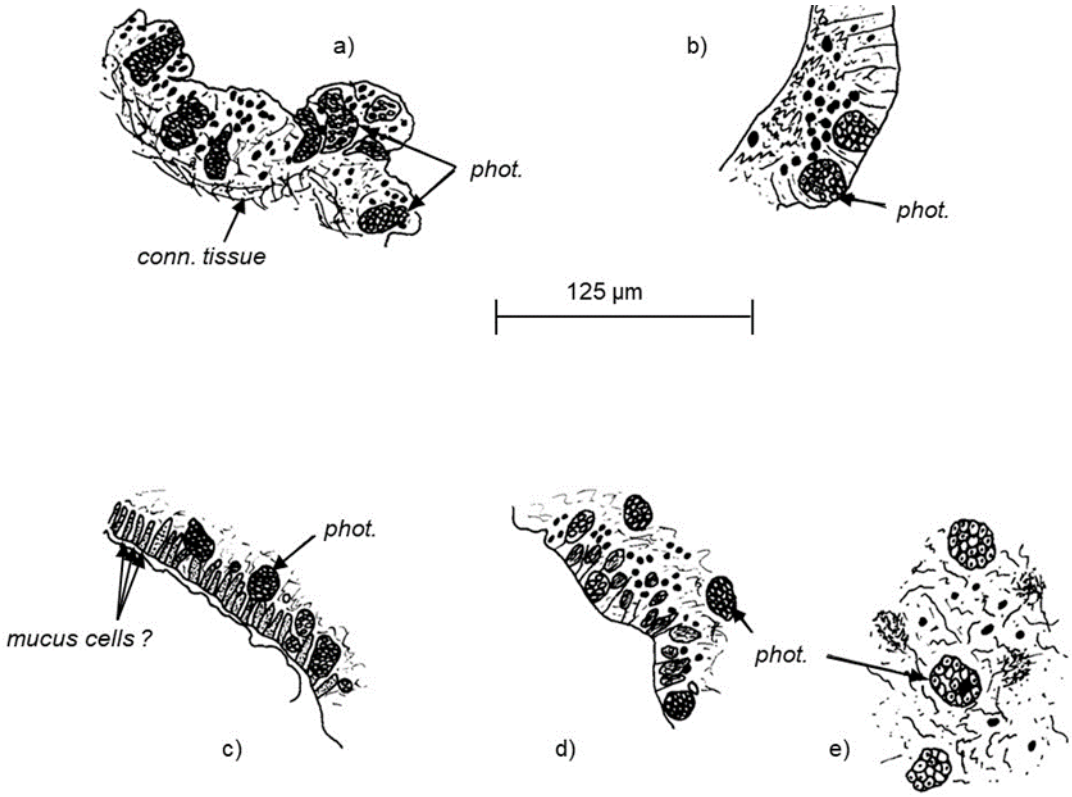

Figure 9. Representation of the possible photogenic cells in Holothuroidea. a) *Kolga hyaline*, b) *Ellipinion* sp., c) *Benthogone rosea*, d) *Laetmogone violacea*, e) *Galatheathuria* sp.. "phot." means photocyte, "conn. tissue" means connective tissue. From Herring, 1974.

to large numbers of glandular cells, both kinds staining rather similarly letting Herring suspect that they may be of similar light emission use (Herring ,1974).

In *Enypniastes* eximia, Robison finds granular bodies, 20 to 60 µm in size, that resemble the bodies that Herring, 1974, suspects to be the Holothuroids' photocytes (Robison, 1992). They are in the first subdermal layer, in concentrations from 52 per cm² on the trunk's surface to 98 per cm² on the veils and emit a green-blue light (maximum emission wavelength 474 nm) (Robison, 1992). Being directly under the skin, they are shed together with the epidermis following mechanical contact (see below) (Robison, 1992). SEM showed that the units exceeding 40 µm are clusters of the smaller subunits (Robison, 1992).

Equally, it is hypothesised that similar with granules filled cells are responsible for luminescence in Asteroidea (Herring, 1974). In fact, they are found just underneath the epidermis of *Hymenaster sp.* and *Calyptraster personatus* (in the article *Cryptaster personatus* Perrier. Herring, 1974). *Hydrasterias ophidion* does not have this type of cell but does present an epidermis with glandular cells whose content can be of granular appearance (Herring, 1974).

In *Thaumatocrinus jurgensis* Herring could not define with certainty a cell type responsible of light emission. He surmises some granular cells in the epidermis of the podia but without certainty (Herring, 1974).

1.3.4 Ecological interests of bioluminescence for echinoderms

General use of bioluminescence has been widely discussed (Morin, 1983; Herring, 1995; Haddock et al., 2010; Widder, 2010). It may accomplish several different roles for one single organism (Haddock et al., 2010).

In many Ophiuroids the photocytes, and thereby light emission, are mainly found in the arms which are also, for many of them, the only body part in the water column (Delroisse et al., 2017a); the non-luminescent disc being often buried in the sea floor. This emphasizes the important role of bioluminescence in the animal's interaction with its biotic environment (Delroisse et al., 2017a).

Avoidance reactions are generally shown by predators in regard to light emitting ophiuroids (Grober, 1988a, 1988b). Therefore, the similarity between light emission signals, in coastal emitters at least, might be due to mimicry (Grober, 1988b). This mimicry links to the hypothesis that bioluminescence is aposematic, a warning signal where the predator learned to associate light emission (instead of colours) to unpalatability (Grober, 1988a). During Grober's experiments, predators seemed to learn the unpalatability of the luminescent ophiuroid as fast as for the non-luminescent ones, but the difference was that the handling time was always lower for luminous brittle stars thus less damage was induced (Grober, 1988a). Hence, the luminescent *Ophiopsila riisei*, when tested, were less harmed while interacting with predators than non-luminescent control species (Grober, 1988a). This does not prove aposematism though but is the first quantitative proof of the use of bioluminescence as a predator deterrent (Guilford and Cuthill, 1989; Grober, 1989).

Aposematic use of bioluminescence has nevertheless been described for *Ophiopsila aranea* (Jones and Mallefet, 2010). Indeed, this species is unpalatable for the tested predators but suffered less predation than the cryptic control brittle star species. Handling time, like in Grober (1988a), diminished with the number of trials and predatory behaviour was significantly superior during the first trial (Jones and Mallefet, 2010). It could not be verified if predators show an initial aversion towards the aposematic prey because light is only emitted by the ophiuroid under mechanical stimulus by the predator thus, the predator is not able to recognise the aposematic display prior to the contact (Jones and Mallefet, 2010). This type of "facultative aposematism" is considered beneficial to the brittle star because it stays cryptic and not exposed to detection (Jones and Mallefet, 2010).

It seems like the sea cucumber *Enypniastes eximia* also uses bioluminescence for defence purposes (Robison, 1992). This pelagothuriid's luminous response also depends on the importance of the mechanical contact. The harder, the brighter it lights up and the more epidermis breaks thus, emitting more luminous tissue into the surrounding water (Robison, 1992). The light emitting capacities will later regenerate together with the skin's regeneration (Robison, 1992). *E. eximia* seems to rely on the burglar alarm effect. This means that the light emitted will attract secondary predators (*i.e.* the predator's predators) (Robison, 1992; Burkenroad, 1943, for original description). The shed skin or a continuous glow of the animal even after ingestion could help mark the predator making him visible and exposed to his own predators (Robison, 1992). A further use of light emissions could be as a warn signal for other holothuroids in the surroundings. In any case, the burglar alarm strategy might rely on kin selection after the sacrifice of one individual. Hence, this animal occurring regularly alone and

having the capacity to regenerate skin and thus luminescence, it can be suspected that light emissions helps the individual to survive the encounter with a predator (Robison, 1992).

The emission of luminous tissue when encountering a predator is also seen in Ophiuroids. *A. squamata* shows an increased luminescent response with an increased stimulus (*i.e.* persistence of the predator. Deheyn et al., 2000). A still persistent contact will lead *A. squamata* to autotomize the arm in contact with the predator (Deheyn et al., 2000). This arm will emit light more intensely while the others (still attached to the animal) start to fade enabling it to flee unseen while the crab handles the glowing autotomized arm (Deheyn et al., 2000). Different colour varieties of this species emit different light intensities, but more luminous individuals do not seem to take any advantage from it because all varieties show the same amount of autotomy (Deheyn et al., 1997).

Mallefet, 2009, did the same experiment and verified the luminescent arm autotomy of *A. squamata* in presence of *Galathea squamifera* but additionally he showed that the sacrificed arm keeps glowing in the galatheid's mouth thus enabling burglar alarm by making the predator detectable to secondary predators (Mallefet, 2009).

Ophiocomina nigra has been observed secreting a luminous mucus produced when attacked (Jones and Mallefet, 2012). Normally, this kind of secretion helps either through burglar alarm effect or as smoke screen, startling or blinding the predator (Jones and Mallefet, 2012). The problem with the previously described strategies is that they rely on bright light emission which is quite the opposite of *O. nigra*'s luminescence (Jones and Mallefet, 2012). Therefore, Jones and Mallefet propose either an aposematic predator deterrence response or a usage to attract prey like decapods.

Another predatory use of bioluminescence by an ophiuroid is recorded by Morin, 1983. Here, a bright flash following the contact between *O. californica* and a polychaete makes the worm stop its movement upon which he is caught and eaten by the ophiuroid (Morin 1983). Herring, 1995, doubts the interpretation of this as a voluntary use of light as a prey-stunning method.

Jones and Mallefet, 2013, verify deterrence, aposematism and burglar alarm effect rigorously using *Amphiura arcystata, A. squamata, O. nigra, O. aranea* and *O. californica* as bioluminescent ophiuroids, *Ophiotrix fragilis* as non-luminescent control, the crab *Carcinus maenas* as primary predator (preying on the brittle stars) and the seabream *Diplodus vulgaris* as secondary predator (predating the crab) (Jones and Mallefet, 2013). Their study verifies once again all three effects of bioluminescence as anti-predatory strategy based on vision.

The seasonal variability shown in *A. squamata* is linked to temperature and the reproductive cycle of the adults, itself guided by photoperiod (Deheyn et al., 2000). The two light emission peaks that arise, one in summer and one in winter, allow to suggest two different uses for bioluminescent: *(i)* the already stated defensive use in summer when predation is highest, and *(ii)* due to the low predation in winter, the winter peak could be explained by intraspecific communication for aggregation during mating season (Deheyn et al., 2000). This would be useful for *A. squamata* because as a brooding species it produces few gametes thus, cross-fertilization may only work when individuals are aggregated (Deheyn et al., 2000).

A recent study on Asteroidea photoperception showed that all three of the aphotic zone species they tested have well-developed compound eyes and that two of them, *Diplopteraster multipes* and *Novodinia americana*, are also luminescent (Birk et al., 2018). This evokes the recognition of light produced by bioluminescence. The authors suggest that it would help

while on the search for a mate; olfaction would not be enough if used alone, thus bioluminescence in Asteroidea could also help for intraspecific communication (Birk et al., 2018). Furthermore, they observed *D. multipes* walking around with extruded stomach leading to the hypothesis that it feeds on organic matter deposits on the sea floor and that it could use biofilm light emission to direct itself towards its food source (Birk et al., 2018).

Interestingly, another ecological role of luminescence may be refuge creation and thus community structuring (Grober, 1988b). Indeed, hermit crabs have been observed in close association with *O. riisei* while their predators avoid *O. riisei* aggregations (Grober, 1988b). Grober implies the refugium hypothesis to explain this observation (Grober, 1988b).

1.3.5 Biochemistry of the light emission in echinoderms

Until Harvey, 1952, not much work had been done on echinoderm bioluminescence biochemistry. Harvey showed in 1926 that oxygen was needed for *A. squamata* to produce light. He also states that, when ground in a mortar, a bright light is emitted but that it does not last long. Harvey was also unable to show if it was a luciferin-luciferase reaction with *Cypridina* luciferase (that doesn't react with coelenterazine).

A. filiformis has a coelenterazine-luciferase system allowing it to emit light from its arm spines (Shimomura, 2006; Delroisse et al., 2017b). Its luciferase was shown to be homologous to the sea pansie *Renilla*'s luciferase (*RLuc*); one would expect that luciferases are different between phylogenetically distinct groups (Delroisse et al., 2017b). Delroisse et al.'s main hypothesis is horizontal gene transfer of a haloalkane dehalogenase with a hydrolase function to the common ancestor of cnidarians and echinoderms. The haloalkane-dehalogenase function became a luciferase in both groups due to the exposure to the same environmental pressures (Delroisse et al., 2017b). Sea pansies and brittle stars live both on soft sediment and are suspension-feeders which allows both to acquire coelenterazine from plankton (Delroisse et al., 2017b). Hence, access to a luciferin and the need of a predation avoidance strategy would have led to the appearance of luminescence (Delroisse et al., 2017b). *A. filiformis* luciferase has a molecular weight of 23 000 kDa, its optimum is at a pH of 7,2, it presents a specific activity of 4 x 10^{12} photons·s^{-1}·mg^{-1} and in the presence of oxygen light emission of coelenterazine will have an emission maximum of 475 nm at optimum pH (Shimomura, 2006).

O. californica is a green light emitter (Shimomura, 1986). At the contrary of *A. filiformis,* it relies on a 45 000 kDa photoprotein with an emission maximum about 482 nm (Shimomura, 1986) a smaller wavelength than the one measured by Brehm and Morin (1977) *in vivo*. In *O. californica*, light emission was induced by electrical, mechanical and chemical (KCl, distilled water) stimulation (Brehm and Morin, 1977) but the photoprotein requires relatively high concentrations of H_2O_2 for light emission (Shimomura, 2006). Its green light is nearly identical with its fluorescence suggesting that the chromophore would be the light emitter (Shimomura, 1986). Nothing more is known about the chromophore or the apoprotein.

Concerning non-ophiuroid echinoderms, Herring, 1974, obtained luciferin-luciferase reactions from fresh Asteroidea *Hydrasterias ophidion* and Crinoidea *Thaumatocrinus jungerseni*. Aqueous extracts made out of all the bioluminescent species he tested (7 asteroids, 9 holothuroids, 3 ophiuroids, 2 crinoids) reacted to Fe^{2+} and H_2O_2 by emitting a blue flash (except for *Hymenaster roseus*. Herring, 1974).

1.3.6 Nervous control

The nervous control of bioluminescence has been demonstrated for many species (*e.g.* fireflies, fish, sharks, annelids, krill,…). Control can be effectuated through induction or reduction of light production or affecting surrounding pigment cells that can thus block light emission from photophores (Trimmer et al., 2001; Claes and Mallefet, 2011). It can allow modulation and adjustment of duration, angle, frequency and intensity of the signal (Gouveneaux and Mallefet, 2013). NO[4], neuropeptides like PACAP[5] (paracrine role), hormones (*e.g.* MT, PRL, α-MSH, ACTH)[6] and general neurotransmitter like Ach, GABA[7], carbachol, octopamine, noradrenaline, adrenalin, can all be involved depending on the clade and species (Trimmer et al., 2001; Zaccone et al., 2011; Claes and Mallefet, 2011; Gouveneaux and Mallefet, 2013, Duchatelet et al., 2019).

The close relation between the photocytes and the nerve cord in ophiuroids led to the assumption that, here too, light emission was under nervous control (Buchanan, 1963; Brehm and Morin, 1977; Deheyn et al., 1996; Mallefet, 2009). Response to Ach and eserine (cholinesterase inhibitor) by *Plutonaster agassizi notatus* (*Plutonaster notatus* in the article) and *Thaumatocrinus jungerseni* lets also suppose control by the nervous system in sea stars and crinoids (Herring, 1974).

Cholinergic, GABAergic and trace aminergic control has been shown for inter alia *A. squamata*, *A. filiformis*, *O. californica* (Mallefet, 2009). The different intensities observed when treating *A. squamata* and *O. californica* or *O. aranea* with Ach, allow to stipulate that Ach is not the main neuromediator in *Ophiopsila* (Dewael and Mallefet, 2002). Nevertheless, it may still have a synergic action with an until this date unknown molecule (Dewael and Mallefet, 2002). These experiments suggest however that there is no common transmission pathway in brittle stars (Dewael and Mallefet, 2002).

One explanation suggested for different kinetics in luminous response is the involvement of different fibre types that conduct impulses at distinct velocities (Dewael and Mallefet, 2002).

1.4 Our work

The goal of this work is to do a first asses of the data concerning deep-sea bioluminescent echinoderms obtained during the *Sampling the Abyss* cruise.

Objectives of the cruise were, among other, testing for bioluminescence and the description of the latitudinal and bathymetric distribution of biodiversity from the lower bathyal (2500m) to the abyssal (4000m).

Thus, the first part of this Master thesis consists on the evaluation of sampling data collected on board. Echinoderm captures are going to be analysed and we will try to find patterns in the

[4] Nitric oxide
[5] Pituitary adenylate cyclase-activating polypeptide
[6] Melatonin, Prolactin, α-Melanocyte-stimulating hormone, Adrenocorticotropic hormone
[7] Acetylcholine, γ-aminobutyric acid

distribution of bioluminescent genera along latitudinal and bathymetric gradients off the south-eastern Australian coast.

In the second part, luminometry measurements taken by Pr. Jérôme Mallefet after capture and following external stimulation (mainly KCl and fresh water) will be described and pictures taken of live luminescence will allow to make *in toto* descriptions of light emission zones in some of the species.

The third part consists in following into Herring's steps in the search for the luminous structures in Echinodermata. We will therefor try to find the photocytes of two crinoids and a holothuroid through epi-fluorescence microscopy.

The fourth and last part is the determination of the light emission system in one of our crinoids.

This shall eventually lead to increase our knowledge on deep-sea bioluminescence and light emission in non-ophiuroid echinoderms as well as updating the ever-growing list of bioluminescent species.

2 Materials and Methods

2.1 Organism sampling

Organisms were sampled during the *Sampling the Abyss* cruise (4/05/2017 – 16/06/2017) and codified with operation number (001 – 136) and sample number. Thus, an animal with the code 006_139 is the sample 139 from operation 006. Several individuals considered from the same species could be put together in one sample thus, 1019 samples contain 12 465 individuals.
Organisms were randomly selected to be tested for bioluminescence. The latter come all from sampling operations where the CSIRO Four Metre Beam Trawl was used (*Table S1*). Organisms were stored in 4% formaldehyde seawater solutions and kept refrigerated. Table S1 contains all the operations and the equipment used to collect the totality of the samples during the cruise.
Only tissues used for histology will now get a detailed description of their sampling. *Monachocrinus* cf. *aotearoa* (Bathycrinidae) and *Psychropotes longicauda* (Psychropotidae) were collected during operation 56 at site 12 at approximately 2600 m depth in the Jervis CMR on May 29th, 2017. The Thalassometridae, initially identified as *Thalassometra* cf. *gracilis*, were collected at two sites namely during operation 80 at site 17 at approximately 1200 m depth in the Central Eastern CMR on June 5th, 2017 and operation 69 at site 15 at approximately 1000 m depth in the Hunter CMR on June 3rd. For both crinoids, arm pieces with their pinnules were stored in formaldehyde. One rather complete specimen of the thalassometrid 69_148 was kept frozen at -80°C. For *P. longicauda* tissue samples were taken from the surrounding brim (formed from the fusion of ventro-lateral tube-feet), dorsum and "tail" appendage and kept in formaldehyde.

Stiremetra breviradia (Thalassometridae) is a bioluminescent crinoid used for preliminary histological studies. These samples date back from the Southern Surveyor SS10 cruise in 2005 and have since been stored in a 4% formaldehyde seawater solution. Even though *S. breviradia* is also a Thalassometridae, the term thalassometrid will designate the thalassometrids collected in 2017.

2.2 Luminometry

Stimulation of the light emission, luminometry measurements and photography were done on board of the RV *Investigator* by Pr. Jérôme Mallefet. Stimulants tested for inducing light emission were mainly KCl (200 mM) and freshwater. Additionally, adrenalin was used to stimulate the thalassometrid 69_148 and acetylcholine was tested as stimulant on *O. rudis*.

Tested samples were classified into three different groups namely bioluminescent, non-bioluminescent and dubious. An animal was considered bioluminescent if it was able to emit light either by itself or following chemical or mechanical stimulation in the laboratory. A sample was considered non-luminescent if no light emission was observed nor measured with the luminometer. A species was considered a dubious light-emitter if samples of the same species responded differently to stimulation but never with a clear light emission or the

measured light was weak, never clearly exceeding 10 000 relative light units (RLU) per second and being close to the stimulant-injection and thereby being a possible artefact. Hence, if two samples from one species gave no response and another from the same species did gave a weak response, the species was counted as dubious. If this single weak response was very close to injection time and consisted only in a single weak peak, then this response was interpreted as an artefact and the species as non-bioluminescent. If one of several samples of the same species did give a clear emission-curve that certainly was the trait of bioluminescence, then the species was counted as bioluminescent despite previous failures to trigger light emission.

A *FB12* single sample luminometer (Berthold Detection Systems GmbH, Pforzheim, Germany) was used with the FB12/Sirius software (Berthold Detection Systems). The mode used was "single kinetics". Animals were kept in 1°C cold sea water and were not anesthetized before being stimulated. Samples were put in sample tubes with up to 12 mm diameter and up to 75 mm length. For larger animals, pieces had to be dissected. Adding of the stimulants was done using a syringe and an injector on the luminometer. To avoid artefacts the syringe was wrapped in black fabric before starting and during the measurement. The injection was normally done 10 s after beginning the measurement in order to have the luminometers baseline. Sometimes stimulation was first followed by photography of the light emitting animal before putting the sample into the luminometer. Light intensity was recorded during 190 s for each measurement. Measurements were recorded in RLU. Calibration was done with a Tritium light source. Knowing the age of the light source we can calculate the intensity of the light it emits with the corresponding formula : $I = 119{,}7e^{-0.056\,t}$ where I is the light emission intensity in Mega-quanta per second (Mq s^{-1}) and t is the time passed since April 1st 1971 expressed in years. Thus, in June 2017; t = 46.167 and I = 9.022 Mq s^{-1}. Measuring this light source with the luminometer we can calculate that 1 RLU = 16.85 q.

If the measurement interval surpassed the measuring range of the luminometer (> 505.5 10^6 Mq s^{-1}) the machine overloaded, and a filter had to be used to dim the emitted light before arriving at the detector (Single photon counter, 370-630 nm). The neutral-density filters used had a transmittance of 1% and 0.1%, meaning they let respectively 1 or 0.1% of the light go through. Actual values of the filters are respectively 1.1% et 0.2%.

In addition, bioluminescence light wavelengths were measured with a spectrometer. Using KCl and freshwater the samples can only be stimulated once thus, if not a lot of tissue is available then the choice must be made to either use the luminometer or the spectrometer.

One sample from each class will be described in more detail

2.2.1 *Dytaster exilis*

A first whole specimen from the sample 56_127 was put into a recipient with freshwater and a picture was taken. A second specimen had 1 cm long pieces cut from the distal and proximal parts of the arm. Both where tested with KCl (200 mM). The arm extremity of a second specimen from the same sample was stimulated with freshwater.

2.2.2 *Psychropotes longicauda*

Two skin pieces of the caudal region were tested from the sample 56_111. Stimulation was done with freshwater and KCl (200 mM). The sample 67_101 was tested using a 1% filter. The first stimulation was done with freshwater the second with KCl (200 mM). The individual 90_111 had one piece tested with KCl (200 mM).

2.2.3 *Ophioplinthaca rudis*

A 1% filter was used. A first arm (a) from the sample 103_106 was taken and 2 cm long parts were cut from the distal and proximal regions. The stimulant used was KCl (200 mM). Two new arms were taken (b1, b2) and cut in three into distal, median and proximal parts (1 - 1.5 cm). All six pieces were tested with KCl (200 mM) and measurements lasted for 360 s except for b2 distal (180 s). Two last pieces (1 cm, 0.5 cm) from a fourth arm (c) were stimulated with ACh (222 µM). The second Ach trial was effectuated without filter.

2.2.4 Thalassometridae 69_148

A first measurement was done with 3 cm of an already spontaneously luminescent arm piece (a). The second measurement consisted on a second arm (b) stimulated with KCl. Then, two arms were taken (c, d) and 2 cm long parts from the distal and proximal regions were stimulated with freshwater. Subsequently, similar arm parts (e-h) from the same individual were taken and put into 1 ml seawater. The stimulation of these samples was done with adrenaline: out of a 1mg mL^{-1} stock solution 0.25, 0.5, 0.75 and 1 mL were taken and added to the arm pieces. Cirri and Calyx were tested with freshwater.

2.3 Histology

Only one individual per species was used for histological studies. When subsequently it is spoken of different samples for one species it means different parts of the same animal.

2.3.1 Decalcification

Decalcification of the crinoid tissues was performed through agitation in a 0.3 M NaCl solution with 2% ascorbic acid. Agitation lasted until the tissue was deemed soft which meant between 3 to 4 h. The tissues for the paraffin and semi-thin sections were all decalcified. For cryosection, decalcification was done on two thalassometrid (80_120) samples but only on one of the two *M.* cf. *aotearoa* samples and on none of the two *Stiremetra* samples.

2.3.2 Cryosections

For cryosection, tissues were cryoprotected with sucrose: 1 h in a 10% sucrose phosphate-buffer saline (PBS) solution, 1 h in a 20% sucrose PBS solution and then let overnight in a 30% sucrose PBS bath (approximately 15 h). The tissues were then transferred into a Cryomold (15 mm x 15 mm x 5 mm) covered in Cryomatrix (Thermo Fisher Scientific, Waltham, Massachusetts, U.S.A.) and frozen at -80°C. The 10 µm thin sections were cut with a Leica CM3050 S Research Cryostat (Leica Microsystems GmbH, Wetzlar, Germany) and mount on Superfrost Plus Microscope slides (Thermo Fisher Scientific). Cryosections were effectuated on *S. breviradia*, *M.* cf. *aotearoa*, the thalassometrid and *P. longicauda* "tail" tissues.

2.3.3 Paraffin sections

For paraffin section, the tissues were first put into a 70% ethanol bath for 24 h, followed by two 1 h baths in 90% ethanol and a 1 h bath in butanol after which the tissues were placed for 12 h in butanol inside a heat chamber at 56°C. Three paraffin (paraffin pastilles, Merck, Darmstadt, Germany) baths were effectuated: one 12 h, one 3 h and eventually one 1 h long bath. The paraffin with the tissue was then poured into a mould. The 10 µm thin sections were done with a Leica Biocut 2030 microtome (Leica Microsystems). Only *M.* cf. *aotearoa* was sectioned using this technique.

2.3.4 Semi-thin sections

For semi-thin section, the tissues were first placed in 3 successive 10 min sodium-cacodylate (0,2 M) and 1,84% NaCl rinsing baths, followed by a 1% osmium tetroxide, sodium-cacodylate (0,1 M) and 2,3% NaCl bath during 1 h before redoing the cacodylate baths and eventually using the above-described decalcification technique. Following decalcification, alcohol baths were used for dehydrating the tissue: 10 min in 25% ethanol, 10 min in 50% ethanol, 20 min in 70% ethanol, 2 times 15 min in 90% ethanol and 2 times 30 min in 100% ethanol. The resin used was a mixture of 10 g of vinylcyclohexene dioxide (ERL 4206), 6 g of DER 736 resin, 26 g nonenyl succinic anhydride and 0,4 g dimethyl amino ethanol. The resin was put into Eppendorfs and the samples were added. These Eppendorfs stayed open overnight and were then placed in a heat chamber during 24 h at 70°C. The sections were done with a Reichert 0mU2 ultramicrotome. This technique allowed us to do 1.5 µm thick sections. One tissue sample of *M.* cf. *aotearoa* (arm with pinnule) and one from the thalassometrid (arm with pinnule) were sectioned using this technique.

2.3.5 Fluorescent microscopy

Observations were done under a Leitz Diaplan Fluorescent Microscope (Leica Microsystems) with an epi-fluorescence 100 W mercury arc lamp used as a light source with a blue filter (420-490 nm). Pictures were taken with a ToupCam UCMOS Series C-mount USB2.0 CMOS Camera

(Hangzhou ToupTek Photonics, Zhejiang, China) associated to a FMAXXX 0,5 x 23,2 mm adapter (ToupTek) and the ToupView software (ToupTek).

2.3.6 Staining

Some cryosection slides were stained via an adapted Masson's Trichrome protocol. Briefly, cryomatrix was dissolved in a 4 min bath of distilled water; then, slides spend 1 min in fuchsine followed by two succeeding 1 min baths in 1% acetic acid water solutions. These were followed by one 4 min bath in orange G and one 4 min bath in fast green ensued by two more consecutive 1 min baths in 1% acetic acid water solutions.

Semi-thin section slides were stained by covering the slide with methylene blue for 1.5 min before rinsing with distilled water.

2.4 Luciferin & luciferase assays

Frozen thalassometrid 69_148 tissues (stored at -80°C) were used for performing coelenterazine and luciferase assays. About 1 cm long arm parts were collected for five coelenterazine replicates, mean weight 31.6 mg, and for seven luciferase replicates, mean weight 28.4 mg. The used arm parts came all from the distal to middle parts of the arm. Luminometry measurements lasted 190 s and were done with a FB12 tube luminometer (Berthold Detection Systems). All components of these experiments were kept on ice while preparing the solutions. The precise weights and volumes are in tables S2 and S3.

For the coelenterazine assay the arm parts were crushed with a small plastic pestle inside an Eppendorf filled with at least 200 µL of cold argon-saturated methanol depending of sample weight. With a syringe, 5 µL of the mixture were drawn and added to 195 µL Tris buffer (20 mM Tris, 0.5 M NaCl, pH 7.4) in a glass sample tube, vortexed and introduced into the *FB12* luminometer. 3 µL *RLuc* solution were added (20 mM Tris, 0.5 M NaCl, Bovine Serum Albumin (BSA) 0.1%) to 197 µL Tris buffer. The luciferase injection took place after 10 seconds of recording in order to have the luminometers base line.

For the luciferase assay the arm parts were crushed with a small plastic pestle inside an Eppendorf filled with at least 200 µL of Tris buffer (20 mM Tris, 0.5 M NaCl, pH 7.4) depending of the sample's weight. A first solution made of 5 µL of a $A_{430,1\ cm}$ 1.0 coelenterazine solution diluted in 995 µL methanol solution was done to create a 1/200 dilution. Then, 5 µL of the diluted solution were added to 195 µL Tris solution, vortexed and put into the *FB12* luminometer. After ten seconds of emission intensity recording, 10, 20 or 40 µL of the arm extract were added to 190, 180 or 160 µL Tris solution respectively. A 0,02% filter was used after the first test showed that the emission was overloading the luminometer.

The luminometry outputs were given in $RLUs^{-1}$. To transform them in Mq s^{-1}, a beta-light source was measured and the previously presented formula $I = 119{,}7e^{-0.056\,t}$ was used with t = 48.75 and I = 7.88 Mq s^{-1}. Thus, 1 RLU = 16,96 q.

To estimate the quantity of coelenterazine in the arm we calculated the total light emitted (L_{tot}) with the formula:

$$L_{tot}(q/g) = \frac{\text{Integral (RLU/s)} \cdot \text{Time (s)} \cdot \text{Filter value} \cdot \text{Calibration value(q/RLU)}}{\text{Weight (g)} \cdot \text{Dilution factor}}$$

Knowing that 1 ng of coelenterazine consumed by *RLuc* emits 252 Gq, we know that 1 Mq will be emitted by 3,968 10^{-6} ng coelenterazine. Thus, we can calculate the amount of coelenterazine in the crushed arm part.

To determine luciferase activity the mean maximal light emission value (L_{max}) between a 40 µL and a 20 µL and 10 µL extract solution from the same arm piece was taken. Mean activity was calculated using the formula:

$$\text{Activity}_{mean}(q/g \cdot s) = \frac{L_{max\,mean}\ (\text{RLU/s}) \cdot \text{Filter value} \cdot \text{Calibration value(q/RLU)}}{\text{Weight (g)} \cdot \text{Dilution factor}}$$

2.5 Data analysis

Data analysis and graphs were done with *R 3.5.3* and *RStudio version1.2.1335.*

2.5.1 Data frames

Two data frames were available for the animal samples. One contained the 956 non-echinoid echinoderms collected during the whole cruise (called the "IN2017_V03 echinoderms sample") and the other data frame contained all 119 samples tested on board (the "tested sample"). The tested sample is a sub-sample of "IN2017_V03".

One operation data set was at hand which contained start and end latitude, longitude and depth for every sampling operation as well as several other parameters like the equipment used, date, time, tow area, etc. (*Table S1*).

Due to its small size and inconsistent sampling, two categories were created to treat latitudinal distribution of the tested samples. The whole latitudinal gradient was categorized into "temperate" and "tropical" waters. The division of both was based on O'Hara et al. 2019's division of temperate and tropical waters at 34° South. The latitude considered to classify the samples to the specific categories was the operation's start latitude.

Three categories were created for the depth distribution to create bigger categories for the data analysis of the tested samples. During the cruise, operations were done at 3 different depths. These depths can be categorized into upper bathyal (actually between 932 and 2000 m but called "above 2000 m"), lower bathyal ("2000-3000 m") and abyssal ("under 3000m"). The depth considered to classify the samples to the specific categories was the operation's start depth.

Thanks to O'Hara et al., 2019, further environmental variables were added. Thus, Carbon flux (gC m^{-2} $year^{-1}$), oxygen (mL L^{-1}), temperature (°C) and salinity (‰) between the latitudes 23° and 43° South and between 100 and 4000 m depth were extracted (*Fig.S2*). O'Hara's measurements are given at every 100 m depth at all latitudinal degree. Start depth and start latitude were thus rounded accordingly to be designated to one of the measurements' latitude-depth coordinates. O'Hara's data represents the mean annual data for a study area between the 30th meridian E and the 90th meridian W putting the centre at 150° E which approximately corresponds to *IN2017_V03*'s longitudinal transect. The operations 1 and 2 were excluded because they are mid-water trials for the McKenna demersal fish trawl nets. Actual data collected during the cruise was not available. We validated this approach by comparing O'Hara's data to maps from Geoscience Australia (Australian Government).

The IN2017_V03 sample being far larger, we created new groups based on Commonwealth marine reserves (CMR) and operation depth. The purpose was to increase the precision on a latitudinal level. Each CMR was subdivided in the 3 previously described depth categories "above 2000 m", "2000 – 3000 m" and "under 3000 m" if samples were available.
Thereafter, the environmental data was grouped into these CMR-depth categories and means were taken for carbon flux, oxygen, temperature, and salinity. This new environmental dataset was standardized.

A Spearman correlation matrix was done to look for significant correlation between the environmental variables depth, latitude, longitude, carbon flux, oxygen, temperature and salinity (*Table S4*). The number of variables was reduced using the Escoufier's equivalent vectors method. This method finds the variables that are most correlated with the principal axes of a principal component analysis. Thus, the remaining variables were oxygen, carbon flux and temperature.

At our sampling depths carbon flux is slightly higher to the south but decreases importantly with depth. Oxygen varies greatly with latitude due to deep oxygenated waters from the Antarctic and low-oxygen shallower zone to the north. Temperature does not vary with latitude at these depths but does continuously decrease with depth.

A contingency table was created per dataset to annotate the number of individuals captured per species at each CMR-depth category. In order to avoid grouping all non-identified samples, the lower-most identified taxonomic level was associated with the operation number to create a different "species".

2.5.2 Proportions

The proportion of luminescent, non-luminescent and dubious light emitters was calculated for the total tested sample. Three categorical variables were used namely class to compare the four bioluminescent echinoderm classes, latitudinal zone to compare between tropical and temperate waters (division at 34° South) and depth zone to differentiate between upper bathyal, lower bathyal and abyssal zone (division at 2000 and 3000 meters). Ratios of blue to green emitters in the tested data set were also studied regarding depth and latitude.

Using the whole 1019 echinoderm samples collected during the *IN_V2017* cruise, the whole current knowledge on bioluminescent species was used to determine bioluminescent families

and genera. Species were logged as bioluminescent if there were literature accounts and/or the bioluminescence had been observed during the "Sampling the Abyss" cruise. Families and Genera were classified as bioluminescent if there were records of bioluminescent species inside them. The number of individuals per sample was used not the number of samples. This is more accurate and increases our sample size from 1019 to 12 465.

2.5.3 Chi-squared tests

Chi-squared tests were performed to compare the different zones and classes considering numbers of bioluminescent, dubious and non-luminescent samples. This was done to the tested samples. The IN2017_V03 data set was also tested once considering bioluminescent genera and once with the bioluminescent families. Here the categories were only bioluminescent and non-bioluminescent. In the case of a too small expected value (<5) the Monte Carlo method (with 2000 replicates) was used to simulate a distribution and thereby a p-value and avoid overestimating the Chi^2 statistic. For the 2x2 tests with the IN2017_V03 data set a Yate's correction was performed to prevent overestimation of the Chi^2 statistic.

Not enough is known about bioluminescence in echinoderms for counting whole families as bioluminescent. Therefore, the following models were only fitted on the individuals basing bioluminescence on belonging to a bioluminescent genus

2.5.4 Similarity profile

A similarity profile (SIMPROF) was calculated to create groups *a posteriori* based on the echinoderm communities in each CMR-depth group. The IN2017_V03 contingency table was used, transformed into a Bray-Curtis dissimilarity matrix between CMR-depth groups. The goal was to see if we were missing relations between animal communities because of our a priori categorisation of the data. New groups could mean unconsidered environmental variables. SIMPROFs were done on the whole data set as well as once individually on bioluminescent and non-bioluminescent genera.

2.5.5 General linear model on proportion

The proportion of samples from bioluminescent genera was calculated for each available CMR-depth group with the IN2017_V03 samples. We tried to fit a generalized linear model (GLM) on a binomial distribution using the variables carbon flux, oxygen and temperature.

Due to overdispersion of the samples we eventually used a quasi-binomial.

2.5.6 Models on Biodiversity indices

Abundance, Species Richness and Shannon diversity index *H* were calculated for the whole IN2017_V03 sample and for bioluminescent genera.

A GLM based on a Poisson distribution was performed on species richness with the variables oxygen, carbon flux and temperature on both total and bioluminescent IN2017_V03. Due to overdispersion, eventually a quasi-poisson distribution was used.

A linear model (LM) was fitted on the Shannon index with the variables carbon flux, oxygen and temperature on both total and bioluminescent IN2017_V03. Stepwise function with AIC criterion was applied. Normality was tested with a Shapiro-Wilk test and homoscedasticity was tested with Levene's test for homogeneity of variance.

3 Results

3.1 Organisms

3.1.1 Identification

Identification of the species remains inconclusive in a lot of cases (*Fig.10*). Thus, up to this date regarding the whole echinoderm sample, for the Asteroidea 50.67% (n=113) were identified until species level or recognized as new species, 34.08% (n=76) until genus, 10.31% (n=23) could be put into a family and 4.93% (n=11) were only identified as Asteroidea. The Holothuroidea samples are described until species level for 73.8% (n=262) samples, 6.2% (n=22) have only a genus assigned, 0.8% (n=3) only a family and 19.7% (n=70) could only be classified as holothuroids. There were 85.98% (n=282) of the Ophiuroidea samples identified until species level, 6.7% (n=22) until genus, 2.1% (n=7) down to the family and 5.18% (n=17) to the class. In crinoids out of the 50 samples 52% (n=26) are assigned to a species, 32% (n=16) to a family and 16% (n=8) are only assigned to Crinoidea.

In the tested Asteroidea, 17 species were identified, and 18 samples were not assigned to a species. Holothuroidea present 18 different species from which three are probable new species. In the tested ophiuroids we have 18 identified species plus six more different non-identified ones. In the tested crinoids we have three probably identified species plus three more unidentified species (currently at family level).

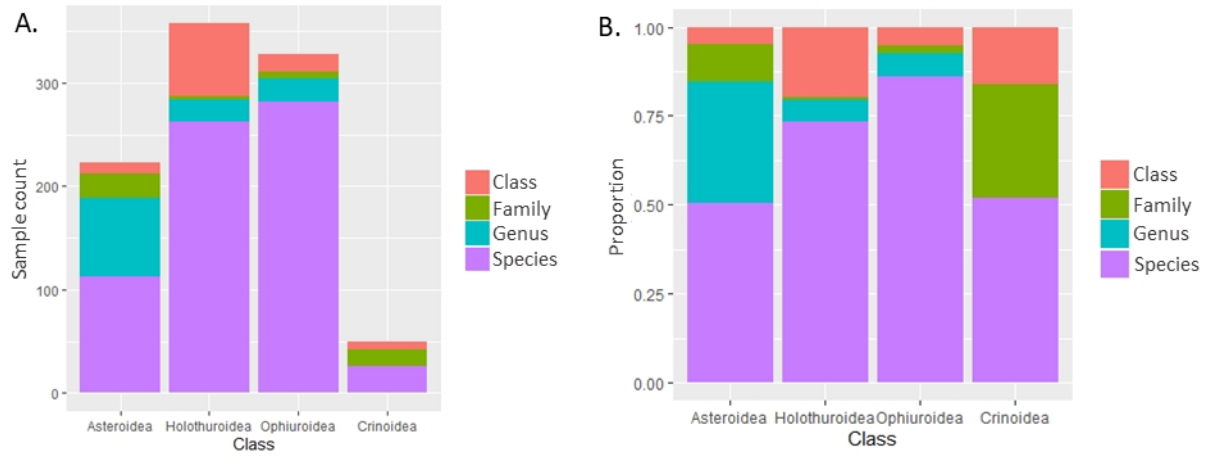

Figure 10. Bar charts representing the number of unidentified samples per echinoderm class. A. Sample count identified until species level (purple), genus (blue), family (green) and class (red). B. Proportion of samples identified down to species level (purple), genus (blue), family (green) and class (red).

3.1.2 Photography

Taken on the boat, pictures of *M.* cf. *aotearoa* and the thalassometrid while emitting light show rows of luminescent dots on the pinnules and arms (*Fig.11C*). The light emitted is blue. The size of the dots in *M.* cf. *aotearoa* is estimated around 0.2 mm with an approximate 0.4 mm interval between dots. The thalassometrid 69_148 also shows a dotted pattern but it

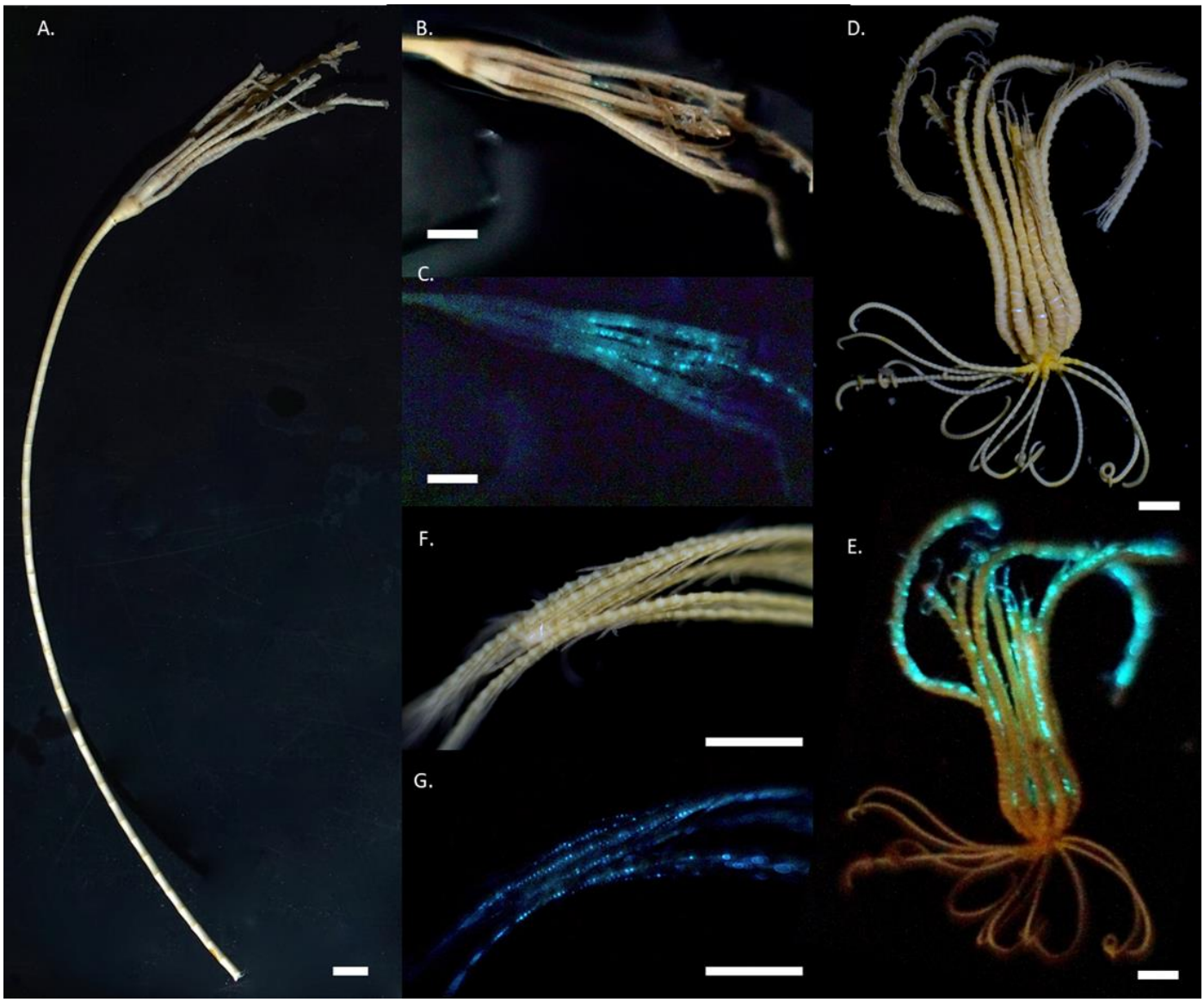

Figure 11. Monachocrinus cf. *aotearoa* (A, B, C), unidentified Thalassometridae 69-148 (D, E), unidentified Thalassometridae 80_120 (F, G). A. nearly whole animal with missing attachment plate and broken arms, B. calyx, arms and pinnules with light emitting dots visible on rays, D. same individual as B but in the dark, D. whole animal with some missing arm parts, E. same individual as D emitting light, F. arm tips and pinnules, G. same individual as F in the dark emitting light. White bars indicate 1 cm. © Jérôme Mallefet.

actually seems as would the whole interarticular section illuminate (*Fig.11E*). In the tested thalassometrid 80_120, the luminescent dots seem to be only on the pinnules and brighter at the base of the latter. Thus, on the pictures, dots are larger at the base (*Fig.11G*). Their size varies between 0.10 and 0.25 mm with interspaces generally about 0.3 mm wide.

Pictures of *P. longicauda* are blurry but still show that the animal is covered in blue dots (*Fig.12A*). We only see the dorsal right side of the animal. The tail seems mainly illuminated along the anteroposterior axis with rather dark sides. There do not seem to be brighter body parts except for the anterior brim regions.

The picture of *S. breviradia* shows that its bioluminescence is completely different than that of the crinoids photographed during the “Sampling the Abyss” cruise (*Fig.12D*). Indeed, the tested *Stiremetra* emits a diffuse green light at the height of the radials instead of rows of blue dots.

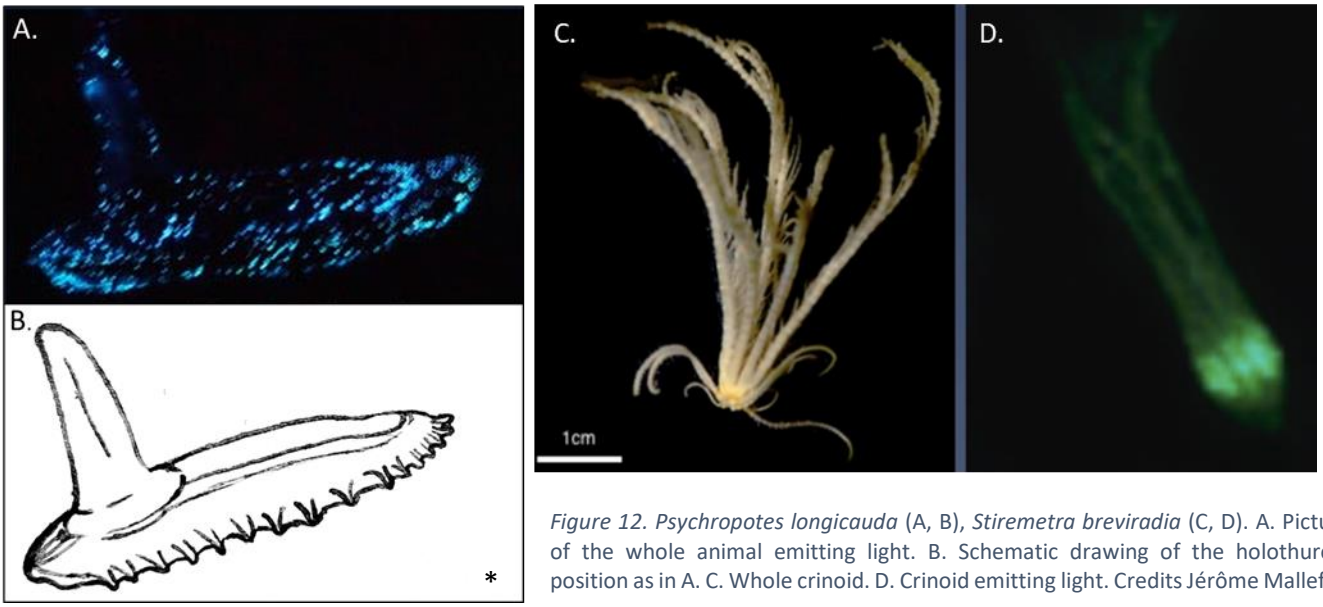

Figure 12. Psychropotes longicauda (A, B), *Stiremetra breviradia* (C, D). A. Picture of the whole animal emitting light. B. Schematic drawing of the holothuroid position as in A. C. Whole crinoid. D. Crinoid emitting light. Credits Jérôme Mallefet.

3.2 Luminometry

3.2.1 Species

Table 2 presents all the tested species for Asteroidea. At least 13 species are counted as bioluminescent. Two unidentified Astropectinidae (22_119; 35_128) were positively tested along with one completely unidentified Asteroidea (40_128). At least five Asteroidea species emitted green light namely *Plutonaster knoxi*, *Pl.* complexus, *Plutonaster* sp., *Dytaster exilis* and *D. pedicellaris*. This means all the bioluminescent Astropectinidae except for the not even to genus level identified samples (22_119; 35_128) - whose colour couldn't be determined - give off green light. Bioluminescent Benthopectinidae captured during this cruise are all blue emitters as do the genera *Freyella*, *Calyptraster*, *Hymenaster* and *Zoroaster*. All bioluminescent species emitted light when stimulated with KCl. Additionally, five species were counted as dubious emitters and 6 were categorized as non-bioluminescent.

The Holothuroidea species tested are presented in Table 3. At least 10 different species were positively tested. All observed bioluminescent species were described as emitting blue wavelengths except for the new *Molpadia* species whose colour was not determined. KCl was able to initiate light emission whenever it was used. Three further species were tested but did not emit light following stimulation and for two species the emission is uncertain.

The tested Ophiuroidea samples are presented in Table 4. In four species we doubt the ability to emit light. The number of species that did not give any light emission on their own or as a response to external stimulation elevates to 11. With only 8 species, Ophiuroidea is the only clade with less bioluminescent than non-bioluminescent species. For the three species of Ophiocanthidae the light emitted was estimated as being green and for three species (*O.glabrum*, *O.paucispina*, *Ophiotoma* sp.) it was marked as blue. KCl was able to stimulate all

as bioluminescent identified species. Acetylcholine was used positively to stimulate *Ophioplinthaca rudis*.

The criniod species tested are all in Table 5. No species was deemed dubious but two out of five were clear non-emitters. Conversely, bioluminescence was recorded for probably three species. *M.* cf. *aotearoa* and both thalassometrids emit blue light. For all three, the emission was verified by luminometry following KCl and freshwater as well as through spontaneous light emission. Adrenaline was successfully used to stimulate the thalassometrid 69_148.

Table 2. Tested Asteroidea species with their families and sample code. The colour column indicates the colour in which the species seemingly emits light.

Bioluminescent		colour	**Dubious**		**Non-bioluminescent**	
	40_128		Astropectinidae	*Proserpinaster neozelanicus* (14_116)	Astropectinidae	Psilaster acuminatus (128_108)
Asteriidae	*Coronaster reticulatus* (122_104)			*Proserpinaster* sp. (69_138)	Goniasteridae	Bathyceramaster sp. (115_105)
Astropectinidae	*Dytaster exilis* (44_119; 56_127)		Odontasteridae	*Hoplaster kupe* (14_109; 70_115)	Porcellanasteridae	*Porcellanaster ceruleus* (14_117; 22_114; 56_160)
	Dytaster pedicellaris (115_103)		Pterasteridae	*Hymenaster carnosus* (14_101)		*Porcellanaster crassus* (22_116; 22_115)
	Plutonaster complexus (14_114; 56_155)		Zoroasteridae	*Zoroaster barathri* (22_129; 22_106; 56_129; 56_167; 70_128; 80_129)		*Porcellanaster inermis* (14_110; 22_117)
	Plutonaster knoxi (22_118;88_103; 104_103; 128_106)				Solasteridae	*Crossaster multispinus* (69_145)
	Plutonaster sp. (56_159)					
	22_119; 35_128					
Benthopectinidae	*Benthopecten* sp. (14_115; 44_125))					
	Cheiraster sp. (69_144; 100_129; 128_109)					
Freyellidae	*Freyella* sp. (78_103; 109_105; 109_107; 109_102					
Pterasteridae	*Calyptraster gracilis* (56_128)					
	Calyptraster sp. (35_171; 69_144; 100_127)					
	Hymenaster nobilis (128_105)					
Zoroasteridae	*Zoroaster microporus* (104_128; 115_108)					

Table 3. Tested Holothuroidea species with their families and sample code. The colour column indicates the colour in which the species seemingly emits light.

Bioluminescent		colour	**Dubious**		**Non-bioluminescent**	
Elpidiidae	*Achlyonice ecalcarea* (53_101)		Deimatidae	*Oneirophanta mutabilis* (56_135; 128_104)	Cucumariidae	*Abyssocucumis abyssorum* (44_130; 56_146)
	Amperima furcate (35_119)		Molpadiidae	*Molpadia* cf *musculus* (53_112)	Synaptidae	*Protankyra brychia* (53_115)
	Peniagone azorica (90_110)				Ypsilothuriidae	*Echinocucumis ampla* (44_130)
Psychropotidae	*Benthodytes* sp. nov. 1 (22_107; 22_112; 56_142; 56_143)					
	Benthodytes sp. nov. 2 (35_173; 78_102; 90_102)					
	Psychropotes depressa (56_150; 67_101)					
	Psychropotes longicauda (56_111; 90_111)					
	Psychropotes scotiae (44_105)					
Molpadiidae	*Molpadia* sp. nov. (53_113, 53_104)					
Synallactidae	*Synallactes* cf. *crucifera* (90_106)					

Table 4. Tested Ophiuroidea species with their families and sample code. The colour column indicates the colour in which the species seemingly emits light.

Bioluminescent		colour	**Dubious**		**Non-bioluminescent**	
Amphiuridae	*Amphiura* sp. (13_112)		Ophiocamacidae	*Ophiocamax applicatus* (69_141)		35_0a; 35_0b (both on seapens)
Ophiocanthidae	*Ophiocantha sollicita* (6_139)		Ophiodermatidae	*Bathypectinura heros* (128_107)	Amphiuridae	*Amphioplus verrilli* (53_118)
	Ophiophthalmus relictus (13_109)		Ophiopyrgidae	*Amphiophiura paraconcava* (122_109; 128_110; 115_104)		*Amphioplus (Unioplus) daleus* (6_105)
	Ophioplinthaca rudis (69_139; 80_125; 103_106)		Ophiuridae	*Ophiocten hastatum* (14_130)	Asteronychidae	*Astrodia tenuispina* (122_113)
Ophiopyrgidae	*Aspidophiura* sp. (100_126)				Ophiactidae	*Ophiactis amator* (6_136; 11_109)
Ophiosphalmidae	*Ophiosphalma glabrum* (122_106; 122_105)					*Ophioactis abyssicola* (13_113)
Ophiotomidae	*Ophiotoma paucispina* (6_137)					*Ophioactis* sp. (13_104)
	Ophiotoma sp. (6_138)				Ophiosphalmidae	*Ophiosphalma armigerum* (6_136; 11_121; 42_102)
					Ophiuridae	*Ophiura clemens* (103_105)
						Ophiura flagellata (13_111; 80_124)
						Ophiura fluctuans (69_147)

Table 5. Tested Crinoidea species with their families and sample code. The colour column indicates the colour in which the species seemingly emits light.

Bioluminescent		colour	Dubious		Non-bioluminescent	
Atelecrinidae	*Adelatelecrinus* cf. *vallatus* (80_121)				Bathycrinidae	86_110
Bathycrinidae	*Monachocrinus* cf. *aotearoa* (56_107)				Rhizocrinidae	*Democrinus* cf. *japonicus* (69_146)
Thalassometridae	69_148; 80_120					

3.2.2 Emission intensity curves

Table S5 summarizes all results for the here presented samples.

Between asteroid taxa that emitted most light we find several unidentified Astropectinidae that cause overload of the luminometer as well as *Calyptraster sp.* and *Dytaster exilis* that both achieve maximal intensities of over 250 Mq s^{-1} when stimulating the whole animal. Proximal and distal arm parts of *D. exilis* were successfully stimulated with KCl and peak height attained 8.9 Mq s^{-1}, proximally and 3.2 Mq s^{-1}, distally (*Fig.13*). The sole arm tip tested with freshwater produced nevertheless a peak height of 5.4 Mq s^{-1} and had a total light emission of 3.67 Mq in 3 minutes compared to 105.5 Mq in 3 min for the distal KCl test (*Fig.13*).

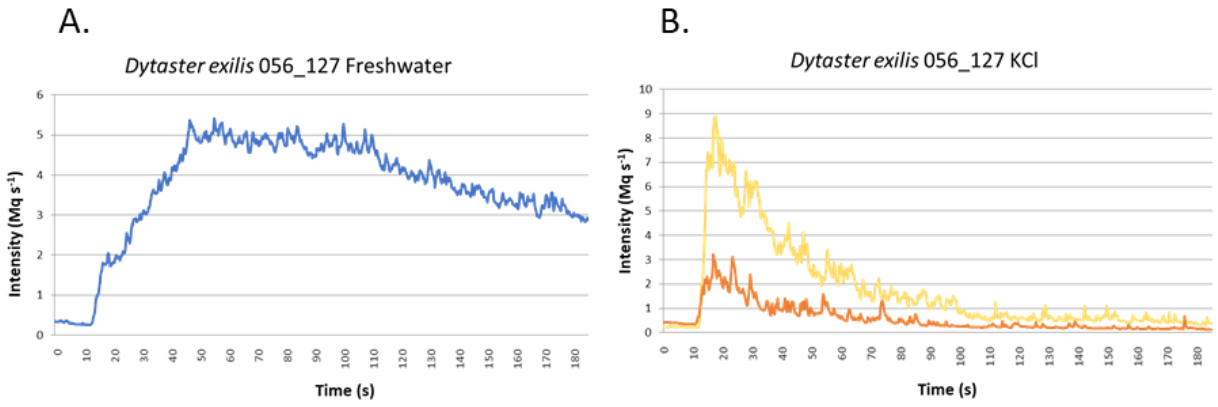

Figure 13. Dytaster exilis (56_127) luminometer measurements. A. Emission intensity of freshwater stimulation of a distal arm piece. B. Emission intensity after KCl stimulation of a distal (orange) and proximal (yellow) arm piece.

Biggest light emitters in Holothuroidea were among others *Psychropotes depressa* and the genus *Peniagone*, both causing overloads. While KCl testing did not give a respons in 56_111, 90_111 gave a light response and 67_101 had a maximun emission of 63.1 Mq s^{-1} (*Fig.14A*). Freshwater exposure gave very good responses with 17,2 Mq s^{-1} in 56_111 and 4 036 Mq s^{-1} in 67_101 (*Fig.14B*).

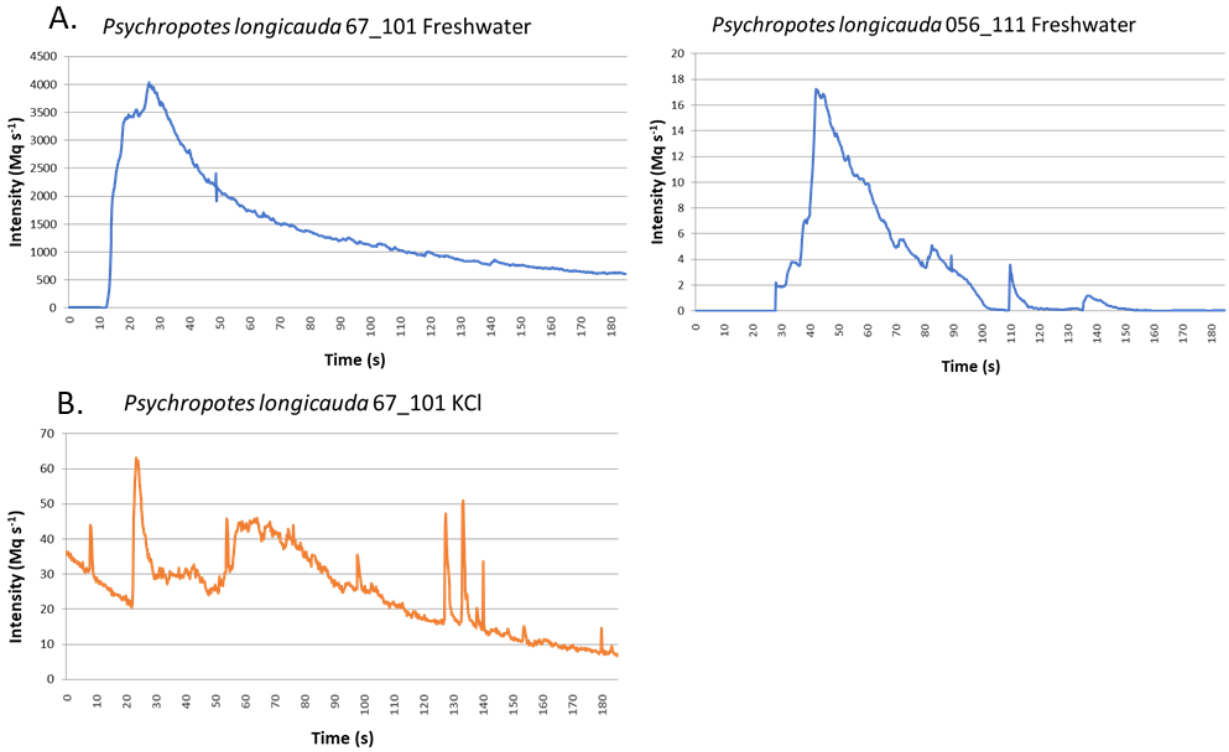

Figure 14. Psychropotes longicauda luminometer measurements. A. Emission intensity after freshwater stimulation of caudal skin pieces from two different individuals (67_101, 56_111). B. Emission intensity from KCl stimulated caudal skin piece from individual (67_101).

In Ophiuroidea, *Ophiophthalmus relictus*, *Ophioplinthaca rudis* and *Ophiacantha sollicita* overloaded the machine and spontaneously had peaks over 160 Mq s^{-1}. Sitmulating with KCl, maximal intensities of 20 000 Mq s^{-1} were attained with the distal part of the arms. The results of the arms a,b1 and b2 show us that there is an intensity gradient along the arm with the tips being by far more luminescent than the central and proximal parts that do not exceed emissions of 14 000 Mq s^{-1} and seem rather variable in their response (*Fig.15*). Effectively in b1 the median piece produces a peak of 13 Gq and the proximal only 4 Gq albeit b2's median region produced 5 Gq and the proximal piece 9 Gq. Let's note that in most KCl stimulation tests we obtain a bimodal curve with a first smaller shoulder approximately 10-20 s after injection. Acetylcholine stimulation seems to have been able to trigger light emission in at least one of the two pieces of the arm c even though both curves seem strange and are low. Nevertheless, c1 produces about 49 Mq in 180 s. The arm c2 produces a very late peak even if injection happened at 60 s instead of 10 s (*Fig.16*).

The cirri and calyx from the thalassometrid emit only very weakly with peaks at 1.3 and 0.2 Mq s^{-1} respectively. As seen in figure 17, both curves are completely different with the cirri emitting three separate peaks and the calyx' emission being relatively constant in time. Arms c and d present opposite results thus, a gradient along the arm cannot been vetted (*Fig.17*). Regarding adrenaline stimulation we do see a tendency for an increased light emission with adrenaline concentration (*Fig.18*). However, the first three concentration are close together. Specially, the curve f creates a discontinuity with a very low integral (0.67 Mq s^{-1}) and a very high peak (5.15 Mq s^{-1}) (*Fig.18B*). Let's note that one of the thalassometrids 80_120's arms achieved a peak of 151.6 Mq s^{-1} after KCl stimulation while 69_148's highest peak is 91.4 Mq s^{-1} (with freshwater) and only made a peak of 1.1 Mq s^{-1} with KCl (arm b) (*Fig.17)*.

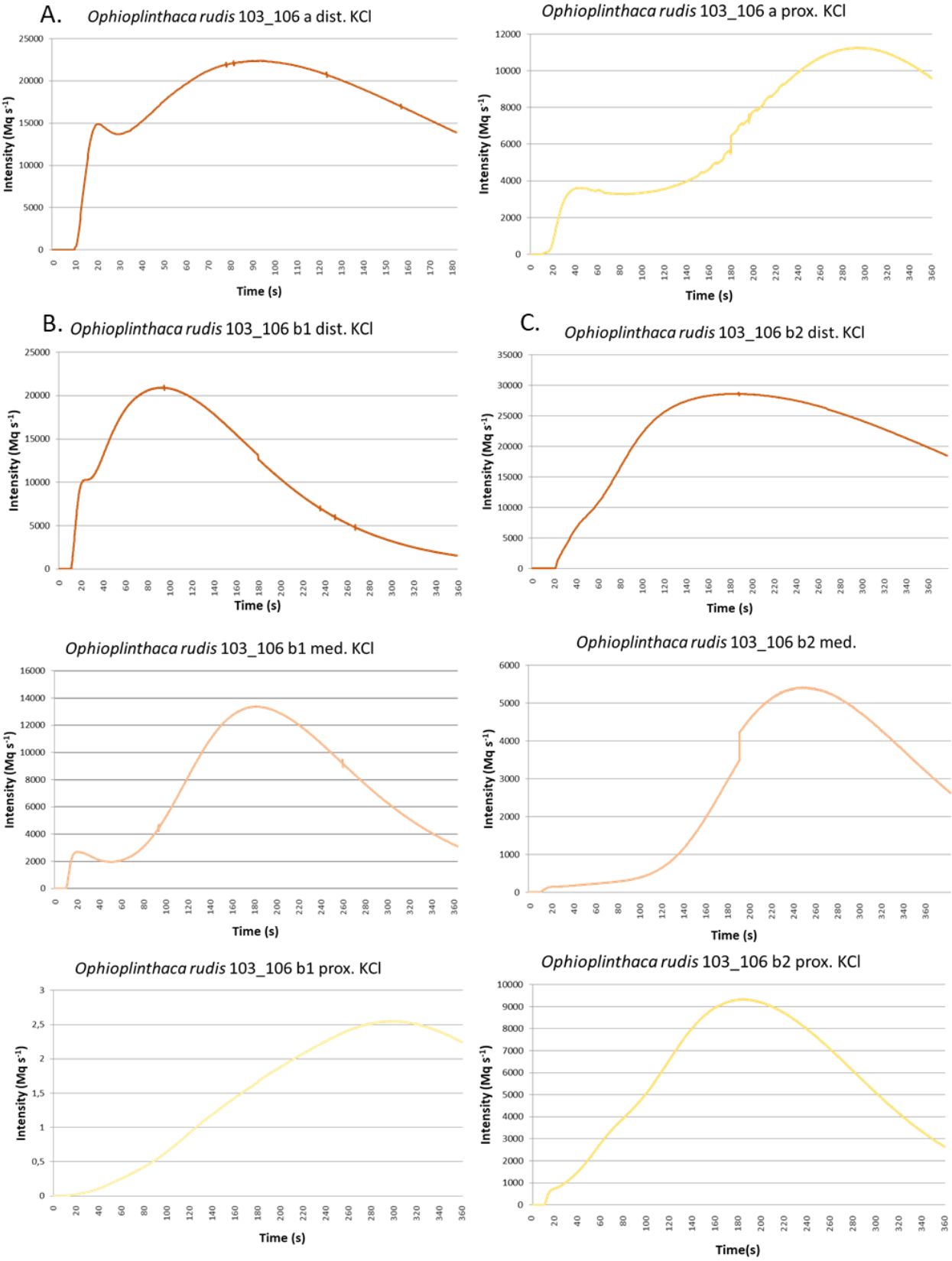

Figure 15. Ophioplinthaca rudis (103_106) luminometer measurements. A. Emission intensity after KCl stimulation of distal (ochre) and proximal (yellow) parts of arm a. B. Emission intensity after KCl stimulation of distal (ochre), median (orange) and proximal (yellow) parts of arm b1. C. Emission intensity after KCl stimulation of distal (ochre), median (orange) and proximal (yellow) parts of arm b2.

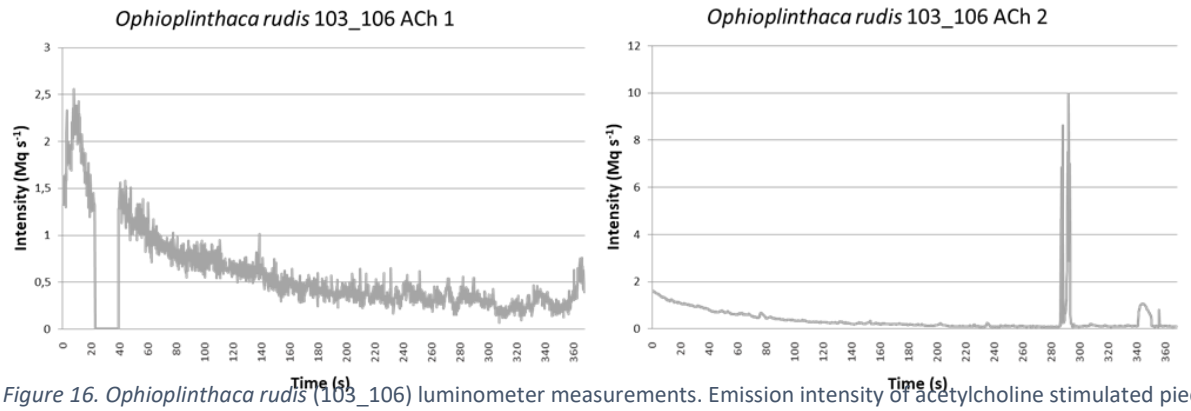

Figure 16. Ophioplinthaca rudis (103_106) luminometer measurements. Emission intensity of acetylcholine stimulated pieces from arm c.

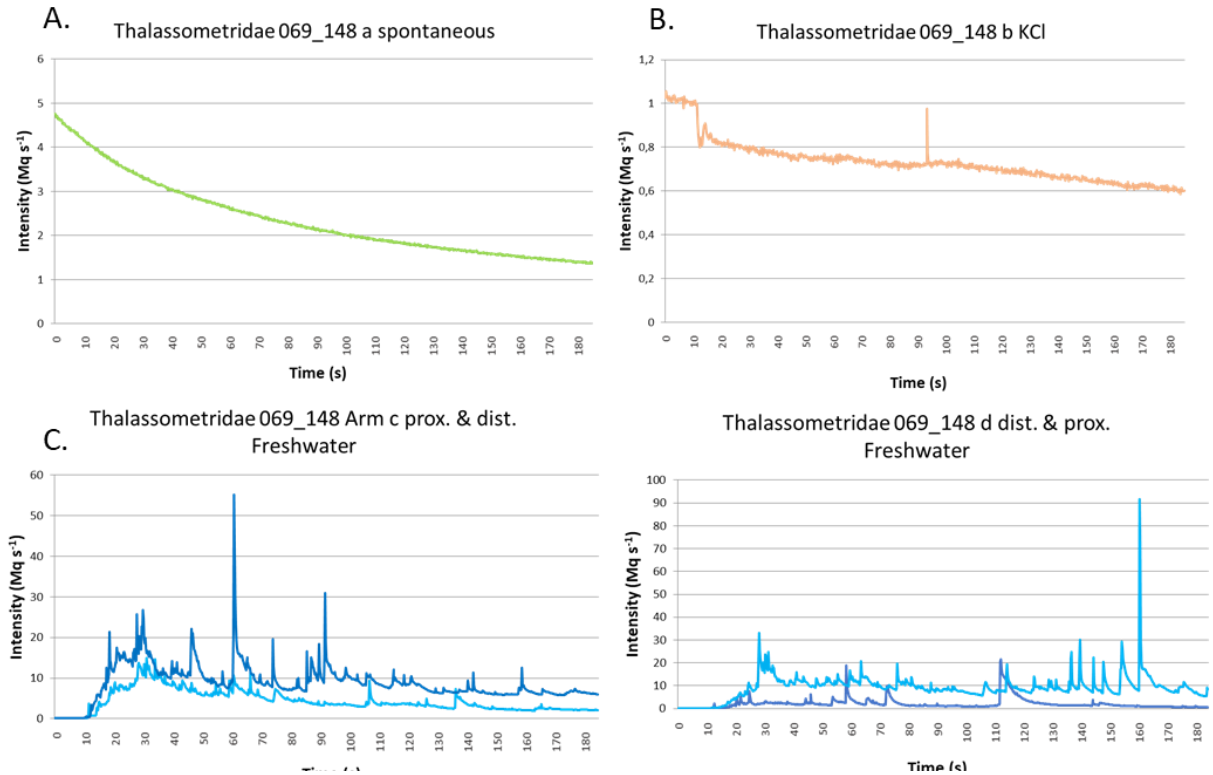

Figure 17. Thalassometrid 69_148 luminometer measurements. A. Spontaneous emission from arm a. B. Emission intensity from the with KCl stimulated arm b. C. Emission intensity of freshwater stimulated arms c and d. Distal (blue) and proximal (light blue) pieces were tested on both arms. D. Emission intensity from the with freshwater stimulated cirri. E. Emission intensity from the with freshwater stimulated calyx.

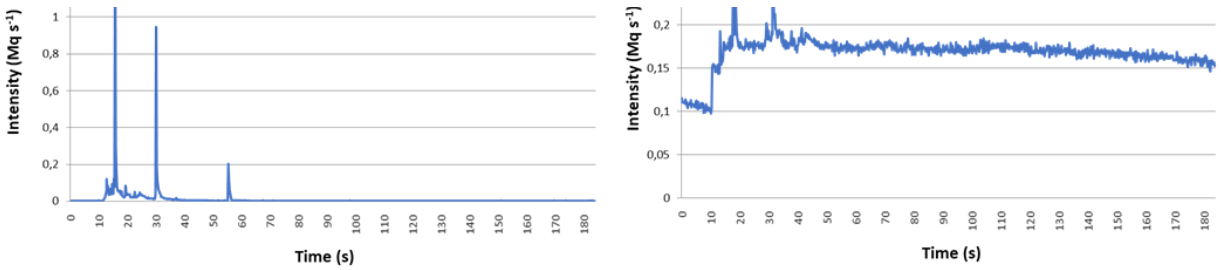

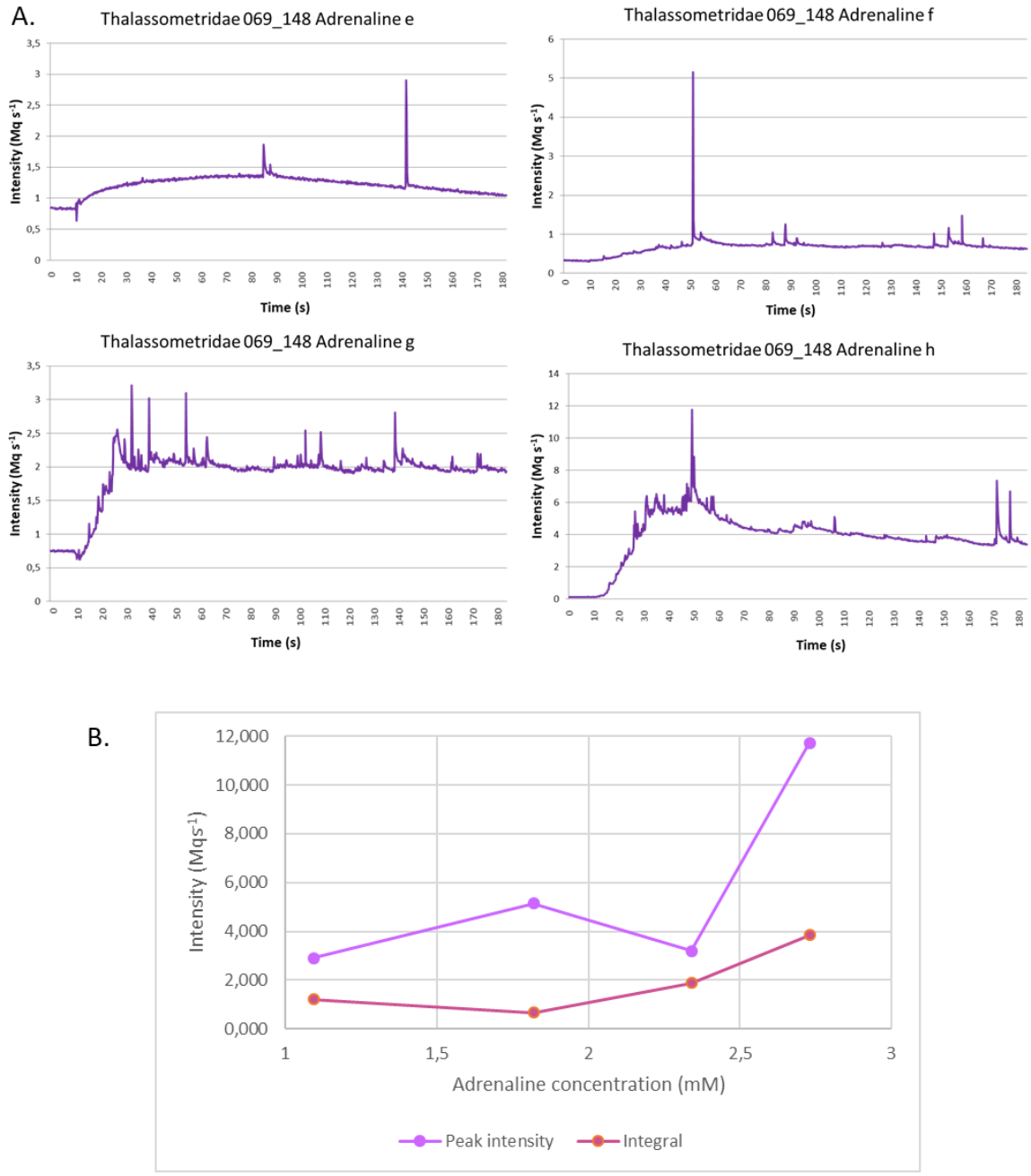

Figure 18. Thalassometrid 69_148 luminometer measurements. A. Emission intensity from adrenaline stimulated arm pieces. Adrenaline concentration (C) increases from e to h. C_e =1.092 mM, C_f =1.819 mM, C_g =2.339 mM, C_h =2.729 mM. B. variation of peak intensity and integral with C.

3.3 Histology

3.3.1 Crinoidea

The transversal, coronal and sagittal cryosections through pinnules and arms of *Stiremetra breviradia* revealed the classical arm structure of comatulid crinoids: a thin epithelium left floating above the underneath lying brachials, movable articulations with ventral muscle and dorsal ligament (MCT) bundles linking the brachial skeletal pieces, coelomic cavities, a nerve that runs all along the centre of the arm and an ambulacral groove with tube feet (*Fig.19A, D*). The same structures were observed with the cryosections of the Thalassometridae 80_120 and *Monachocrinus* cf. *aotearoa* (*Fig.19B*). In the latter, developing gonads were observable in the pinnules which suggests that our arm pieces are rather proximal to the calyx (*Fig.19C*) (Heinzeller and Welsch, 1994).

Saccules were observed all along the ventral side of the arms and pinnules in all three species, but their presence is rather low in *Stiremetra*. In *Monachocrinus* cf. *aotearoa* we have two or three sacculi between arm articulations and one or two sacculi between pinnule articulations (*Fig19B, E*). We find sacculi on the arm, near the pinnule bifurcation and on the pinnules where saccules zigzag on the proximal part before forming a line (*Fig.19E*). On the pinnules of the thalassometrid, we observed one sacculi per pinnular forming a row all along the pinnule, while on the arm we found mostly one sacculi around the articulation (*Fig.19F*).

Epifluorescence observations on the whole animal and in sections show that the saccules are fluorescent (*Fig.19D, E, F, H*). Their fluorescence, on the arms and on the pinnules, stands out compared to the surrounding epifluorescence from the other parts of the animal in *M.* cf. *aotearoa* and in the thalassometrid but not in *S. breviradia*. The sacculi of *M.* cf. *aotearoa* differ in size but they tend to lay between 0.15 and 0.2 mm long, with seemingly no size difference between arm and pinnule saccules. Spaces in-between are 0.35 mm to 0.5 mm wide. Sometimes agglomerations of two or three saccules are visible (*Fig.19G*). The tested thalassometrid has smaller saccules on the pinnules (~0.09 mm) compared to those on its arms (~0.12 mm). The mean interspaces are 0.38 mm on the pinnules and 0.34 mm on the arm. A closer look to some saccules shows different granulation of their content. What seems darker under the light microscope is brighter under stimulation (*Fig.19G, H*).

3.3.2 Holothuroidea

In *Psychropotes longicauda*, sub-epithelial granular cells were found. These are brighter than their surrounding and their fluorescence colour differs from the epithelium and the cells laying deeper in the connective tissue. These fluorescent cells are distributed from directly underneath the epithelium to about 0.8 mm with some cells being even found deeper but not under 1 mm into the connective tissue. The largest have a size of some 80 µm and the smaller still as granular cell recognizable ones lay around 30 µm. Larger fluorescent masses (0.6 mm) were observed in which individual cells are not recognizable. Still, the colour in which they fluoresce also seems similar albeit in some of them the granulations are bigger than the granulation of the former.

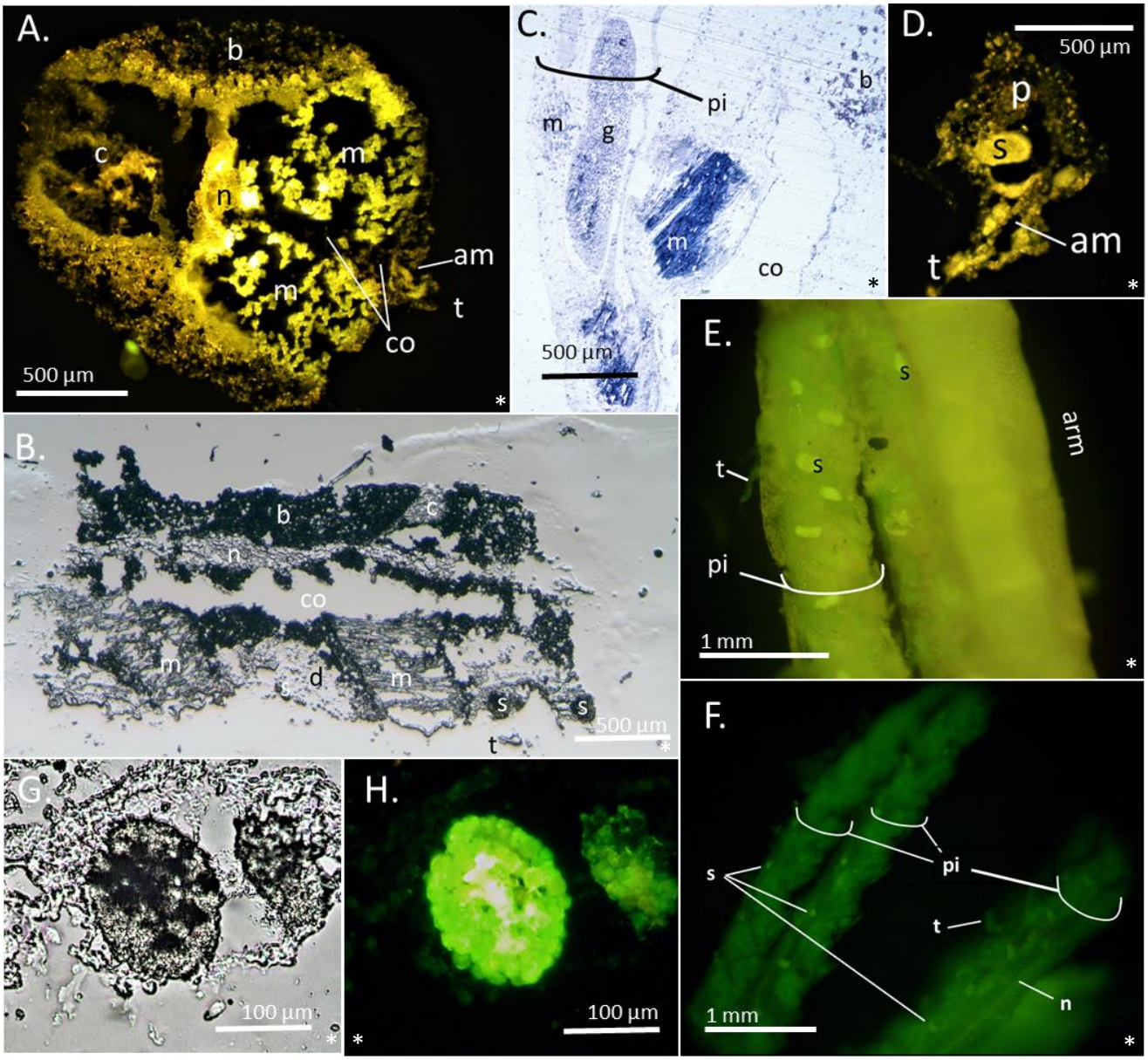

Figure 19. Stiremetra breviradia (A,D), *Monachocrinus* cf. *Aotearoa* (B,C,E,G,H), Thalassometridae 80_120 (F). A. Transversal cryosection into an arm at the height of a muscular synarthry under blue light stimulation. B. Sagittal cryosection of an arm unstained. C. Semi-thin section at the height of a pinnule insertion. Stained with methylene blue. D. Cryosection into a pinnule under blue light stimulation. E. *In toto* observation of arm and pinnule under blue light stimulation. F. *In toto* observation of pinnules under blue light stimulation. G. Sagittal cryosection into a saccule. Unstained. H. Saccule seen in G under blue light stimulation. am: ambulacral groove, b: brachial, c: connective tissue, co: coelomic space, d: dermis, g: gonad, m: muscle, n: nerve, p: pinnular, pi: pinnule, s: saccule, t: tentacle.

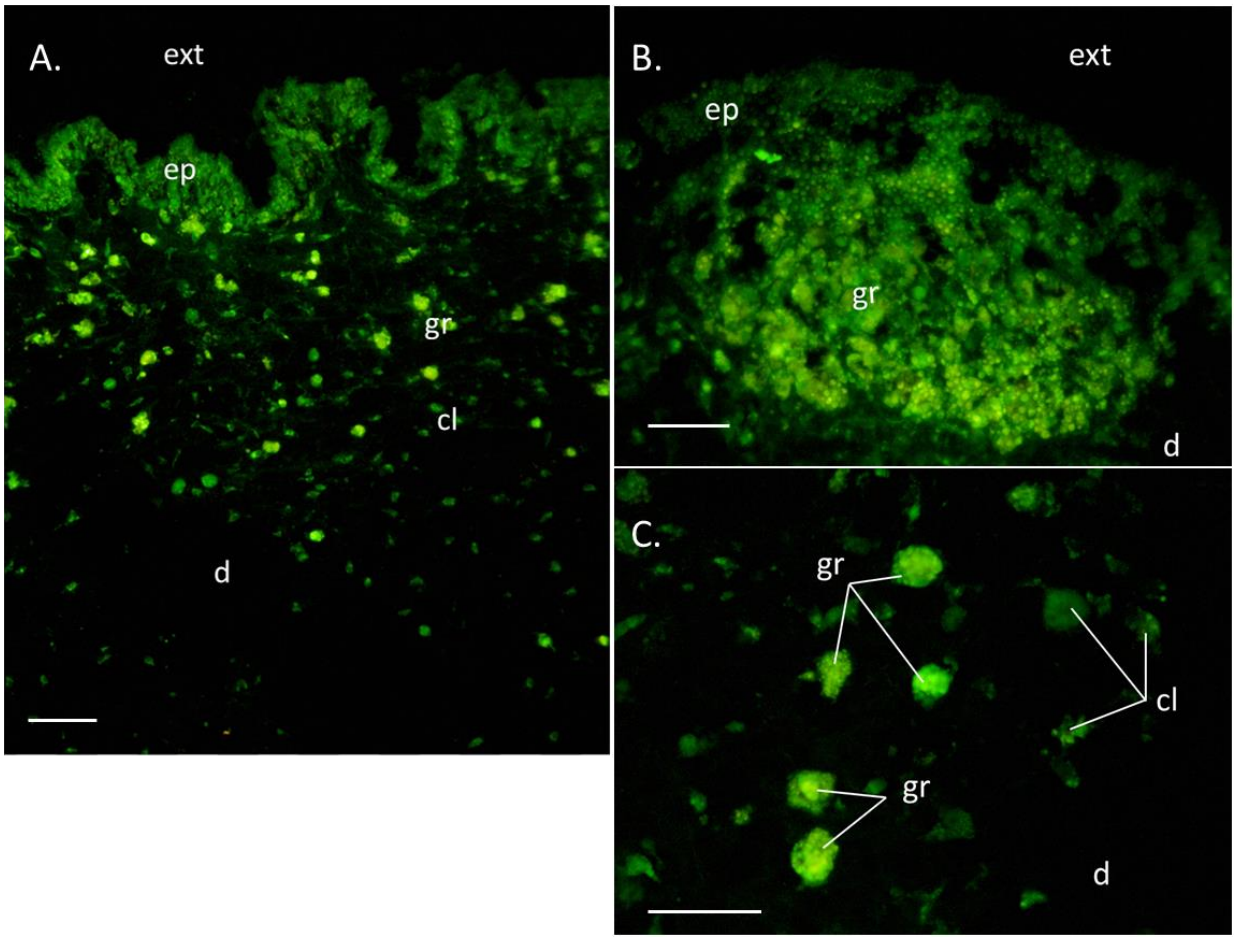

Figure 20. Psychropotes longicauda cryosection of tail skin. A. Section into the dermis showing the epithelium and the layer containing granular cells underneath B. Fluorescent mass with undistinguishable individual cells a big granulation C. Close up of the granular cells. ep: epithelium, cl: connective tissue cells, ext: exterior of the animal d: dermis, gr: granular cells. Bar represent 100 µm.

3.4 Luciferin and luciferase assays

Effectively, mixing *RLuc* with our crushed thalassometrid did induce light emission as did the addition of coelenterazine to it.

The following results should all be considered as minimum values because the amounts of coelenterazine and luciferase may diminish during storage even while frozen. Imidazolpyrazines are unstable, photolabile molecules that can easily autoxidize (Campbell and Herring, 1990). Around 80% can be lost overnight while kept in methanol at -20°C (Campbell and Herring, 1990).

Tables 14 and 15 report all the measurements made.

Per arm weight, coelenterazine assay results are 0.01 nmol g^{-1} with an average deviation from the mean of 0.0027 nmol g^{-1}. Luciferase activity's result mean is 4.53 10^{12} q $s^{-1}g^{-1}$ with an average deviation from the mean of 1.49 10^{12} q $s^{-1}g^{-1}$.

3.5 Data analysis

3.5.1 Proportions

From de total 119 samples tested for bioluminescence, 53.8% (n=64) are bioluminescent animals, for 18.5% the emission is dubious (n=22), and in 27.7% (n=33) of the cases we can be sure that there was no emission.

Samples were sometimes not available in enough quantities as to test both emission intensity and colour, therefore, for 6 species no colour was reported. Hence, in total, for 29.4% of the samples (n=35) light emitted was deemed as blue and for 10.1% (n=12) as green.

Our samples come to 26 % (n=31) come from above 2000 m depth, 56.3% (n=67) were collected between 2000 and 3000 m depth while only 17.7 % (n=21) come from waters deeper than 3000 m. Figure 21A indicates the proportions of light emission for each depth group. Above 2000 m, 54.8% (n=17) of the samples are bioluminescent, 19.4% (n=6) are dubious and 25.8% (n=8) are non-luminescent (*Fig.21A*). Between 2000 and 3000 m depth 50.7% (n=34) of the samples are bioluminescent, 22.4% (n=15) are dubious light emitters and 26.9% (n=18) are non-bioluminescent. Under 3000 m, 61.9% (n=13) are bioluminescent, 4.8% (n=1) are dubious emitters and 33.3% (n=7) don't emit light. The blue/green ratio is above 3 to 1 underneath 2000 m (3.5 under 3000 m; 3.3 between 2000 and 3000 m). Above 2000 the ratio is 1.7 blue emitters for every green emitter.

By dividing our sample in two latitudinal zones, we have 44,53% (n=53) from tropical waters and 55.47% (n=66) from temperate latitudes. Figure 21B indicates the proportions of light emission categories for each latitudinal group. In the tropical latitudes 62.2% of the samples emit light (n=33), for 20.8% the bioluminescence is dubious (n=11) and in 17% of the samples no luminescence was observed (n=9). In temperate waters 47% (n=31) are bioluminescent, only 16.7% are dubious (n=11) and 36.3% (n=24) of the samples did not emit any light. In both zones the blue/green ratio stays around 3 to 1 (3.2 and 2.7).

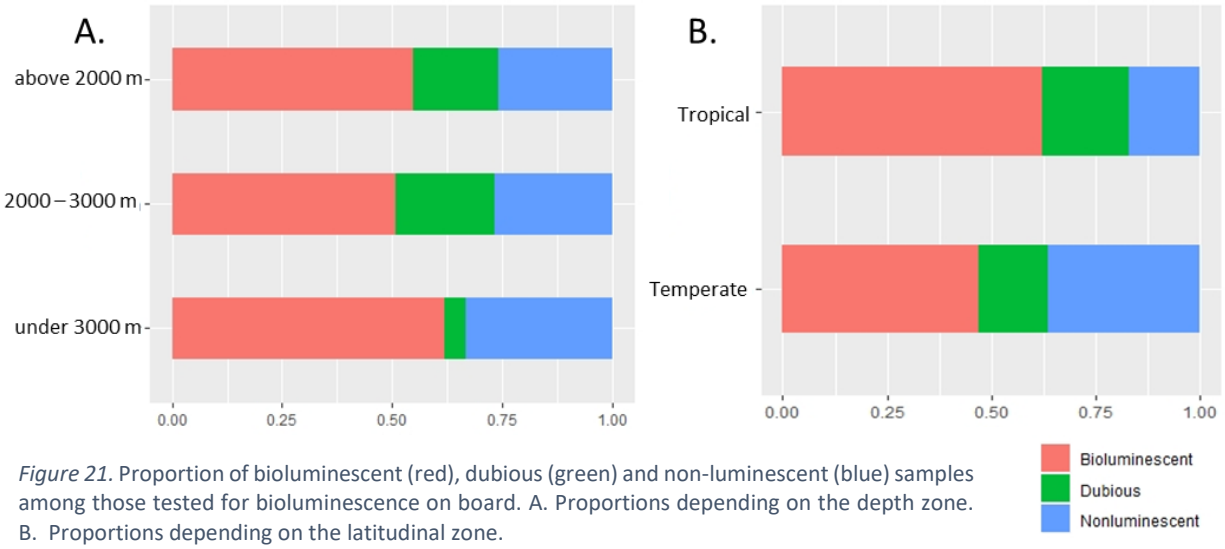

Figure 21. Proportion of bioluminescent (red), dubious (green) and non-luminescent (blue) samples among those tested for bioluminescence on board. A. Proportions depending on the depth zone. B. Proportions depending on the latitudinal zone.

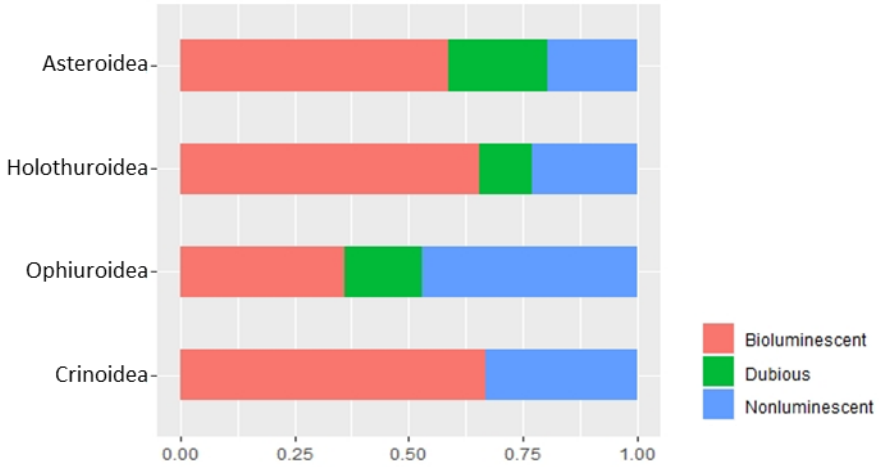

Figure 22. Proportion of bioluminescent (red), dubious (green) and non-luminescent (blue) samples per echinoderm class among those tested for bioluminescence on board. As of today, the clade Echinoidea is completely non-luminescent.

The same data set can be subdivided into classes (*Fig.22*). Doing this we obtain 58.82% (n=30) luminescent, 21.57% (n=11) dubious and 19.61% (n=10) non-luminescent Asteroidea. In Holothuroidea, 65.38% (n=17) emit light, 11.54% (n=3) are dubious and 23.08% (n=6) are non-light-emitters. The percentage of luminescent brittle stars lays at 36.1% (n=13) while 16.7% (n=6) are dubious and 47.2% (n=17) are non-luminescent ophiuroids. Percentages of light-emitting Crinoidea is 66.67% (n=4) and 33.33% (n=2) are non-bioluminescent.

The total IN2017_V03 sample presents 41% (n=5162) samples from bioluminescent genera and 59% (n=7303) from non-bioluminescent genera. Considering latitude, 74% (n=9241) come from waters south from the 34th parallel and 26% (n=3224) from northern waters. Depth zones also strongly differ in the number of samples namely 35% (n=4416) are from the upper bathyal, 58% (n=7193) from the lower bathyal, and only 7% (n=856) from abyssal waters. Also, samples come mostly from Ophiuroidea with 73% (n=9192), followed by Holothuroidea with 16% (n=1948) of the samples and Asteroidea, 7% (n=832), and Crinoidea, only 4% (n=493).

With this sample not only Ophiuroidea have less individuals from bioluminescent genera but also Holothuroidea.
When putting all the echinoderms together, bioluminescence decreases with depth and towards the South. However, Holothuroidea have more bioluminescent samples in temperate waters. Also, only Crinoidea show a decrease in samples from bioluminescence genera with depth. Holothuroidea show an increase in the lower bathyal followed by a decrease in deeper waters, Asterozoa, in the contrary, show first a decrease and then an increase in bathyal waters (*Fig.23*).

3.5.2 Chi-squared tests

Chi-squared test on the tested samples comparing both latitudinal zones gave a p-value of 0.063. Therefore, the null hypothesis that states that both zones are equal could cautiously be rejected. The chi-squared test between waters above 2000 meters and waters between 2000 and 3000 meters produced a p-value of 0.92 by which we concluded that they do not differ. While comparing both upper layers with the deepest, in both cases we do not reject

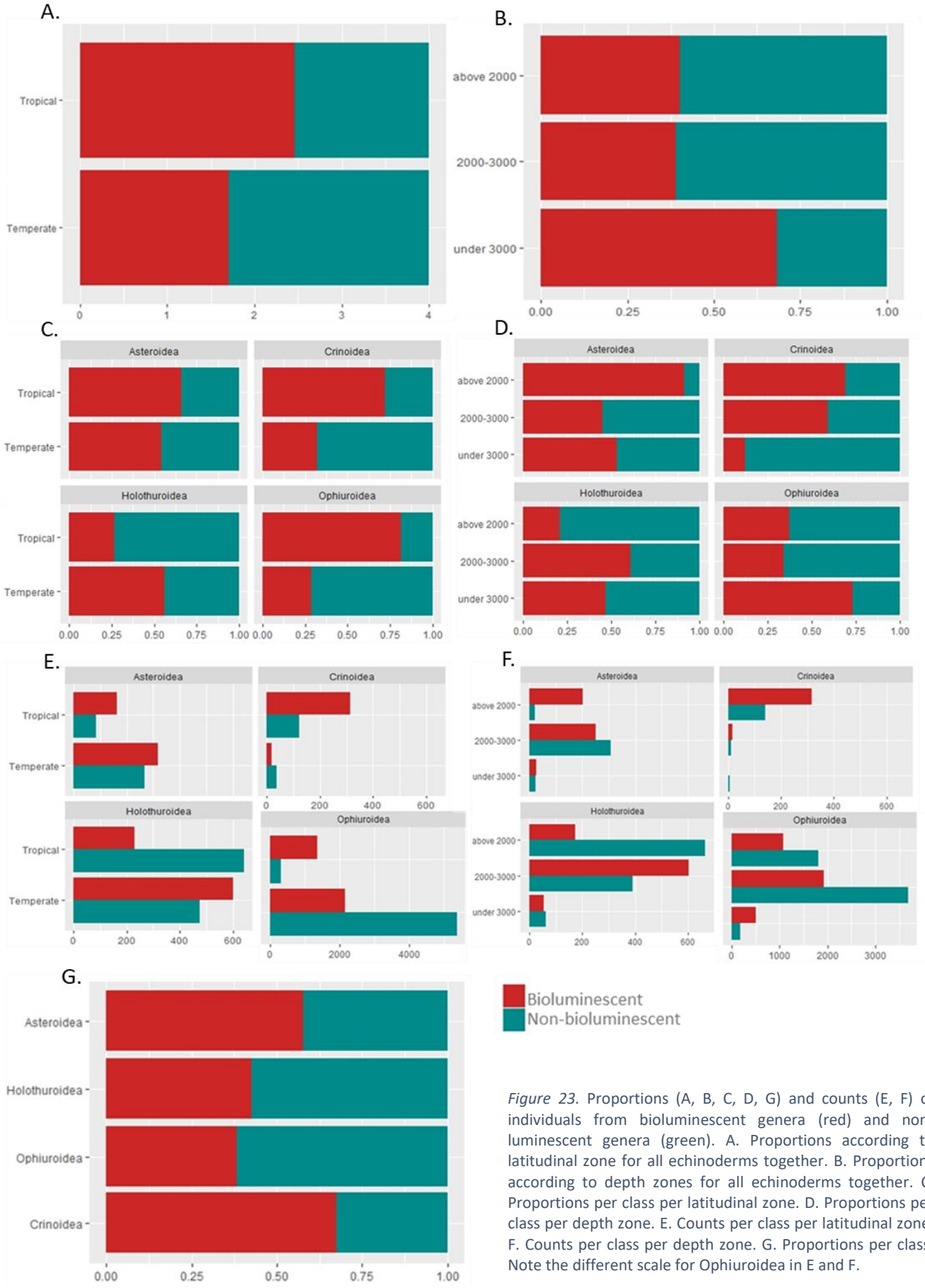

Figure 23. Proportions (A, B, C, D, G) and counts (E, F) of individuals from bioluminescent genera (red) and non-luminescent genera (green). A. Proportions according to latitudinal zone for all echinoderms together. B. Proportions according to depth zones for all echinoderms together. C. Proportions per class per latitudinal zone. D. Proportions per class per depth zone. E. Counts per class per latitudinal zone. F. Counts per class per depth zone. G. Proportions per class. Note the different scale for Ophiuroidea in E and F.

the null hypothesis (p-value=0.31 and p-value=0.18). No difference is to be considered between Asteroidea and Crinoidea (p-value=0.4), Asteroidea and Holothuroidea (p-value=0.53), Crinoidea and Holothuroidea (p-value=0.57) and Crinoidea and Ophiuroidea (p-value=0.23). Differences exist between Ophiuroidea and both other well represented classes namely Asteroidea (p-value=0.027) and Holothuroidea (p-value=0.02).

A Chi-squared test on the IN2017_V03 sample (*Table 6*) comparing the proportions of samples from bioluminescent and non-luminescent genera gave us a p-value of smaller than $2\ 10^{-16}$ between latitudinal zones. Between upper and lower bathyal, the p-value scores at 0.11 by which we deem the proportions equal. While comparing above 2000 and under 3000 we do reject the null hypothesis (p-value<$2\ 10^{-16}$). As well, the two deeper layers are significantly different (p-value<$2\ 10^{-16}$). Comparing the different classes together we obtained a completely new image than what was seen with the tested samples. Now, all classes have a significantly different number of samples from bioluminescent genera, $2.8\ 10^{-4}$ (between asteroids and crinoids) and $2.4\ 10^{-4}$ (between holothuroids and ophiuroids) being here the biggest p-values.

Chi-squared test considering bioluminescence at family level instead of genus on the same IN2017_V03 sample gave us again different p-values (*Table 6*). Hence, the p-value between latitudinal zones is now at 0.997. The difference between depths is now significant between all zones. The difference between classes also changes. All are significantly different except for Asteroidea and Crinoidea for which the p-value=0.48.

Table 6. Chi-squared test results for the IN2017_V03 sample between A. Latitudinal zones, B. depth categories, C. echinoderm classes. Red squares give the results while testing according to bioluminescent genera. Green squares give the results while testing according to bioluminescent families

A.	Tropical	Temperate
Tropical		0.997
Temperate	< $2\ 10^{-16}$	

B.	above 2000 m	2000 – 3000 m	under 3000
above 2000 m		< $2\ 10^{-16}$	< $2\ 10^{-16}$
2000 – 3000 m	0.11		$1.5\ 10^{-11}$
under 3000 m	< $2\ 10^{-16}$	< $2\ 10^{-16}$	

C.	Asteroidea	Holothuroidea	Ophiuroidea	Crinoidea
Asteroidea		< $2\ 10^{-16}$	< $2\ 10^{-16}$	0.48
Holothuroidea	$2.9\ 10^{-11}$		< $2\ 10^{-16}$	$5.5\ 10^{-11}$
Ophiuroidea	< $2\ 10^{-16}$	$2.4\ 10^{-4}$		< $2\ 10^{-16}$
Crinoidea	$2.8\ 10^{-4}$	< $2\ 10^{-16}$	< $2\ 10^{-16}$	

3.5.3 Similarity profile

The SIMPROF test created three significantly different groups with the total IN2017_V03 based on the species found at each CMR-depth group (*Fig.24A*). The first group contains two sub-groups: (i) all sites above 2000 meters depth and (ii) all southern sampling sites between

2000 and 3000 m up to New Castle (33.4° S). The second group covers the remaining sites sampled between 2000 and 3000 m depth (iii). The third group comprises all sites under 3000 meters. This last group is also made of two main sub-groups: (iv) one northern sub-group, from the Coral Sea CMR down to the Central Eastern CMR, and (v) one southern sub-group, from Freycinet CMR up to Hunter CMR. The division between North and South is here made between the 30th and the 32nd parallel south.

Taking only the bioluminescent genera from IN2017_V03 we see very similar groups appear (*Fig.24B*). Four significantly different groups are created: the first can again be subdivided into two subgroups (i) the first contains all the southern sites between 2000 and 3000 m depth up until Jervis CMR (35° South), (ii) the second subgroup contains all the southern sites under 3000 m depth up to Hunter CMR plus New Castle CMR's 2000-3000 depth range. (iii) The second group created contains the remaining sites under 3000 m. They all lay to the North of Hunter CMR. (iv) The third group the SIMPROF creates englobes all sites above 2000 m and eventually, (v) the 4th group is formed from the remaining, and thus from Hunter CMR to the north laying, sites between 2000 and 3000 m depth.

The similarity profile of the non-bioluminescent species creates two significantly different groups that can be subdivided into the exact same five sub-groups of the total IN2017_V03 sample (*Fig.24C*).

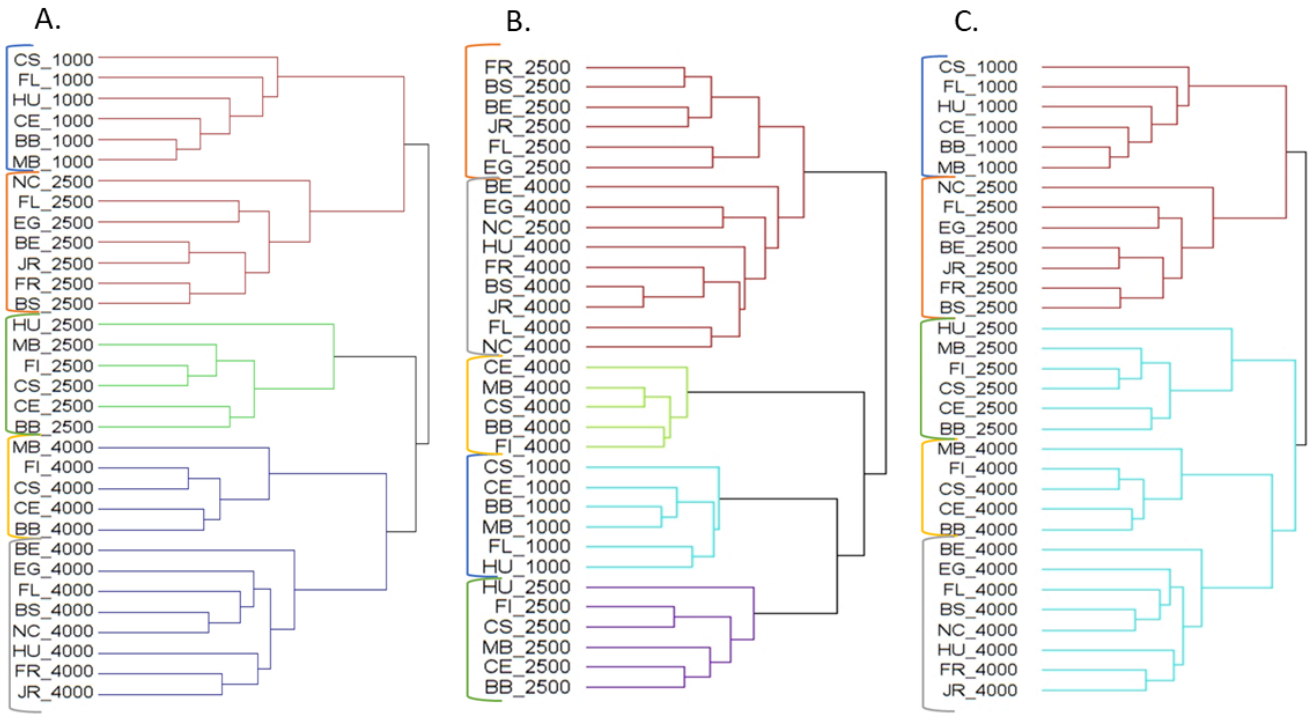

Figure 24. SIMPROF output trees. Significantly different groups have branches of different colour. A. Whole echinoderm IN2017_V03 dataset. B. Only samples from bioluminescent genera. C. Only samples from non-luminescent genera. Blue accolades contain the CMR-depth groups from above 2000 m depth; orange, southern waters between 2000 and 3000 m depth; yellow, southern waters from underneath 3000 m depth; green, northern waters between 2000 and 3000 m depth; grey, northern waters from underneath 3000 m depth. CMR name codes are from south to north as follows: FR: Freycinet CMR, FL: Flinders CMR, BS: Bass Strait, EG: East Gippsland CMR, BE: off Bermagui, JR: Jervis CMR, NC: off Newcastle, HU: Hunter CMR, CE: Central Eastern CMR, BB: off Byron Bay, MB: off Moreton Bay, FI: Fraser Island, CS: Coral Sea CMR. Note that in B. NC_2500 is in the group with the southern samples from under 3000 m depth.

3.5.4 GLM on proportion

A GLM was tested to describe the proportion of samples from bioluminescent genera considering the available environmental data. The only significant variable was oxygen (coefficient=0.524, p-value=0.01). Same happens to the non-luminescent samples who present the opposite coefficient and the same p-value.

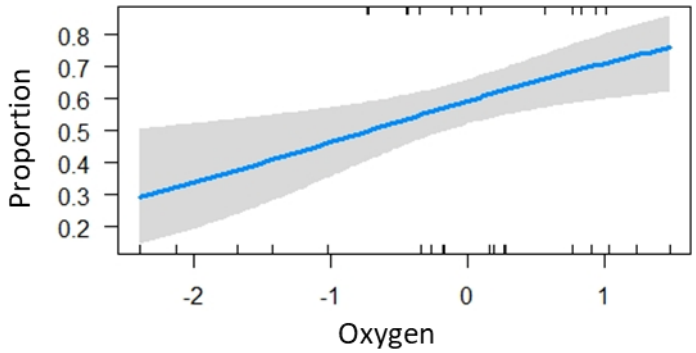

Figure 25. Plot showing the variation of the proportion of bioluminescent genera with oxygen concentration (mL L^{-1}) (standardized) fitted with a GLM. The blue line is the expected value. The grey bands represent the 95% confidence interval. Dots on the upper and lower margin indicate the observations' positions in relation to the expected value.

3.5.5 LM on Shannon diversity index

With our three environmental variables, the Shannon diversity index of the whole IN2017_V03 data could not be explained. However, an LM on the Shannon index only from the bioluminescent genera states significant explanation by the carbon variable (coefficient: 0.63, p-value=7.8 10^{-5}; R^2=0.47) while computing it together with carbon flux and temperature. Shannon index of non-bioluminescent genera does not obey to any of our three variables.

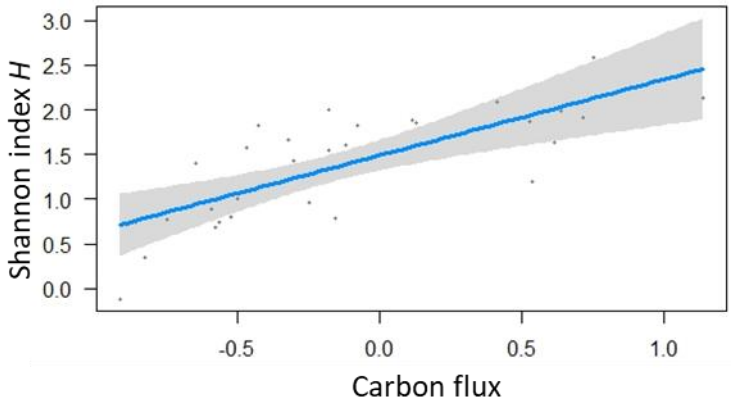

Figure 26. Plot showing the variation of the Shannon index *H* of bioluminescent genera with carbon flux (gC m^{-2} $year^{-1}$) (standardized) fitted with a LM. The blue line is the expected value. The grey bands represent the 95% confidence interval. Dots indicate the observations' positions.

3.5.6 GLM on species richness

A GLM on species richness shows a significant relation between this index and carbon flux (coefficient: 0.864, p-value=9.8 10^{-5}), oxygen (coefficient: -2.289, p-value=0.003) and nearly a significant contribution of temperature (coefficient: -0.304, p-value=0.055) (the dispersion parameter for the quasi-poisson family taken to be 3.7). With the bioluminescent genera we again have carbon (coefficient: 0.911, p-value=0.001) and oxygen (coefficient: -0.276, p-value=0.026) as significant variables. The non-bioluminescent genera samples species richness varies significantly with carbon flux (coefficient: 0.81, p-value=5.8 10^{-5} and) oxygen (coefficient: -0.307, p-value=0.0008) and temperature (coefficient: -0.351, -value=0.02) (the dispersion parameter for the quasi-poisson family taken to be 3.7).

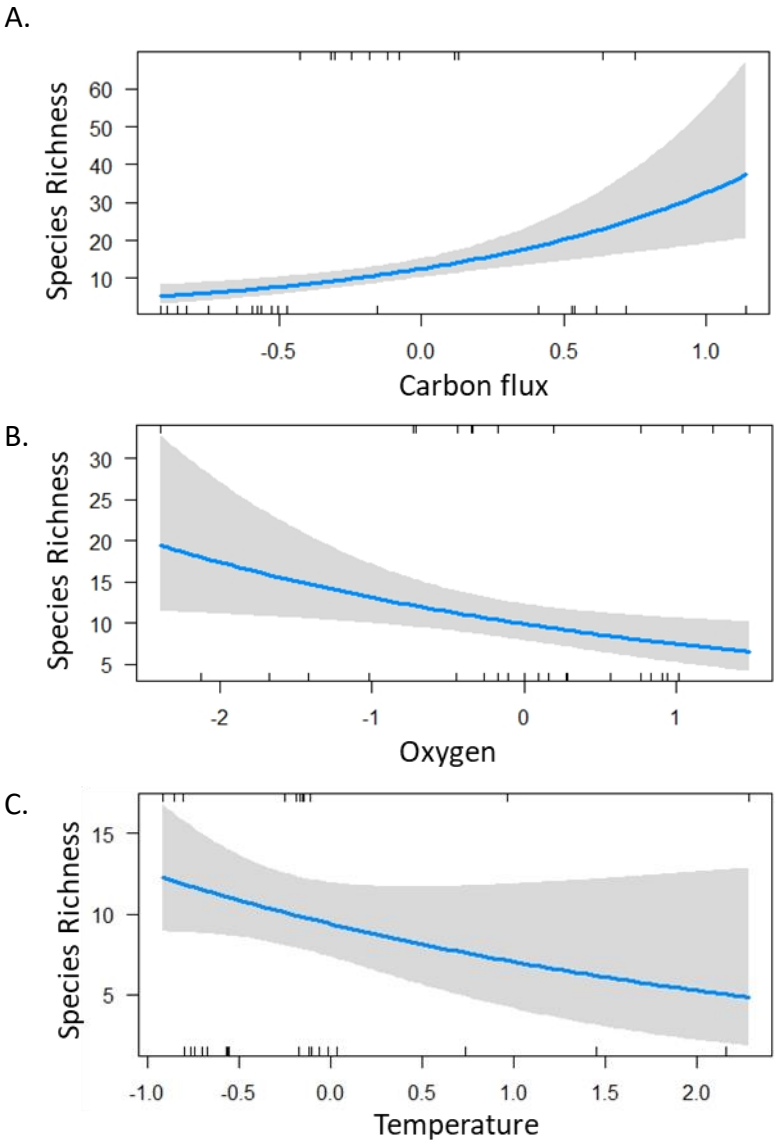

Figure 27. Plots showing the variation of species richness of non-bioluminescent genera with A. carbon flux (gC m^{-2} $year^{-1}$) (standardized), B. oxygen (mL L^{-1}) (standardized), C. temperature (°C)(standardized) fitted with a GLM (non-significant). The blue line is the expected value. The grey bands represent the 95% confidence interval. Dots on the upper and lower margin indicate the observations' positions in relation to the expected value.

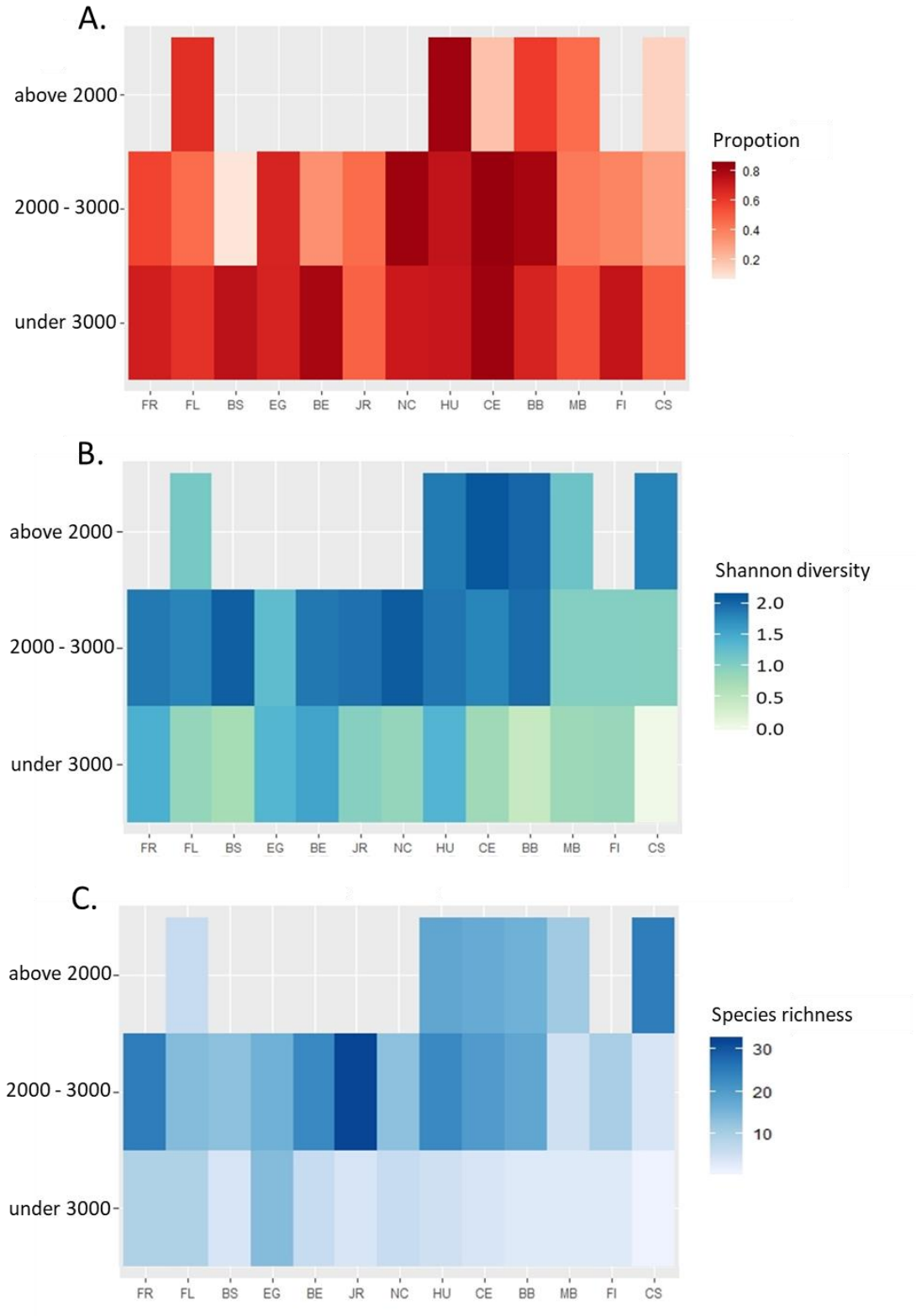

Figure 28. Tile graphs representing A. proportion of individuals from bioluminescent genera, B. Shannon diversity, C. species richness for each CMR-depth group. Darker colours mean higher values. FR: Freycinet CMR, FL: Flinders CMR, BS: Bass Strait, EG: East Gippsland CMR, BE: off Bermagui, JR: Jervis CMR, NC: off Newcastle, HU: Hunter CMR, CE: Central Eastern CMR, BB: off Byron Bay, MB: off Moreton Bay, FI: Fraser Island, CS: Coral Sea CMR

4 Discussion

4.1 Distribution of Echinodermata in the south-eastern Australian deep-sea

Recent work on biogeographic provinces of the deep ocean floor by Watling et al., 2013, puts the south-eastern Australian deep sea in single lower bathyal and abyssal provinces namely the New Zealand-Kermadec bathyal province and the Indian abyssal province based on environmental variables such as carbon flux, temperature, oxygen and salinity (*Fig.29*).

4.1.1 Depth

In the pelagic environment, Martini and Haddock, 2017, state that numbers of pelagic animals in the north-east Pacific decreases with depth (0 to 3900 m). Yet, the percentage of bioluminescent creatures stays over 50% even if the effect of depth varies between taxa (Martini and Haddock, 2017). The bioluminescence of the deep-sea benthos in this region seems to depend above all on the habitat and not specially on depth (Martini et al., 2019). According to them, the low proportions (30 to 40%) of bioluminescent benthic animals can probably be explained by the cost and ineffectiveness for communication because of recurrent mechanical stimulation by involuntary plankton impacts, currents and other roaming animals.

The occurrence of natural bioluminescent events in the benthic environment has been studied in the north-east Atlantic from 970 to 4800 m depth and in the Mid-Atlantic reach between 1659 to 2622 m depth (Craig et al., 2011; Gillibrand et al., 2007). Both found a decrease in the number of events with depth and associate this with the decrease in biomass that is depth related.

It seems as if in the south-east Pacific, bioluminescence in echinoderms increases with depth. Similarly, when considering the whole sample, the SIMPROF shows that bathyal communities differ from communities from deeper waters. However, taking bioluminescent families for calculating proportions portrays instead a significant decrease (unshown data). We consider that current knowledge on echinoderm bioluminescence has shown how variable luminescence capacities is inside families and therefore, we deem that grouping at family level would not be a precise enough representation.

As stated in the results, observed separately, only Ophiuroidea show this increase pattern. The increase-decrease pattern shown by proportions of bioluminescent Holothuroidea with depth is also present in Martini et al., 2019, yet, their maximum is in shallower waters than ours. They also show that numbers of bioluminescent Asterozoa increase with depth (Martini et al., 2019) which for us is mostly the case for Ophiuroidea. Through their sheer numbers, Ophiuroidea are probably pulling the data set in this direction.
Deeper water samples were done mainly on the abyssal plain or the lower slope. Thus, it may be that the plain is more suitable for the way in which Ophiuroidea use bioluminescence while the slope may be better for Holothuroids. Both use light emission seemingly mainly for burglar alarm and aposematism. Thereby, differences in habitat may be related to differences in

predator occurrence. Not enough is known about their ecology as to fully understand these patterns.

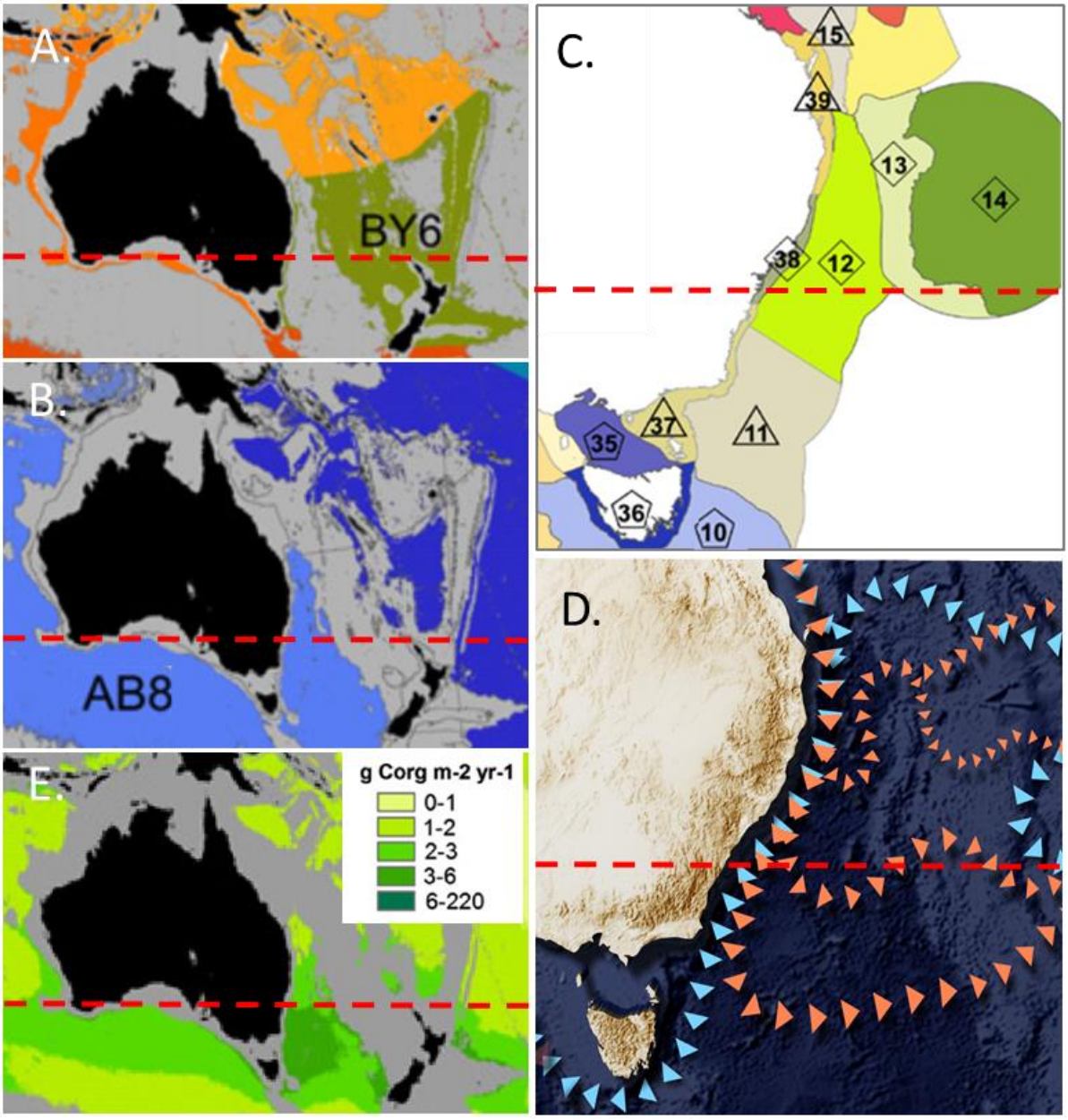

Figure 29. Maps of Australia and the whole Tasman Sea with New Zealand (A, B, E) and maps from the south-eastern Australian coast (C, D). A. The green area indicates the lower bathyal province of New Zealand-Kermadec (BY6) for depths between 800 and 3500 m. B. The light blue area indicates Indian abyssal province (AB8) for depths between 3500 and 6500 m. C. Provincial bioregions according to IMCRA v4.0. IN2017_V03 sampling took place in the bioregions 10: Tasmania province, 11: South-east transition, 12: Central-eastern province, 15: Central-eastern transition. Note that we consider the Central eastern province to be the transition zone fore echinoderms. D. Schematic representation of hot surface currents (red arrowheads) and cold deep currents (blue arrowheads) in the Tasman Sea along the south-eastern coast of Australia. Arrow heads indicate flow direction. E. Representation of carbon flux to the bottom at depths between 3500 and 6500 m. Data from Lutz et al., 2007. All red dashed lines indicate the 34th parallel. A, B and E are adapted from Watling et al., 2013. C is adapted from Commonwealth of Australia and Department of the Environment and Heritage, 2006. D is adapted from CSIRO Tasman sea currents image.

4.1.2 Latitude

While the region is considered one single biogeographic province (Watling et al., 2013) differences are apparent within this zone.

In their work on Ophiuroidea distribution, O'Hara et al., 2011, create a boundary for shelf fauna at approximately 30° South and reminds the presence of the Tasman Front at these heights. They suggest that this warm surface current diminishes the connectivity between North and South. Furthermore, based on the work of Lutz et al., 2007, Watling et al. show that the quantity of particulate organic carbon reaching the bottom at depths of 3500 to 6000 m increases towards south approximately between parallels 32 and 34 South (*Fig.29*). Moreover, this zone between Moreton Bay and Jervis CMR is considered the Central-eastern bioregion (*Fig.29*) based on demersal fish regionalization (Commonwealth of Australia and Department of the Environment and Heritage, 2006). Eventually, O'Hara et al., 2019, finds a boundary at 34° South based on beta diversity in Ophiuroidea.

We too find that our echinoderm communities present a North-South division at these heights: around 31° South underneath 3000 m and in the lower bathyal separation happens around 33.5° South for non-luminescent echinoderms and around 34° South for bioluminescent ones. This Central-eastern bioregion seems to be a transition region for echinoderm communities.

Southern waters have a higher carbon input and thus support a richer biomass (Gillibrand et al., 2007; Wooley et al., 2016). This is clearly seen with the number of individuals taken in these latitudes. Yet, we see an unexpected decrease in the proportion of samples from bioluminescent genera in waters south of the 34th parallel. Observed separately, only Holothuroidea show the opposite pattern. We here propose to use Martini et al. 's explanation: recurrent mechanical stimulation by involuntary plankton impacts and other roaming animals might make the use of bioluminescence ineffective and costly. These impacts increase with biomass, thereby, bioluminescence decreases.

4.1.3 What variables do really matter?

Two variables stand out for bioluminescent genera: carbon flux and oxygen. Proportions of samples from bioluminescent genera increase with oxygen concentration; Shannon diversity increases with carbon flux; species richness increases with carbon and decreases with oxygen.

The increased proportion of samples from bioluminescent genera with depth may thus be explained with the increased oxygen concentration. Also, the increased proportion from the North towards the Central-eastern bioregion (*Fig.28*) may also be explained with an oxygen increase.

The decrease of carbon and oxygen with depth explains the loss of species richness with depth.

Surprisingly, Shannon diversity increases with the carbon input. O'Hara et al., 2019, describes the biggest species richness and diversity in upper tropical waters. Yet, our data presents the higher diversity in waters between 2000 and 3000 m from the Central-eastern bioregion to

the south which is congruent with an increased carbon flux. A biological explanation may be that an increased biomass may in this case be responsible for supporting more diversity.

Nevertheless, all our GLMs present overdispersion and our LM has a rather low R^2. Thus, there are probably other variables that may better explain the distribution of bioluminescent genera. The type of seafloor is thought to play a role in the presence or absence of benthic bioluminescence because it determines the turbidity of the water and the presence of obstacles that could hinder the transmission of light (Herring, 1983; Martini et al., 2019).

4.1.4 Colour distribution

The ration of blue to green emitting samples in the sample that we tested for bioluminescence varies with depth. Taking the tested data set only, the numbers are too small to do real statistical comparisons, but we see that this relation is close to 1 in waters above 2000 m and close to 3 in waters underneath. Green emitters are less numerous in deeper waters.

Different propositions have been made to explain different wavelengths in bioluminescent animals. While some suggested that green light would be related with coastal waters and blue light with oceanic animals (Young, 1983), others proposed the idea that green emitters would be benthic and blue emitters oceanic (Herring, 1983; Johnsen et al., 2012). In both cases the basic proposal is that green light is better transmitted in turbid waters (Herring, 1983) and that it does not match the surrounding light for counterillumination (Young, 1983). Haddock and Case, 1999, showed for gelatinous zooplankton that the colour is depth related with shorter (bluer) wavelengths in deeper living animals.

Our data too shows that green emission diminishes with depth yet, we are speaking of benthic deep-sea animals. Thereby, our data would be congruent with Haddock and Case's proposal but not with the relation of green spectra to a benthic lifestyle.

Birk et al., 2018, hypothesized that the sea star *Novodinia americana* is, based on its eye's high spatial resolution, perhaps able to use its bioluminescence to communicate with and locate its conspecifics. If this was the case and the environment was effectively turbid like it is proposed for the benthic environments, then the ideal wavelength would be larger. Yet, *N. americana* emits in the short part of the spectrum (Birk et al., 2018). Knowing that currents on the abyssal plains tend to be rather weak it could be envisaged that the environment is not turbid thus the wavelengths of the animals do not need to adapt becoming longer.

One could also consider that the ecological use of bioluminescence does not need far travelling wavelengths hence, a blue spectrum would be as good as a green one. Indeed, Young, 1991, proposed that the action range of bioluminescence in marine systems would be of less than a meter.

The analysis of the wavelengths of further benthic animals (echinoderms and non-echinoderms), the study of the actual ecology of the bioluminescent creatures, the visual sensitivity of their predators as well as the actual environmental conditions will certainly provide further insight into this question.

4.2 Organisms

The proportions of bioluminescent species between classes in the tested data set is difficult to compare due to the small number of samples. Crinoids, with n=6, have a way to small sample thus, they are not significantly different from any of the other classes. Ophiuroidea is significantly different because it is the only class for which there are more non-luminescent than luminescent samples and species.

Ophiuroids and holothuroids show this same pattern when looking at the number of individuals from bioluminescent genera. These results are quite surprising given that ophiuroids and holothuroids have always been considered the most bioluminescent classes (Mallefet, 2009; Martini et al., 2019).

Thus, the first conclusion that has to be made is that we do not know enough about the bioluminescence capacities of echinoderms.

4.2.1 New Species

From the 34 species found to be bioluminescent at least 26 are new records, meaning it is the first time that these animals are described as bioluminescent.

Hymenaster nobilis is the sixth species of its genus to be described as bioluminescent. With *Calyptraster gracilis* and *Calyptraster sp.* we have the first two records of *Calyptraster* as being a bioluminescent genus. *Plutonaster complexus*, *Plutonaster knoxi* and *Plutonaster sp.* are the forth to fifth species of the genus *Plutonaster* to be recognized as light emitters. The genus *Dytaster* had already two records of bioluminescent species. Here we add two more, namely *Dytaster exilis* and *Dytaster pedicellaris. Coronaster reticulatus* is the first of its genus and *Zoroaster microporus* is the second of its. Interestingly, *Coronaster reticulatus* is the first bioluminescent Asteriidae.
Moreover, before "S*ampling the Abyss*", *Benthopecten* and *Freyella* had two species described as bioluminescent and *Cheiraster* none. We cannot state that the two unidentified bioluminescent samples of *Benthopecten* are two different species nor that they are neither *B.simplex* nor *B.spinosus* (the two bioluminescent species that have been described in this genus so far). The same type of uncertainty counts for the four *Freyella* samples, the three *Cheiraster* samples and the two unidentified Astropectinidae.
We can still conclude that there are five orders of sea stars that have bioluminescent species with at least 8 families and at least 17 genera and at least 31 species from which 9 are new records gained through *"Sampling the Abyss"*.

Achlyonice ecalcarea and *Synallactes* cf. *crucifera* are both the first of their respective genera with bioluminescent capabilities. *Amperima furcate* is the second, *Peniagone azorica* is the sixth and *Psychropotes scotiae* and *P. longicauda* are the third and fourth species of their genus found to emit light. The two new species of *Benthodytes* discovered during this cruise are also bioluminescent and thus the number of light emitters in this genus increases to four. The newly discovered *Molpadia* species is not only the first of the genus *Molpadia* and Family Molpadiidae to be successfully tested but, more importantly, it is the first record of a

bioluminescent species from the order Molpadida.
Thus, for holothuroids, we can conclude that there are at least five orders with bioluminescent species, at least 9 families, at least 26 genera and at least 38 species with 9 new species from this cruise.

Regarding our findings in Ophiuroidea, *Ophiocantha sollicita* adds itself in one of the most bioluminescent echinoderm genera with already 14 prior descriptions. *Ophiophthalmus relictus*, *Ophiosphalma glabrum* are all the first records of bioluminescence in their respective genera. *O. glabrum* is also the first record for the family Ophiosphalmidae.
Like in Asteroidea, we have here the uncertainty with unidentified species in the genera *Amphiura, Aspidophiura* and *Ophiotoma.* Nevertheless, our *Aspidophiura* sample is the first record of bioluminescence in this genus. In the case of *Ophiotoma* we record with certainty *O. paucispina* (that is the first) in this genus. As for *Ophiotoma* sp., it probably is a different species, but we still don't know which one.
Thereby, we can state that in Ophiuroidea there are at least 5 bioluminescent orders with at least 20 bioluminescent families, at least 38 genera and at least 74 bioluminescent species with 5 new ones coming from this cruise.

Before the "Sampling the Abyss" expedition, only 5 crinoids were described as being able to emit light. Here we ad *Adetelecrinus* cf. *vallatus* and *Monachocrinus* cf. *aotearoa* as the first of their respective genera and families. Also, the thalassometrids we studied should also count as a new bioluminescent species in the Thalassometridae family.
The number of bioluminescent orders in Crinoidea does not change (Comatulida and one Insocrinida), but now there are 6 bioluminescent families and 7 genera with 8 bioluminescent species from which three records result from this expedition.

4.2.2 Stimulation of the luminescence

Adding freshwater to a marine animal creates an osmotic shock destroying his cells, spilling out its content and thus, mixing all compounds needed for light emission if present. This gives us the maximal light emission of the tissue if the animal was not previously overstimulated in which case there might be a lack of substrate or cofactor.

Injection of potassium chloride creates a general depolarization of the membrane of any cell thereby inducing the liberation of vesicle contents indiscriminately as long as it is linked to the membrane potential. Thus, induction of luminescence after addition of KCL is also a maximal response (Deheyn et al., 1996; Dewael and Mallefet, 2002). Most of the time when KCl was tested on bioluminescent echinoderms during the cruise, we got a stimulation.

We would expect a similar response in both cases because in both treatments we suspect that all the luminous compounds are liberated. But we actually see that freshwater stimulation often gives more intense responses than KCl does (seven times higher peak intensity in *P. longicauda*). This could have many reasons. It could depend on the initial state of the sample meaning that an overstimulated and stressed animal/body-part will have a lesser response than an unstimulated individual/body-part of the same species/individual. It might also be that different parts of the animal react per se different meaning that testing freshwater on one part and KCl on another may give different results due to inherent differences in bioluminescent compound content. Eventually, we also see the possibility that the difference

may be due to the quantity of compound being made available in each treatment in two identical samples. Thus, while KCl induces an unnatural physiological response where all the cellular content mixes, the compounds needed for light emission remain confined to the cell (if the bioluminescence is intracellular). Contrariwise, freshwater makes the cells explode and hence, the content of one cell mixes with the content of several other cells. Thereby, if the substrate is not actually limited to the photocytes but is also contained somewhere else in the animal, like the gut in the case of external coelenterazine acquisition, or in the liver in the case of coelenterazine storage (Duchatelet et al., 2019; Mallefet and Shimomura, 1995). It could be imagined that the luciferase would have more substrate available and thus, would induce a bigger response.

A light gradient is supposed in the arms of *D. exilis*. The distal part of the arm creates in our test a 2.78 times lower peak than the proximal part of the arm. Generally, gradients with brighter distal parts have been associated to distractive body part sacrifice (Jones and Mallefet, 2012) but the opposite pattern has not been associated to any behavior yet but is probably an aposematic display. A bigger sample would be needed to make any conclusions.

A gradient is also plausible in *Ophioplinthaca rudis*. While the arm *b1* has a constant increase towards the tip (*Fig.15B*), in the individual *b2* the median part of the arm emits less light than both other segments. Intriguingly, the median part of *b2* emits approximately as much light as the proximal part of *b1* and the proximal part of *b2* emits approximately as much light as the median part of *b1*. We could consider an annotation error. It could also be that there is no error, in that case median and proximal segments are probably equal in emission capacity and would still differ from the distal portion. A bigger sample would be needed to effectuate statistical tests.
Like shown in many other ophiuroids (Mallefet, 2009), acetylcholine induces light emission in *O. rudis*. It can be said that (i) in *O. rudis* light emission is under extrinsic cholinergic control and (ii) cholinergic muscarinic and/or nicotinic receptors are present on the walls of the photocytes. Also, seen its acceptance as a neurotransmitter in echinoderms it is highly probable that this is also the case for *O. rudis*. The presence of both muscarinic and nicotinic receptors has been shown in *A. filiformis* and *A. arcystata*. In Ophioneriedae, muscarinic receptors were proven in *Ophionereis schayeri* and nicotinic receptors are present in *O. fasciata* (Mallefet 2009). Further pharmacological test and a bigger sample will be needed to find out the type of receptors present in *O. rudis*.

No gradient was observable in the thalassometrid 69_148. This is compatible with the pictures taken in which no real gradient is visible along the arm.
De Bremaeker et al., 2000, suggest that in *A. squamata* catecholamines have an inhibitory effect on ACh-induced luminescence. In the thalassometrid 69_148, in the contrary, we see an increase in the light production. Meanwhile, catecholamines induce a potentiation of light emission in *O. californica* and *A. filiformis* but gave no response in *O. fasciata*, *O. schayeri* and *O. aranea* (Mallefet, 2009). As far as we have researched no information seems to be available on catecholamines in crinoid except of their presence in *Antedon bifida* (Pentreath and Cobb, 1972) and the participation of dopamine during arm regeneration (Candia Carnevali and Bonasoro, 2001). Nevertheless, we can suppose that (i) in some Thalassometridae light emission is under extrinsic adrenergic control, (ii) adrenergic receptors are present, (iii) the response is positively correlated to the adrenalin concentration.

Regarding Holothuroidea it would have been interesting to test different parts of the animal to compare if differences exist between body regions.

4.2.3 Photocytes in Crinoidea

Regarding the similarities in size and position between the blue light dots on the pictures of the thalassometrid and *M.* cf. *aotearoa* and the size and position of their sacculi as well as the sacculi's outstanding fluorescence in comparison to the rest of the tissue it seems acceptable to hypothesize that light emission spots and sacculi are one and the same structure.

Like Brehm and Morin, 1977, Gandelman et al., 1993 and Mallefet et al., 2004, we use autofluorescence as a proxy for bioluminescence supposing that the by-products of bioluminescence will be more fluorescent than other compounds in the animal's body. Nevertheless, fluorescent compounds are relatively common in echinoderms and given the proven proteinaceous content of the sacculi (Holland, 1967; Noccart, 1993) we deemed necessary to check the fluorescence of sacculi with two control species: *Stiremetra breviradia* and *Antedon mediterranea*, the latter being a non-luminescent species. As of the writing *A. mediterranea* did not arrive thus, it won't be covered.

S. breviradia, as already described, is also a bioluminescent species from the family Thalassometridae, but it is currently known to emit light with a diffuse glow at the height of its axils without any light points. When sections of *S. breviradia* are observed under epifluorescence, the sacculi do not fluoresce more intensely than the rest of the arm (*Fig.19D*). This could confirm two things: (i) the content of sacculi is not *per se* more fluorescent than the rest of the body; (ii) different ways of light emission exist inside the same family.

Let's note that we were unable to determine the origin of the bioluminescence around the axils. We deem that sections of the decalcified arm tissue could bring further insight because it would remove the fluorescence produced by the ossicles. However, *Thaumatocrinus jungerseni* possesses seemingly both types of luminescence: the diffuse emission around the calyx and the dots on the arms that, we suspect, are probably luminous sacculi (Herring, 1974). Hence, we cannot confirm that this is a valid control because it may be that *S. breviradia* is also capable of both emission systems and the lesser fluorescence of the sacculi could be due to a certain degradation of the tissue with time.

An additional observation is the granulation density inside the saccules visible in some sections. Darker irregular spots are seen inside, often more to the center of the organ. In epifluorescence, these darker spots are brighter than the surrounding parts of the saccule. These seem to be parts were the autofluorescent by-product accumulates thus, it could be the ultrastructural changes following light emission. Albeit, the different appearance of the content under light and electron microscope has been described in *A. mediterranea* and has been interpreted as an indication of a maturation process of the saccule (Heinzeller and Welsch, 1994).

4.2.4 Photocytes in Holothuroidea

Basing ourselves again on epifluorescence to determine the origin of bioluminescence in *P. longicauda*, we found sub-epithelial granular cells that are brighter than their surrounding and their fluorescence colour differs from the epithelium and the cells laying deeper in the connective tissue. This remembers the description of the potential photocytes in Holothuroidea described by Herring 1974 and Robison 1992. Herring speaks of granular cells filled with spherical to subspherical granules in the luminous areas of the holothuroids he tested. His drawings (*Fig.9*) show about 40 µm large cells just below the epidermis. In Robison's study of *E. eximia* he described granular bodies 20-60 µm in size that were observed to emit light. Our cells have approximately the same size range albeit a bit larger.

Due to the quality of the picture we are not able to estimate the size of the luminescent blue dots on *P. longicauda* but given the size of the animal they do seem larger than individual cells. Thus, it is conceivable that agglomerations of these cells exist. It could also be that the dots visible on the picture are the emission of the large mass that were observed (*Fig.22B*). However, these masses seem to have a connection to the animals exterior and could therefore be some kind of gland.

So called morula cells and spherulocytes have been described in holothurian connective tissue (San Miguel-Ruiz and García-Arrarás, 2007). They have the same size than our and Herring's cells and are, as their names suggest, filled with vesicles. They have been shown to participle during wound healing in *Thyone briareus*, *Eupentacta quinquesemita* and in *Holothuria glaberrima* (San Miguel-Ruiz and García-Arrarás, 2007). These are all non-luminescent genera as far as known. Several possibilities exist like (i) the thought that these cells are the photocytes is erroneous, (ii) photocytes participate in wound healing, (iii) there are actually also morula and spherulocytes besides the photocytes, but they were not observable, (iv) some species have one cell family other species have the other. Clearly not enough is known about deep-sea holothurian anatomy, histology and bioluminescence and further research will be needed. A good start would be to stain the sections to differentiate the cell types.

4.2.5 Luciferin luciferase system

Through luciferin-luciferase assays we were able to demonstrate that the bioluminescence system in the thalassometrid 69_148 is a luciferin luciferase system based on coelenterazine. It is the second time this type of system is described for Echinodermata and the first time coelenterazine is proven as the luciferin in a non-ophiuroid echinoderm (Shimomura, 2006).

Coelenterazine has previously been described for depths of about 1000 m. In vertebrates, Myctophidae tend to migrate down to a 1000 m during daytime and it has been shown that they use coelenterazine as their luciferin (Campbell and Herring 1990; Duchatelet et al, 2019). In invertebrates, Campbell and Herring report coelenterazine from depths of 1500 m in, among others, the squid *Pterygioteuthis giardia*, the decapod *Systellapspis debilis* and the copepods *Euaugaptilus magnus* and *Pleuromamma xiphias* (Campbell and Herring 1990).

Our mean coelenterazine concentration in the thalassometrid 69_148 is 0,01 ±0,0027 nmol g^{-1} (*Table 7*). Thus, our concentration is similar to that of the euphausiids *Meganyctiphanes*

Table 7. Coelenterazine content (nmol g^{-1}) for different marine species from different classes. The coelenterazine column indicates the amount of coelenterazine present in the tissue indicated in the tissue column. The weight column indicates the weight from the tissue presented in the tissue column. Coelenterazine content is the amount of coelenterazine in the tissue divided by its weight. Adapted from Shimomura 2006.

CLASS	SPECIES	COELENTERAZINE (nmol)	WEIGHT (g)	COELENTERAZINE CONTENT (nmol g^{-1})	TISSUE
Hydrozoa	*Mitrocoma cellularia*	0.5	8	0.063	Whole body
Anthozoa	*Cavernularia obesa*	20	30	0.667	Whole body
	Renilla muelleri	2	6	0.333	Whole body
Tentaculata	*Mnemiopsis leidyi*	0.25	10	0.025	Whole body
Malacostraca	*Meganyctiphanes norvegica*	0.015	1.5	0.010	Whole body
	Euphausia pacifica	0.008	0.8	0.010	Whole body
Cephalopoda	*Chiroteuthis imperator*	7	150	0.047	Liver
	Watasenia scintillans	120	10	12.000	Liver
Actinopterygii	*Diaphus coeruleus*	12	18	0.667	Liver
Ophiuroidea	*Amphiura filiformis*	0.012	1	0.012	Whole body

norvegica and *Euphausia pacifica* (0.01 nmol g^{-1}) as well as that of the other echinoderm from which the coelenterazine concentration is known, *Amphiura filiformis* (0.012 nmol g^{-1}) (Shimomura, 2006). These concentrations are rather low compared to the 0.667 nmol g^{-1} when considering the whole body of some antozhoans and the up to 12 nmol g^{-1} in the liver of the firefly squid *Watasenia scintillans* (Shimomura, 2006).

Like the coelenterazine content, the here found luciferase has a similar activity than the activity of *RLuc* and the luciferase of *A. filiformis* (*Table 8*). The latter is homologues to the former (Delroisse et al., 2017b). Seen the similar activity and substrate of our thalassometrid's luciferase and given Delroisse et al.'s hypothesis of horizontal gene transfer in the ancestor of cnidarians and echinoderms, the presence of a *RLuc* homologue in our crinoid would not be out of place.

As stated, this unidentified thalassometrid is the third echinoderms for which the bioluminescent system has been described a bit more in detail. Up to this date the only well described bioluminescence systems in echinoderms are those of *Amphiura filiformis* (*RLuc*-coelenterazine system) and *Ophiopsila californica* (H_2O_2 dependant photoprotein system). Luciferin-luciferase systems have furthermore been assessed for non-ophiuroid echinoderms by Herring, 1974. With hot and cold dark extracts, he obtained the confirmation of luciferin-luciferase systems for *Hydrasterias sexradiata* and the crinoid *T. jungerseni*, that, as discussed before, also presents the same type of luminescent dots than the thalassometrid 69_148.

The green light emitted from the calyx by *S. breviradia* lets us rather think of a photoprotein system like in *O. californica* (Shimomura 2006) or a system based on another type of luciferin

Table 8. Luciferase activity (q s^{-1} g^{-1}) for different marine species from different classes. The luciferase activity column indicates the amount of quanta emitted by tissue indicated in the tissue column. The weight column indicates the weight from the tissue presented in the tissue column. Luciferase activity per gram is the activity of the tissue divided by its weight. Adapted from Shimomura 2006.

CLASS	SPECIES	ACTIVITY (q s^{-1})	WEIGHT (g)	PER GRAM (q s^{-1} g^{-1})	TISSUE
Anthozoa	*Cavernularia obesa*	$6{,}60\ 10^{13}$	30	$2{,}20\ 10^{12}$	Whole body
	Renilla muelleri	$7{,}80\ 10^{12}$	6	$1{,}30\ 10^{12}$	Whole body
Cephalopoda	*Chiroteuthis imperator*	$1{,}30\ 10^{11}$	150	$8{,}67\ 10^{8}$	Liver
Actinopterygii	*Argyropelecus hemigymnus*	$7{,}00\ 10^{10}$	3	$2{,}33\ 10^{10}$	Stomach
	Diaphus coeruleus	$6{,}00\ 10^{10}$	18	$3{,}33\ 10^{9}$	Liver
Ophiuroidea	*Amphiura filiformis*	$1{,}00\ 10^{12}$	1	$1{,}00\ 10^{12}$	Whole body

at least. If this is the case, then two different systems would be present inside the same family which is rather surprising. Yet, considering the bioluminescence in *T. jungerseni* it might even be that there are two different systems inside one animal. *A. filiformis* and *O. californica* have two different systems but are in different families (Amphiuridae and Ophiopsilidae) that are nevertheless in the same order (Amphilepidida).

Seen the great taxonomical and ecological diversity of bioluminescent species in Echinodermata, it would not be surprising to have several different systems of light emission appear during their more than 500 MY old history (early Cambrian). This diversity is seen in other deuterostomians namely in fish like *Melanocetous johnsoni* who have developed symbiosis with bioluminescent bacteria, coelenterazine systems like in myctophids and vargulin systems like in *Porichthys notatus* (Widder, 2010). In ostracods too, luciferin-luciferase systems have been described using coelenterazine and vargulin (Widder, 2010).

The biosynthesis of coelenterazine has been described in the copepod *Metridia pacifica* (Oba et al., 2009). Yet, coelenterazine is often considered a molecule that for most taxa is obtained through nutrition thus explaining its ubiquitousness (Haddock et al., 2010; Haddock et al., 2001; Frank et al., 1984). Most recently it has been shown for *A. filiformis* (Mallefet et al., 2020). Thereby, supposing that the acquisition of coelenterazine in bioluminescent crinoids happens through nutrition is not unreasonable specially when considering that crinoids are filter feeders and have been recorded capturing bioluminescent plankton (Gillibrandt et al., 2007). The study of the gut content in bioluminescent crinoids could be a first approach to give further insight into this hypothesis.

4.3 On Crinoidea

4.3.1 How to luminesce

Why and how would and could saccules in crinoids evolve to become bioluminescent organs? One thing that is most probably true is that sacculi do not only serve for bioluminescence. They are present in most Comatulida but only 6 species (considering our thalassometrids)

have been so far certified as bioluminescent and not all of them have shown light dots on their arms (Herring, 1974; Johnsen et al., 2012; Mallefet personal communication).

One first approach to the question is that while Comatulida extended their range towards deeper waters, sacculi lost their initial function and selection pressure promoted light emission instead. This could specially be true if, because of the new environment and the characteristics of the deep sea, the initial function was not needed anymore or at least became secondary.

This loss of initial function is the main hypothesis regarding luciferin and bioluminescence evolution (Widder, 2010). Luciferin would have been an antioxidant that, due to released pressure of reactive oxygen species with depth, lost is initial purpose or shifted it and reconverted into the substrate molecule for bioluminescence (Rees et al., 1998).

Superoxide anions can be produced photochemically (Rees et al., 1998) thus, it could be of considerable interest for the crinoid to contain antioxidants in an organ that easily lets light through (Umpathy et al., 2013). Thereafter, introduction to deeper waters would reduce the risk of reactive oxygen species and allow coelenterazine inside the sacculi to develop into a luciferin.

Given that coelenterazine chemiluminusces easily in aprotic solvents, sacculi with their basic protein content (at least in *Antedon*. Holland, 1967; Noccart, 1993) could effectively be a good environment for light production as long as it is hydrophobic enough (Rees et al., 1998).

Also, if our luciferase turns effectively out to be homologous to *RLuc*, an initial haloalkane dehalogenase function can be hypothesized (Delroisse et al., 2017b). These enzymes are hydrolases (and not oxygenases) used for the detoxification of haloalakanes (Delroisse et al., 2017b). Hence, a detoxification role for sacculi could seem plausible.

Holland, 1977, proposed that saccules of *A. mediterranea* could be used as light receptors because they are not covered by pigmented epithelium and they possess a clear and homogenous content. Light would pass through them and stimulate the subjacent nerve. These are also characteristics that would be expected from a light emitting organ. The clear content and the lack of pigments above would allow a good transmission of the light. Furthermore, the connection with the nervous system would allow the control of the emission. But, if sacculi were initially sensitive organs then the neurons would have to be changed from sensory to motor types.

Does the transformation into a light emitting organ eliminate the original function? We do not know. It does seem plausible to lose light sensitivity in an environment without light but loosing supposed excretion, secretion or chalk production functions would be less convenient.

4.3.2 Why to luminesce

Pictures show that in *M.* cf. *aotearoa* and in the thalassometrids 69_148 and 80_120 bioluminescence occurs only on the arms and pinnules. Thus, the use of light emission capacities should be related to the ways in which they use their arms.

The combination of bioluminescence with autotomy seems very plausible seen the likeliness at which crinoids autotomize (Carnevali et al., 2001) and given that this has been reported in

other echinoderms: Ophiuroidea (Deheyn et al., 2000; Mallefet, 2009; Jones and Mallefet, 2013) and Holothuroidea (Robison, 1992).

However, it does not seem plausible for crinoids to use their bioluminescence in combination with autotomy to create a distractive body-part allowing the crinoid to escape as seen in some ophiuroids (Deheyn et al., 2000; Mallefet, 2009). Many crinoids are not fast enough to escape highly movable predators like fish (Meyer and Ausich, 1983). This is especially the case for stalked crinoids like *M. aotearoa*. Instead, the use of bioluminescence combined to autotomy as a sacrificial tag attracting secondary predators seems more plausible (Haddock et al., 2010; Deheyn et al., 2000; Mallefet, 2009). Classical burglar alarm without autotomy may also be a possible utility.

A startle effect and the use of light emission as aposematic signal also seems a possible use of bioluminescence in crinoids. These uses have been demonstrated for ophiuroids (Grober, 1998a, Jones and Mallefet, 2010).

In bioluminescent Asteroidea with eyespots, Birk et al., 2018, proposed the use of bioluminescence as an intraspecific communication method to find mates. Crinoids do create aggregations where good current conditions are present (Meyer and Ausich, 1983). But, given the limited visual capacities associated with crinoids and the creation of aggregation in non-luminous species it does seem rather unlikely to rely on bioluminescence for this purpose.

A very attractive theory that has already been proposed by Holland, 1991, is the use of bioluminescence to attract prey. This is especially interesting when one considers that crinoids do not really have a lot of predators (Meyer and Ausich, 1983). Thus, it might not have a role in predator deterrence. The deep sea is considered an environment with low food availability and relying on particulate organic matter from upper layers. Thereby, it could be judicious for crinoids to attract plankton, especially in species that do not move a lot and cannot find a more suitable place to filter feed. Also, this kind of suggestion of a predatory utility has been proposed in the ophiuroid *Ophiocomina nigra* (Jones and Mallefet, 2012) but no real prove exists. The most iconic users of light as attraction method are probably anglerfishes (Pietsch, 2009), but it is suggested to also be the case in cephalopods like the genus *Staurotheutis* and siphonophores like the genus *Erenna* that use light organs on tentacles to attract prey mostly thought to be of planktonic nature (Haddock et al., 2010; Johnsen et al., 1999; Haddock et al., 2005).

4.4 Limits and Perspectives

A lot is to say about our work.

We could have created a recapitulative table of all the luminometry measurements and perhaps extract information at class level.

We could have had earlier the idea of finding a non-luminescent crinoid and holothuroid to compare our findings with.

We could have tried harder to get access to the environmental data collected during the cruise as well as pictures from the sites and add an habitat variable.

We could have guarded more variables to fit our models knowing that, even if strongly correlated, other variables may have explained better.

We probably overestimate the number of species in the contingency table with our method.

We could have done the SIMPROF before dividing the sample into temperate and tropical waters or redo and compare with the new division.

But many problems are inherent to the type of research.

4.4.1 Deep-sea and bioluminescence research

The major problem with deep-sea research is the difficult access to the samples. Important logistics and financial means are needed thus, the numbers of sampling occasions and samples are limited. The largest environment on earth is also the least studied (Brökeland and George, 2009). Moreover, patchiness, low abundance and inability to resample the same site creates doubts on the representativeness of the samples taken.

A lack of taxonomists creates a lack of knowledge on the species presents which produces a lack of information that causes a lack of accuracy in the conclusions made. The subsequent extrapolations, predictions and conservations approaches can only be as good as the original data on which they base themselves (Brökeland and George, 2009). We here show that the taxonomical level at which this study is made completely changes the outcomes.

An initial approach wanted was the creation of indicator values for species in the different communities but eventually we realized that information on the ecology and habitat lacks for deep-sea species.

Regarding bioluminescence, one may never be really sure about the animal's capacity to luminesce especially when capture was done harming the creature and stressing it. Herring, 1987, sets a lot of difficulties inherent to intraspecific diversity in luminescence capacities like seasonal and sex related variations.

Also, we do not study the distribution of bioluminescent individuals but only the distribution of samples from genera known to contain bioluminescent species. Compared, to Martini et al.'s categorisation it is probably neither worst nor better, but while making more categories presenting uncertainties is certainly an asset, they do mix everything in their later analysis and conclusion. Also, our method of taking only one clearly defined taxonomical level, makes comparisons between animal groups certainly more accurate.

Whatever method taken, it is clear that both approaches are limited by the current knowledge on bioluminescence and studies will have to be done again in the future just to adjust to new records of bioluminescence.

Let's note that often very abundant and easily accessible species, like ophiuroids, are taken for studies then used to extrapolate on other taxa. This might be an erroneous approach seen how differently taxa may react to same environmental variables.

4.4.2 Further analysis: Histology and transcriptomics

Along with different perspectives already presented in the text, we would like to point some further analysis that would help improve and make it progress.

Transcriptomics would be interesting to use to find possible luciferase sequences. This method does not always give answers - like for sharks (Duchatelet personal communications) – but has a lot of potential and did allow to determine the luciferase of *A. filiformis* (Delroisse et al., 2017b).

Like, Delroisse et al., 2017b, a further step would be immunodetection. We had planned to perform this with an anti-*RLuc* polyclonal antibody even before knowing the similarities between *RLuc* and our luciferase, but eventually not enough time was available. This method would allow to determine the place where the luminous reaction takes place.

Purification of the luciferase could also be tried using and adapting protocols from Shimomura (and if enough tissue is available).

Nevertheless, comparing with non-luminescent animals is an important approach that has to be done.

As a final word, more sampling and research will be needed to elucidate the mysteries associated with deep-sea animals and bioluminescence. Specially in times of overfishing, global warming and not so distant deep-sea mining, we certainly do not know enough for mitigating anthropogenic impacts on this environment that not only could contain interesting genetic resources but bears an intrinsic value.

5 References

Birk, M.H., Blicher, M.E., Garm, A., 2018. Deep-sea starfish from the Arctic have well-developed eyes in the dark. Proceedings of the Royal Society of London. Series B. Biological Sciences 285, 20172743. https://doi.org/10.1098/rspb.2017.2743

Brehm, P., Morin, J.G., 1977. Localization and characterization of luminescent cells in *Ophiopsila californica* and *Amphipholis squamata* (Echinodermata: Ophiuroidea). The Biological Bulletin 152, 12–25. https://doi.org/10.2307/1540723

Bremaeker, N.D., Baguet, F., Mallefet, J., 2000. Effects of catecholamines and purines on luminescence in the brittlestar *Amphipholis squamata* (Echinodermata). The Journal of Experimental Biology 203, 2015–2023.

Brökeland, W., George, K.H., 2009. Editorial: Deep-sea taxonomy - a contribution to our knowledge of biodiversity. Zootaxa 2096, 3.

Buchanan, J.B., 1963. Mucus secretion within the spines of ophiuroid echinoderms. Proceedings of the Zoological Society of London 141, 251–259. https://doi.org/10.1111/j.1469-7998.1963.tb01611.x

Byrne, M., O'Hara, T., 2017. Australian Echinoderms: Biology, Ecology and Evolution, CSIRO Publishing. ed. Clayton.

Campbell, A.K., Herring, P.J., 1990. Imidazolopyrazine bioluminescence in copepods and other marine organisms. Marine Biology 104, 219–225. https://doi.org/10.1007/BF01313261

Candia Carnevali, M.D., Bonasoro, F., 2001. Microscopic overview of crinoid regeneration. Microscopy Research and Technique 55, 403–426. https://doi.org/10.1002/jemt.1187

Carnevali, M.D.C., Saita, A., 1985. Muscle system organization in the echinoderms: II. Microscopic anatomy and functional significance of the muscle-ligament-skeleton system in the arm of the comatulids (*Antedon mediterranea*). Journal of Morphology 185, 59–74. https://doi.org/10.1002/jmor.1051850105

Chalfie, M., Tu, Y., Euskirchen, G., Ward, W.W., Prasher, D.C., 1994. Green fluorescent protein as a marker for gene expression. Science 263, 802–805. https://doi.org/10.1126/science.8303295

Claes, J.M., Mallefet, J., 2011. Control of luminescence from lantern shark (*Etmopterus spinax*) photophores. Communicative & Integrative Biology 4, 251–253. https://doi.org/10.4161/cib.4.3.14888

Commonwealth of Australia, Department of the Environment and Heritage, 2006. A guide to the integrated marine and coastal regionalization of Australia: IMCRA Version 4.0. Australian Government, Department of the Environment and Heritage, Canberra, A.C.T.

Craig, J., Jamieson, A.J., Bagley, P.M., Priede, I.G., 2011. Naturally occurring bioluminescence on the deep-sea floor. Journal of Marine Systems 88, 563–567. https://doi.org/10.1016/j.jmarsys.2011.07.006

David, V., 2017. Traitement de données en sciences environnementales, ISTE. ed, Ecologie. St. George's Road.

Deheyn, D., Alva, V., Jangoux, M., 1996. Fine structure of the photogenous areas in the bioluminescent ophiuroid *Amphipholis squamata* (Echinodermata, Ophiuridea). Zoomorphology 116, 195–204.

Deheyn, D., Mallefet, J., Jangoux, M., 2000. Evidence of seasonal variation in bioluminescence of *Amphipholis squamata* (Ophiuroidea, Echinodermata): effects of environmental factors. Journal of Experimental Marine Biology and Ecology 245, 245–264. https://doi.org/10.1016/S0022-0981(99)00166-5

Deheyn, D., Mallefet, J., Jangoux, M., 1997. Intraspecific Variations of Bioluminescence in a Polychromatic Population of *Amphipholis squamata* (Echinodermata: Ophiuroidea). Journal of the Marine Biological Association of the United Kingdom 77, 1213–1222. https://doi.org/10.1017/S0025315400038728

Delroisse, J., Ullrich-Lüter, E., Blaue, S., Eeckhaut, I., Flammang, P., Mallefet, J., 2017a. Fine structure of the luminous spines and luciferase detection in the brittle star *Amphiura filiformis*. Zoologischer Anzeiger 269, 1–12. https://doi.org/10.1016/j.jcz.2017.05.001

Delroisse, J., Ullrich-Lüter, E., Blaue, S., Ortega-Martinez, O., Eeckhaut, I., Flammang, P., Mallefet, J., 2017b. A puzzling homology: a brittle star using a putative cnidarian-type luciferase for bioluminescence. Open Biology 7, 160300. https://doi.org/10.1098/rsob.160300

Denton, E.J., Herring, P.J., Widder, E.A., Latz, M.F., Case, J.F., 1985. The roles of filters in the photophores of oceanic animals and their relation to vision in the oceanic environment. Proceedings of the Royal Society of London. Series B: Biological Sciences 225, 63–97. https://doi.org/10.1098/rspb.1985.0051

Dewael, Y., Mallefet, J., 2002. Luminescence control in ophiuroids (Echinodermata) does not share a common nervous control in all species. The Journal of Experimental Biology 205, 799–806.

Duchatelet, L., Hermans, C., Duhamel, G., Cherel, Y., Guinet, C., 2019. Coelenterazine detection in five myctophid species from the Kerguelen Plateau. The Kerguelen Plateau: Marine Ecosystem + Fisheries: Proceedings of the second Symposiom (Hobart, Tasmania, Australia 13/11/2017 to 15/11/2017) 31–41.

Frank, T.M., Widder, E.A., Latz, M.I, Case, J.F., 1984. Dietary maintenance of bioluminescence in a deep-sea mysid. The Journal of Experimental Biology 109, 385-389.

Gandelman, O.A., Brovko, L.Yu., Ugarova, N.N., Chikishev, A.Yu., Shkurimov, A.P., 1993. Oxyluciferin fluorescence is a model of native bioluminescence in the firefly luciferin—luciferase system. Journal of Photochemistry and Photobiology B: Biology 19, 187–191. https://doi.org/10.1016/1011-1344(93)87083-Y

Gillibrand, E.J.V., Bagley, P., Jamieson, A., Herring, P.J., Partridge, J.C., Collins, M.A., Milne, R., Priede, I.G., 2007. Deep sea benthic bioluminescence at artificial food falls, 1,000–4,800 m depth, in the Porcupine Seabight and Abyssal Plain, North East Atlantic Ocean. Marine Biology 150, 1053–1060. https://doi.org/10.1007/s00227-006-0407-0

Gouveneaux, A., Mallefet, J., 2013. Physiological control of bioluminescence in a deep-sea planktonic worm, *Tomopteris helgolandica*. The Journal of Experimental Biology 216, 4285–4289. https://doi.org/10.1242/jeb.090852

Grober, M.S., 1989. Bioluminescent Aposematism: a reply to Guilford & Cuthill. Animal Behaviour 37, 341–343. https://doi.org/10.1016/0003-3472(89)90127-9

Grober, M.S., 1988a. Brittle-star bioluminescence functions as an aposematic signal to deter crustacean predators. Animal Behaviour 36, 493–501. https://doi.org/10.1016/S0003-3472(88)80020-4

Grober, M.S., 1988b. Responses of tropical reef fauna to brittle-star luminescence (Echinodermata: Ophiuroidea). Journal of Experimental Marine Biology and Ecology 115, 157–168. https://doi.org/10.1016/0022-0981(88)90100-1

Guilford, T., Cuthill, I., 1989. Aposematism and Bioluminescence. Animal Behaviour 37, 339–341.

Haddock, S.H.D., Case, J.F., 1999. Bioluminescence spectra of shallow and deep-sea gelatinous zooplankton: ctenophores, medusae and siphonophores. Marine Biology 133, 571–582. https://doi.org/10.1007/s002270050497

Haddock, S.H.D., Moline, M.A., Case, J.F., 2010. Bioluminescence in the Sea. Annual Review of Marine Science 2, 443-493. http://www.annualreviews.org/doi/10.1146/annurev-marine-120308-081028

Haddock, S.H.D., Casey, D.W., Pugh, P.R., Schnitzler, C.E., 2005. Bioluminescent and Red-Fluorescent Lures in a Deep-Sea Siphonophore. Science 309, 263-263.

Haddock, S.H.D., Rivers, T.J., Robison, B.H., 2001. Can coelenterates make coelenterazine? Dietary requirement for luciferin in cnidarian bioluminescence. Proceedings of the National Academy of Sciences 98, 11151.

Harvey, E.N., 1956. Evolution and Bioluminescence. The Quarterly Review of Biology 31, 270–287.

Harvey, E.N., 1952. Bioluminescence, Academic Press. ed. New York.

Heger, A., King, N.J., Wigham, B.D., Jamieson, A.J., Bagley, P.M., Allan, L., Pfannkuche, O., Priede, I.G., 2007. Benthic bioluminescence in the bathyal North East Atlantic: luminescent responses of *Vargula norvegica* (Ostracoda: Myodocopida) to predation by the deep-water eel (*Synaphobranchus kaupii*). Marine Biology 151, 1471–1478. https://doi.org/10.1007/s00227-006-0587-7

Heinzeller, T., Welsch, U., 1994. Crinoidea, in: Microscopic Anatomy of Invertebrates. Wiley-Liss, Inc., pp. 9–148.

Herring, P.J., 1985. How to survive in the dark: bioluminescence in the deep sea. Symposia of the Society for Experimental Biology 39, 323-350

Herring, P.J., 1995. Bioluminescent echinoderms: Unity of function in diversity of expression? in: Echinoderm Research 1995. Emson, Smith & Campbell, Rotterdam.

Herring, P.J., 1987. Systematic distribution of bioluminescence in living organisms. Journal of Bioluminescence and Chemiluminescence 1, 147–163. https://doi.org/10.1002/bio.1170010303

Herring, P.J., 1983. The spectral characteristics of luminous marine organisms. Proceedings of the Royal Society of London. Series B. Biological Sciences 220, 183–217. https://doi.org/10.1098/rspb.1983.0095

Herring, P.J., 1974. New observations on the bioluminescence of echinoderms. Journal of Zoology 172, 401–418. https://doi.org/10.1111/j.1469-7998.1974.tb04116.x

Herring, P.J., Widder, E.A., 2004. Bioluminescence of deep-sea coronate medusae (Cnidaria: Scyphozoa). Marine Biology 146, 39–51. https://doi.org/10.1007/s00227-004-1430-7

Holland, N.D., 1967. Some observations on the saccules of *Antedon mediterranea* (Echinodermata, Crinoidea). Pubblicazioni de la Stazione Zoologica di Napoli 35, 257_262.

Holland, N.D., Grimmer, J.C., Wiegmann, K., 1991. The structure of the sea lily *Calamocrinus diomedae*, with special reference to the articulations, skeletal microstructure, symbiotic bacteria, axial organs, and stalk tissues (Crinoida, Millericrinida). Zoomorphology 115–132.

Johnsen, S., Frank, T.M., Haddock, S.H.D., Widder, E.A., Messing, C.G., 2012. Light and vision in the deep-sea benthos: I. Bioluminescence at 500-1000 m depth in the Bahamian

Islands. The Journal of Experimental Biology 215, 3335–3343. https://doi.org/10.1242/jeb.072009
Johnsen, S., Balser, E.J., Fisher, E.C., Widder, E.A., 1999. Bioluminescence in the Deep-Sea Cirrate Octopod *Stauroteuthis syrtensis* Verrill (Mollusca: Cephalopoda). the Biological Bulletin 197, 26-39.
Jones, A., Mallefet, J., 2013. Why do brittle stars emit light? Behavioural and evolutionary approaches of bioluminescence. Cahiers de Biologie Marine 54, 729–734.
Jones, A., Mallefet, J., 2012. Study of the luminescence in the black brittle-star *Ophiocomina nigra*: toward a new pattern of light emission in ophiuroids. Zoosymposia 7, 139–145.
Jones, A., Mallefet, J., 2010. Aposematic use of bioluminescence in *Ophiopsila aranea* (Ophiuroidea, Echinodermata). Luminescence 25, 81–216.
Kaskova, Z., Tsarkova, A., Yampolski, I., 2016. 1001 lights: luciferins, luciferases, their mechanisms of action and applications in chemical analysis, biology and medicine. Chemical Society Reviews 45, 6048-6077.
Mallefet, J., 2009. Echinoderm bioluminescence: Where, how and why do so many ophiuroids glow? in: Bioluminescence in Focus: A Collection of Illuminating Essays. Victor Benno Meyer-Rochow, Kerala, India.
Mallefet, J., Shimomura, O., 1995. Presence of coelenterazine in mesopelagic fishes from the Strait of Messina. Marine Biology 124, 381–385. https://doi.org/10.1007/BF00363911
Mallefet, J., Duchatelet, L., Coubris, C., 2020. Bioluminescence induction in the ophiuroid *Amphiura filiformis* (Echinodermata). The Journal of Experimental Biology. In press.
Martini, S., Kuhnz, L., Mallefet, J., Haddock, S.H.D., 2019. Distribution and quantification of bioluminescence as an ecological trait in the deep sea benthos. Sci Rep 9, 14654. https://doi.org/10.1038/s41598-019-50961-z
Meyer, D.L., Ausich, W.I., 1983. Biotic Interactions among Recent and Fossil Crinoids, in: Biotic Interactions in Recent and Fossil Benthic Communities, Topics in Geobiology. Springer, New York, pp. 378–420.
Morin, J.G., 1983. Coastal Bioluminescence: Patterns and Functions. Bulletin of Marine Science 33, 787–817.
Noccart, C., 1993. Etude Morphologique des saccules chez la comatule *Antedon bifida* (Pennant) (Echinodermata, Crinoidea) (Zoological Science Licentiate). Université Libre de Bruxelles, Brussels.
Oba, Y., Kato, S., Ojika, M., Inouye, S., 2009. Biosynthesis of coelenterazine in the deep-sea copepod, *Metridia pacifica*. Biochemical and Biophysical Research Communications 390, 684–688. https://doi.org/10.1016/j.bbrc.2009.10.028
O'Hara, T., 2017. Sampling the Abyss (Voyage Summary No. INV2017_V03).
O'Hara, T.D., Hugall, A.F., Thuy, B., Moussalli, A., 2014. Phylogenomic Resolution of the Class Ophiuroidea unlocks a Global Microfossil Record. Current Biology 24, 1874–1879. https://doi.org/10.1016/j.cub.2014.06.060
O'Hara, T.D., Hugall, A.F., Woolley, S.N.C., Bribiesca-Contreras, G., Bax, N.J., 2019. Contrasting processes drive ophiuroid phylodiversity across shallow and deep seafloors. Nature 565, 636–639. https://doi.org/10.1038/s41586-019-0886-z
O'Hara, T.D., Rowden, A.A., Bax, N.J., 2011. A Southern Hemisphere Bathyal Fauna is distributed in Latitudinal Bands. Current Biology 21, 226–230. https://doi.org/10.1016/j.cub.2011.01.002

Ophiuroidea - The World Ophiuroidea Database [WWW Document], n.d. URL http://www.marinespecies.org/ophiuroidea/aphia.php?p=browser (accessed 12.24.19).

Prenant, M., 1928. Notes sur les Saccules de la Comatule *Antedon bifida* (Pennant). Bulletin de la Société zoologique de France 10.

Rees, J.-F., Wergifosse, B.D., Noiset, O., Dubuisson, M., Janssens, B., Thompson, E.M., 1998. The origins of marine bioluminescence: turning oxygen defence mechanisms into deep-sea communication tools. The Journal of Experimental Biology 201, 1211–1221.

Renwart, M., Delroisse, J., Claes, J.M., Mallefet, J., 2014. Ultrastructural organization of lantern shark (*Etmopterus spinax* Linnaeus, 1758) photophores. Zoomorphology 133, 405–416. https://doi.org/10.1007/s00435-014-0230-y

Renwart, M., Delroisse, J., Flammang, P., Claes, J.M., Mallefet, J., 2015. Cytological changes during luminescence production in lanternshark (*Etmopterus spinax* Linnaeus, 1758) photophores. Zoomorphology 134, 107–116. https://doi.org/10.1007/s00435-014-0235-6

Robison, B.H., 1992. Bioluminescence in the benthopelagic holothurian *Enypniastes eximia*. Journal of the Marine Biological Association of the United Kingdom 72, 463–472. https://doi.org/10.1017/S0025315400037826

San Miguel-Ruiz, J.E., García-Arrarás, J.E., 2007. Common cellular events occur during wound healing and organ regeneration in the sea cucumber *Holothuria glaberrima*. BMC Developmental Biology 7, 115. https://doi.org/10.1186/1471-213X-7-115

Shimomura, O., 2006. Bioluminescence: chemical principles and methods, World Scientific Publishing Co.Pt.Ltd. ed. Hackensack.

Shimomura, O., Johnson, F.H., Saiga, Y., 1962. Extraction, Purification and Properties of Aequorin, a Bioluminescent Protein from the Luminous Hydromedusan *Aequorea*. Journal of Cellular and Comparative Physiology 59, 223–239. https://doi.org/10.1002/jcp.1030590302

The World Asteroidea Database [WWW Document], n.d. URL http://www.marinespecies.org/asteroidea/aphia.php?p=browser&id[]=254801&id[]=369151&id[]=369152&id[]=254802&id[]=582528&id[]=123087&id[]=123126&id[]=123240#focus (accessed 12.24.19).

Thompson, E.M., Toya, Y., Goto, T., Tsuji, F.I., 1988. Induction of bioluminescence capability in the marine fish, *Porichthys notatus*, by *Vargula* (Crustacean) [^{14}C] luciferin and unlabelled analogues. The Journal of Experimental Biology 137, 39–51.

Trimmer, B.A., Aprille, J.R., Dudzinski, D.M., Lagace, Chr.J., Lewis, S.M., Michel, Th., Qazi, S., Zayas, R.M., 2001. Nitric Oxide and the Control of Firefly Flashing. Science 292, 2486–2488. https://doi.org/10.1126/science.1059833

Watling, L., Guinotte, J., Clark, M.R., Smith, C.R., 2013. A proposed biogeography of the deep ocean floor. Progress in Oceanography 111, 91–112. https://doi.org/10.1016/j.pocean.2012.11.003

Widder, E.A., 2010. Bioluminescence in the Ocean: Origins of Bioluminescence, Chemical, and Ecological Diversity. Science 328, 704–708.

Widder, E.A., Latz, M.I., Case, J.F., 1983. Marine bioluminescence measured with an optical multichannel detection system. The Biological Bulletin 165, 791–810. https://doi.org/10.2307/1541479

Woolley, S.N.C., Tittensor, D.P., Dunstan, P.K., Guillera-Arroita, G., Lahoz-Monfort, J.J., Wintle, B.A., Worm, B., O'Hara, T.D., 2016. Deep-sea diversity patterns are shaped by energy availability. Nature 533, 393–396. https://doi.org/10.1038/nature17937

Young, R.E., 1983. Oceanic Bioluminescence: An Overview of General Functions. Bulletin of Marine Biology 33, 829-845

Young, R.E., Arnold, J.M., 1982. The functional morphology of a ventral photophore from the mesopelagic squid, *Abralia trigonura*. Malacologia 22, 135–163.

Yuste, R., 2005. Fluorescence microscopy today. Nature Methods 2, 902–904. https://doi.org/10.1038/nmeth1205-902

Zaccone, G., Abelli, L., Salpietro, L., Zaccone, D., Macrì, B., Marino, F., 2011. Nervous control of photophores in luminescent fishes. Acta Histochemica 113, 387–394. https://doi.org/10.1016/j.acthis.2010.03.007

6 Supplementary data

Table S1. Table indicating Operation number, Site (represented in *Fig.S1*), Name code, Equipment used, the date, hour, latitude, longitude and depth at the start of the operation as well as date, hour, latitude, longitude and depth at the end of the operation. Yellow indicates operations from which echinoderm samples were tested. Green indicates other sites at which echinoderms where collected. Adapted from O'Hara 2017.

Operation	Site	Station name	Equipment	Start date	start time	start lat	start lon	start depth	End date	End time	End lat	End lon	End depth
1	1	Freycinet (outside)	McKenna demersal fish trawl nets	16-mai-17	18:11:00	-41,4915	148,9407		16-mai-17	18:11:00	-41,5522	148,997	
2	1	Freycinet (outside)	McKenna demersal fish trawl nets	17-mai-17	8:56:00	-41,6268	149,1493	0	17-mai-17	11:34:00	-41,5127	149,0753	1500
3	1	Freycinet (outside)	McKenna demersal fish trawl nets	17-mai-17	16:27:00	-41,651	149,298	2948	17-mai-17	21:09:00	-41,6742	149,054	2787
4	1	Frey_2500_BT	CSIRO Four Metre Beam Trawl	18-mai-17	1:03:00	-41,7305	149,1197	2820	18-mai-17	2:59:00	-41,7913	149,1558	2751
5	1	Frey_2500_BS	Brenke Epibenthic Sledge	18-mai-17	7:15:00	-41,7303	149,135	2789	18-mai-17	8:06:00	-41,753	149,147	2779
6	2	Frey_4000_BT	CSIRO Four Metre Beam Trawl	18-mai-17	14:14:00	-41,62555	149,5515	4022	18-mai-17	16:38:00	-41,6892	149,5843	4052
7	2	Frey_4000_BC	Biological Box Corer	18-mai-17	22:05:00	-41,6472	149,5695	4030					
8	2	Frey_4000_BC	Biological Box Corer	19-mai-17	2:51:00	-41,6472	149,5693	4012					
9	2	Frey_4000_BS	Brenke Epibenthic Sledge	19-mai-17	7:39:00	-41,626	149,56	4021	19-mai-17	9:06:00	-41,662	149,574	4035
10	2	Frey_2500_TC	Deep Towed Camera System	19-mai-17	3:22:00								
11	2	Frey_2500_BC	Biological Box Corer	19-mai-17	17:58:00	-41,7207	149,1252	2793					
12	2	Frey_2500_TC	Deep Towed Camera System	19-mai-17	21:12:00	-41,7242	148,9845	1671	19-mai-17	23:25:00	-41,7267	149,0489	2516
13	3	Flin_1000_BT	CSIRO Four Metre Beam Trawl	20-mai-17	11:51:00	-40,386	148,928	932	20-mai-17	12:32:00	-40,383	148,951	1151
14	3	Flin_2500_BT	CSIRO Four Metre Beam Trawl	20-mai-17	16:02:00	-40,464	149,1015	2298	20-mai-17	17:16:00	-40,4613	149,1467	2486
15	4	Flin_4000_BT	CSIRO Four Metre Beam Trawl	20-mai-17	23:39:00	-40,4732	149,3967	4114	21-mai-17	0:44:00	-40,464	149,4255	4139
16	4	Flin_4000_BS	Brenke Epibenthic Sledge	21-mai-17	7:38:00	-40,463	149,415	4129	21-mai-17	9:28:00	-40,4612	149,364	4131
17	4	Flin_2500_BC	Biological Box Corer	21-mai-17	15:16:00	-40,4598	149,1085	2331					
18	4	Flin_2500_Manta_1	Manta plankton net	21-mai-17	16:28:00	-40,4563	149,1013	0	21-mai-17	16:43:00	-40,4537	149,0958	0
19	4	Flin_2500_Manta_2	Manta plankton net	21-mai-17	16:50:00	-40,4527	149,0938	0	21-mai-17	17:04:00	-40,4507	149,09	0
20	4	Flin_2500_Manta_3	Manta plankton net	21-mai-17	17:06:00	-40,4503	149,0893	0	21-mai-17	17:21:00	-40,4475	149,0842	0
21	4	Flin_2500_TC	Deep Towed Camera System	21-mai-17	20:00:00								
22	5	Bass_2500_BT	CSIRO Four Metre Beam Trawl	22-mai-17	8:05:00	-39,462	149,276	2760	22-mai-17	9:08:00	-39,465	149,242	2692
23	5	Bass_2500_BS	Brenke Epibenthic Sledge	22-mai-17	13:00:00	-39,462	149,277	2774	22-mai-17	10:00:00	-39,465	149,246	2694
24	5	Bass_2500_Manta_1	Manta plankton net	22-mai-17	15:32:00	-39,469	149,2155	0	22-mai-17	15:47:00	-39,4672	149,2307	0
25	5	Bass_2500_Manta_2	Manta plankton net	22-mai-17	15:49:00	-39,467	149,2333	0	22-mai-17	16:04:00	-39,4655	149,248	0
26	5	Bass_2500_Manta_3	Manta plankton net	22-mai-17	16:06:00	-39,4652	149,2505	0	22-mai-17	16:21:00	-39,4632	149,2655	0
27	5	Bass_2500_BC	Biological Box Corer	22-mai-17	18:33:00	-39,4623	149,2712	2741					
28	6	Bass_4000_BC	Biological Box Corer	22-mai-17	23:53:00	-39,4995	149,5348	4147					
29	6	Bass_4000_MesoZoo	Meso zooplankton net	23-mai-17	1:55:00	-39,5068	149,5313	1	23-mai-17	2:14:00	-39,5173	149,5268	1
30	6	Bass_4000_BT	CSIRO Four Metre Beam Trawl	23-mai-17	4:30:00	-39,552	149,553	4197	23-mai-17	5:57:00	-39,496	149,598	4133
31	6	Bass_4000_BS	Brenke Epibenthic Sledge	23-mai-17	11:09:00	-39,422	149,604	4150	23-mai-17	12:30:00	-39,391	149,597	4170
32	7	East_Gipps_4000_BT	CSIRO Four Metre Beam Trawl	24-mai-17	1:03:00	-38,479	150,1845	3850	24-mai-17	2:02:00	-38,453	150,186	3853
33	7	East_Gipps_4000_BS	Brenke Epibenthic Sledge	24-mai-17	9:00:00	-38,521	150,213	4107	24-mai-17	10:00:00	-38,498	150,207	4064
34	8	East_Gipps_2500_TC	Deep Towed Camera System	24-mai-17	15:39:00	-38,3653	150,0627	2357	24-mai-17	16:02:00	-38,3565	150,0652	2594
35	8	East Gipps_2500_BT	CSIRO Four Metre Beam Trawl	25-mai-17	13:16:00	-37,792	150,382	2338	25-mai-17	14:33:00	-37,8178	150,353	2581
36	8	East_Gipps_2500_Manta_1	Manta plankton net	25-mai-17	15:46:00	-37,8687	150,3098	0	25-mai-17	16:03:00	-37,8668	150,3122	0
37	8	East_Gipps_2500_Manta_2	Manta plankton net	25-mai-17	16:06:00	-37,8665	150,3125	0	25-mai-17	16:21:00	-37,8642	150,3145	0
38	8	East_Gipps_2500_Manta_3	Manta plankton net	25-mai-17	16:23:00	-37,864	150,3148	0	25-mai-17	16:38:00	-37,8617	150,3167	0
39	8	East_Gipps_2500_MesoZoo	Meso zooplankton net	25-mai-17	16:43:00	-37,861	150,3173	0	25-mai-17	16:58:00	-37,8593	150,319	1
40	8	East_Gipps_2500_BS	Brenke Epibenthic Sledge	25-mai-17	19:22:00	-37,815	150,3733	2746	25-mai-17	20:05:00	-37,8177	150,3558	2600
41	9	Berm_4000_BT	CSIRO Four Metre Beam Trawl	26-mai-17	8:33:00	-36,418	150,8	3980	26-mai-17	8:43:00			
42	9	Berm_4000_BS	Brenke Epibenthic Sledge	26-mai-17	17:02:00	-36,3853	150,863	4744	26-mai-17	18:30:00	-36,4335	150,8632	4716
43	9	Berm_4800_BT	CSIRO Four Metre Beam Trawl	27-mai-17	1:19:00	-36,3507	150,9143	4000	27-mai-17	2:38:00	-36,384	150,913	
44	10	Berm_2500_BT	CSIRO Four Metre Beam Trawl	27-mai-17	10:39:00	-36,355	150,644	2821	27-mai-17	12:14:00	-36,315	150,651	2687
45	10	Berm_2500_BS	Brenke Epibenthic Sledge	27-mai-17	19:05:00	-36,3603	150,6435	2835	27-mai-17	20:28:00	-36,3232	150,6502	2739
46	10	Berm_2500_BC	Biological Box Corer	27-mai-17	23:44:00	-36,2838	150,6578	2643					
47	10	Berm_2500_Manta_1	Manta plankton net	27-mai-17	14:01:00	-36,2913	150,6555	0	27-mai-17	14:16:00	-36,3017	150,6548	0
48	10	Berm_2500_Manta_2	Manta plankton net	27-mai-17	14:18:00	-36,3053	150,6538	0	27-mai-17	14:33:00	-36,3132	150,653	0
49	10	Berm_2500_Manta_3	Manta plankton net	27-mai-17	14:36:00	-36,3147	150,6528	0	27-mai-17	14:51:00	-36,3252	150,6522	0
50	10	Berm_2500_MesoZoo_1	Meso zooplankton net	27-mai-17	14:56:00	-36,3288	150,6518	1	27-mai-17	15:11:00	-36,3395	150,6512	1
51	10	Berm_2500_MesoZoo_2	Meso zooplankton net	27-mai-17	15:14:00	-36,342	150,6508	1	27-mai-17	15:29:00	-36,3515	150,6495	1
52	10	Berm_2500_MesoZoo_3	Meso zooplankton net	27-mai-17	15:31:00	-36,3528	150,6492	1	27-mai-17	15:46:00	-36,3617	150,6478	1
53	11	Jervis_4000_BT	CSIRO Four Metre Beam Trawl	28-mai-17	11:42:00	-35,114	151,469	3952	28-mai-17	13:13:00	-35,084	151,441	4011
54	11	Jervis_4000_BS	Brenke Epibenthic Sledge	28-mai-17	17:11:00	-35,1168	151,473	4026	28-mai-17	18:29:00	-35,0992	151,4547	3881
55	12	Jervis_2500_BS	Brenke Epibenthic Sledge	28-mai-17	23:36:00	-35,3352	151,2593	2667	29-mai-17	0:45:00	-35,334	151,2185	2665
56	12	Jervis_2500_BT	CSIRO Four Metre Beam Trawl	29-mai-17	5:13:00	-35,333	151,258	2650	29-mai-17	6:29:00	-35,332	151,214	2636
57	12	Jervis_2500_BC	Biological Box Corer										
58	12	Jervis_2500_TC	Deep Towed Camera System	29-mai-17	15:50:00	-35,2958	151,1545	2126	29-mai-17	16:42:00	-35,3038	151,1353	2355
59	12	Jervis_2500_Manta_1	Manta plankton net	29-mai-17	15:10:00	-35,2977	151,1518	0	29-mai-17	15:25:00	-35,3017	151,1433	0
60	12	Jervis_2500_Manta_2	Manta plankton net	29-mai-17	15:27:00	-35,302	151,1423	0	29-mai-17	15:42:00	-35,306	151,1332	0
61	12	Jervis_2500_Manta_3	Manta plankton net	29-mai-17	15:44:00	-35,3065	151,1322	0	29-mai-17	15:59:00			0
62	12	Jervis_2500_MesoZoo_1	Meso zooplankton net	29-mai-17	16:05:00	-35,3123	151,119	0	29-mai-17	16:20:00	-35,3162	151,1095	1
63	12	Jervis_2500_MesoZoo_2	Meso zooplankton net	29-mai-17	16:22:00	-35,317	151,1078	0	29-mai-17	16:37:00	-35,3213	151,098	1
64	12	Jervis_2500_MesoZoo_3	Meso zooplankton net	29-mai-17	16:39:00			0	29-mai-17	16:54:00	-35,3265	151,0877	1
65	13	Newc_4000_BT	CSIRO Four Metre Beam Trawl	30-mai-17	13:16:00	-33,441	152,702	4280	30-mai-17	14:22:00	-33,435	152,665	4173

66	13	Newc_4000_BS	Brenke Epibenthic Sledge	30-mai-17	19:27:00	-33,4482	152,7328	4378	30-mai-17	21:13:00	-33,4368	152,6737	4195
67	14	Newc_2500_BT	CSIRO Four Metre Beam Trawl	31-mai-17	9:04:00	-32,985	152,952	2704	31-mai-17	7:33:00	-33,015	152,913	2902
68	14	Newc_2500_BS	Brenke Epibenthic Sledge	31-mai-17	10:52:00	-32,993	152,957	2745	31-mai-17	12:20:00	-33,023	152,943	2963
69	15	Hunter_1000_BT	CSIRO Four Metre Beam Trawl	03-juin-17	11:59:00	-32,479	152,994	1006	03-juin-17	12:51:00	-32,507	152,991	1036
70	15	Hunter_2500_BT	CSIRO Four Metre Beam Trawl	03-juin-17	16:22:00	-32,575	153,1617	2595	03-juin-17	17:34:00	-32,63164	153,142	2474
71	15	Hunter_2500_Manta_1	Manta plankton net	03-juin-17	15:19:00	-32,5798	153,1612	0	03-juin-17	15:34:00	-32,5905	153,1578	0
72	15	Hunter_2500_Manta_2	Manta plankton net	03-juin-17	15:36:00	-32,592	153,1575	0	03-juin-17	15:51:00	-32,6035	153,1542	0
73	15	Hunter_2500_Manta_3	Manta plankton net	03-juin-17	15:53:00	-32,6047	153,1538	0	03-juin-17	16:08:00	-32,6145	153,1497	0
74	15	Hunter_2500_MesoZoo_1	Meso zooplankton net	03-juin-17	17:45:00	-32,6515	153,1368	1	03-juin-17	18:00:00	-32,6628	153,1335	1
75	15	Hunter_2500_MesoZoo_2	Meso zooplankton net	03-juin-17	18:02:00	-32,6648	153,133	1	03-juin-17	18:17:00	-32,6768	153,1288	1
76	15	Hunter_2500_BS	Brenke Epibenthic Sledge	03-juin-17	21:22:00	-32,5772	153,1607	2534	03-juin-17	22:38:00	-32,613	153,1488	2480
77	15	Hunter_1700_TC	Deep Towed Camera System	04-juin-17	4:20:00	-32,094	153,253	1741	04-juin-17	5:33:00	-32,115	153,251	2115
78	16	Hunter_4000_BT	CSIRO Four Metre Beam Trawl	04-juin-17	11:01:00	-32,138	153,527	3980	04-juin-17	12:48:00	-32,182	153,524	4029
79	16	Hunter_4000_BS	Brenke Epibenthic Sledge	04-juin-17	17:48:00	-32,1308	152,5273	4000	04-juin-17	19:09:00	-32,1626	153,5236	4031
80	17	Cent_East_1000_BT	CSIRO Four Metre Beam Trawl	05-juin-17	11:07:00	-30,099	153,596	1257	05-juin-17	12:24:00	-30,128	153,571	1194
81	17	Cent_East_1500_TC	Deep Towed Camera System	05-juin-17	16:29:00	-30,0444	153,7513	1511	05-juin-17	18:26:00	-30,09635	153,7296	2246
82	17	Cent_East_1500_Manta_1	Manta plankton net	05-juin-17	15:58:00	-30,0392	153,7543	0	05-juin-17	16:13:00	-30,0483	153,7505	0
83	17	Cent_East_1500_Manta_2	Manta plankton net	05-juin-17	16:16:00	-30,05	153,7497	0	05-juin-17	16:31:00	-30,061	153,745	0
84	17	Cent_East_1500_Manta_3	Manta plankton net	05-juin-17	16:33:00	-30,0618	153,7445	0	05-juin-17	16:48:00	-30,0695	153,741	0
85	17	Cent_East_1500_MesoZoo_	Meso zooplankton net	05-juin-17	16:54:00	-30,0725	153,7395	0	05-juin-17	17:09:00	-30,0802	153,7367	1
86	17	Cent_East_2500_BT	CSIRO Four Metre Beam Trawl	05-juin-17	23:48:00	-30,0977	153,8987	2429	06-juin-17	0:52:00	-30,1193	153,8745	2518
87	17	Cent_East_2500_BS	Brenke Epibenthic Sledge	06-juin-17	3:56:00	-30,113	153,898	2634	06-juin-17	5:18:00	-30,116	153,867	2324
88	18	Cent_East_4000_BT	CSIRO Four Metre Beam Trawl	06-juin-17	14:17:00	-30,264	153,87	4481	06-juin-17	16:26:00	-30,2867	153,8302	4401
89	18	Cent_East_4000_BS	Brenke Epibenthic Sledge	06-juin-17	22:48:00	-30,2633	153,8587	4436	07-juin-17	0:03:00	-30,2893	153,8438	4414
90	19	Byron_2500_BT	CSIRO Four Metre Beam Trawl	07-juin-17	16:28:00	-28,6765	154,2032	2587	07-juin-17	17:56:00	-28,709	154,1897	2562
91	19	Byron_2500_Manta_1	Manta plankton net	07-juin-17	15:18:00	-28,6695	154,2073	0	07-juin-17	15:33:00	-28,6747	154,2052	0
92	19	Byron_2500_Manta_2	Manta plankton net	07-juin-17	15:35:00	-28,6757	154,2048	0	07-juin-17	15:50:00	-28,6817	154,2027	0
93	19	Byron_2500_Manta_3	Manta plankton net	07-juin-17	15:53:00	-28,6827	154,2022	0	07-juin-17	16:08:00	-28,6887	154,1998	0
94	19	Byron_2500_MesoZoo_1	Meso zooplankton net	07-juin-17	16:13:00	-28,6903	154,1992	0	07-juin-17	16:28:00	-28,6962	154,1968	1
95	19	Byron_2500_MesoZoo_2	Meso zooplankton net	07-juin-17	16:31:00	-28,697	154,1965	0	07-juin-17	16:49:00	-28,704	154,1937	1
96	19	Byron_2500_BS	Brenke Epibenthic Sledge	07-juin-17	21:13:00	-28,6778	154,2037	2591	07-juin-17	22:43:00	-28,7158	154,189	2566
97	20	Byron_4000_BT	CSIRO Four Metre Beam Trawl	08-juin-17	10:54:00	-28,355	154,636	3762	08-juin-17	12:38:00	-28,414	154,615	3803
98	20	Byron_4000_BS	Brenke Epibenthic Sledge	08-juin-17	18:31:00	-28,3713	154,6472	3811	08-juin-17	19:53:00	-28,3888	154,6123	3754
99	20	Byron_4000_BT_2	CSIRO Four Metre Beam Trawl	09-juin-17	0:14:00	-28,371	154,6487	3825	09-juin-17	1:33:00	-28,3875	154,617	3754
100	20	Byron_1000_BT	CSIRO Four Metre Beam Trawl	09-juin-17	7:27:00	-28,0544	154,083	999	09-juin-17	8:47:00	-28,097	154,081	1013
101	21	Moreton_2500_BT	CSIRO Four Metre Beam Trawl	09-juin-17	17:43:00	-26,9458	153,945	2520	09-juin-17	18:48:00	-26,9712	153,9512	2576
102	22	Moreton_4000_BT	CSIRO Four Metre Beam Trawl	10-juin-17	1:32:00	-27,0078	154,2232	4274	10-juin-17	3:07:00	-27,049	154,224	4264
103	22	Moreton_4000_BS	Brenke Epibenthic Sledge	10-juin-17	8:52:00	-27,0003	154,223	4260	10-juin-17	10:30:00	-27,061	154,223	4280
104	22	Moreton_1000_BT	CSIRO Four Metre Beam Trawl	10-juin-17	16:00:00	-26,9613	153,8475	1071	10-juin-17	17:01:00	-26,9913	153,8468	1138
105	22	Moreton_1000_Manta_1	Manta plankton net	10-juin-17	15:45:00	-26,9622	153,8477	0					
106	22	Moreton_1000_Manta_2	Manta plankton net	10-juin-17	16:03:00	-26,9713	153,848	0	10-juin-17	16:18:00			0
107	22	Moreton_1000_Manta_3	Manta plankton net	10-juin-17	16:19:00	-26,98	153,848	0	10-juin-17	16:34:00	-26,9882	153,8478	0
108	22	Moreton_1000_MesoZoo_1	Meso zooplankton net	10-juin-17	16:37:00	-26,9895	153,8478	1	10-juin-17	17:00:00	-27,0013	153,8475	1
109	23	Fraser_4000_BT	CSIRO Four Metre Beam Trawl	11-juin-17	7:46:00	-25,221	154,164	4006	11-juin-17	9:22:00	-25,253	154,192	4005
110	23	Fraser_4000_BS	Brenke Epibenthic Sledge	11-juin-17	14:09:00	-25,2198	154,1602	4005	11-juin-17	15:53:00	-25,2605	154,2	4010
111	23	Fraser_4000_Manta_1	Manta plankton net	11-juin-17	14:32:00	-25,2562	154,1945	0	11-juin-17	14:47:00	-25,2628	154,2008	0
112	23	Fraser_4000_Manta_2	Manta plankton net	11-juin-17	14:49:00	-25,2637	154,2018	0	11-juin-17	15:04:00	-25,2697	154,2078	0
113	23	Fraser_4000_Manta_3	Manta plankton net	11-juin-17	15:06:00	-25,2703	154,2085	0	11-juin-17	15:21:00	-25,2768	154,2147	0
114	23	Fraser_4000_MesoZoo_1	Meso zooplankton net	11-juin-17	15:20:00	-25,2768	154,2147	0	11-juin-17	15:44:00	-25,2818	154,2192	1
115	24	Fraser_2500_BT	CSIRO Four Metre Beam Trawl	11-juin-17	20:56:00	-25,3253	154,0683	2350	11-juin-17	21:56:00	-25,3513	154,076	2342
116	24	Fraser_2500_MesoZoo_2	Meso zooplankton net	11-juin-17	20:08:00	-25,3193	154,0665	1	11-juin-17	20:24:00	-25,3278	154,0695	1
117	24	Fraser_2500_MesoZoo_3	Meso zooplankton net	11-juin-17	20:27:00	-25,3295	154,0702	3	11-juin-17	20:47:00	-25,3398	154,0733	3
118	24	Fraser_2500_BS	Brenke Epibenthic Sledge	11-juin-17	20:56:00	-25.3253	154.0683	2350	11-juin-17	21:56:00	-25.3513	154.076	2342
119	24	Fraser_2500_BS	Brenke Epibenthic Sledge	12-juin-17	4:48:00	-25,206	153,991	2247	12-juin-17	6:10:00	-25,178	153,979	2369
120	23	Fraser_4000_FT	McKenna demersal fish trawl nets	12-juin-17	11:00:00	-25,1478	154,1557	3993	12-juin-17	17:45:00	-25,0577	154,1463	
121	25	Coral_Sea_1000_BT	CSIRO Four Metre Beam Trawl	13-juin-17	2:31:00	-23,587	154,194	1013	13-juin-17	3:31:00	-23,617	154,1947	1093
122	25	Coral_Sea_2500_BT	CSIRO Four Metre Beam Trawl	13-juin-17	10:41:00	-23,751	154,639	2369	13-juin-17	11:56:00	-23,773	154,616	2329
123	25	Coral_Sea_2500_BS	Brenke Epibenthic Sledge	13-juin-17	14:46:00	-23,7485	154,6413	2271	13-juin-17	15:56:00	-23,774	154,6172	2339
124	25	Coral_Sea_2500_Manta_1	Manta plankton net	13-juin-17	13:58:00	-23,746	154,6435	0	13-juin-17	14:13:00	-23,7497	154,6407	0
125	25	Coral_Sea_2500_Manta_2	Manta plankton net	13-juin-17	14:15:00	-23,7502	154,6402	0	13-juin-17	14:30:00	-23,7568	154,634	0
126	25	Coral_Sea_2500_Manta_3	Manta plankton net	13-juin-17	14:32:00	-23,7578	154,6278	0	13-juin-17	14:49:00	-23,7653	154,6278	0
127	25	Coral_Sea_2500_MesoZoo_	Meso zooplankton net	13-juin-17	14:54:00	-23,7673	154,6257	1	13-juin-17	15:15:00	-23,7757	154,6177	1
128	25	Coral_Sea_2000_BT	CSIRO Four Metre Beam Trawl	13-juin-17	21:05:00	-23,6312	154,6597	1770	13-juin-17	22:17:00	-23,659	154,6438	1761
129	25	Coral_Sea_2000_MesoZoo_	Meso zooplankton net	13-juin-17	20:33:00	-23,6297	154,661	3	13-juin-17	20:53:00	-23,6378	154,6568	3
130	25	Coral_Sea_2000_MesoZoo_	Meso zooplankton net	13-juin-17	20:56:00	-23,639	154,6562	1	13-juin-17	21:16:00	-23,6467	154,6518	1
131	25	Coral_Sea_2500_BS_2	Brenke Epibenthic Sledge	14-juin-17	3:21:00	-23,748	154,643	2297	14-juin-17	4:43:00	-23,778	154,613	2358
132	25	Coral_Sea_2500_BS_3	Brenke Epibenthic Sledge	14-juin-17	7:53:00	-23,756	154,568	2181	14-juin-17	9:13:00	-23,78	154,54	2132
133	25	Coral_Sea_1700_TC	Deep Towed Camera System	14-juin-17	12:10:00	-23,6312	154,6597	1753	14-juin-17	16:35:00	-23,659	154,6438	
134	25	Coral_Sea_2500_BS_4	Brenke Epibenthic Sledge	14-juin-17	18:32:00	-23,7503	154,5718	2093	14-juin-17	19:46:00	-23,7739	154,5464	2156
135	26	Coral_Sea_4000_BT	CSIRO Four Metre Beam Trawl	15-juin-17	4:36:00	-24,352	154,291	3968	15-juin-17	6:18:00	-24,384	154,325	4034
136	26	Coral_Sea_4000_CTD	Brenke Epibenthic Sledge										

Table S2. Samples used for the luciferin assays come from the same thalassometrid 69_148. Weight is the sample weight. Volume indicates the volume of cold argon-saturated methanol. Dilution corresponds to the 5 µL extracted from the tissue mixture divided by the whole methanol volume. Filter indicates how much light comes through where 1 is the total light emitted. Source is the value obtained measuring the tritium source that allows conversion from RLU to q. Time indicates the total measurement time.

Family	Code IN2017_V03	Sample	Test	Weight (g)	Volume (µl)	Dilution	Filter	Source (q/RLU)	Time (s)
Thalassometridae	69_148	2	luciferine	0.0600	400	0.0125	1	16.96	190
Thalassometridae	69_148	4	luciferine	0.0155	200	0.0250	1	16.96	190
Thalassometridae	69_148	6	luciferine	0.0297	200	0.0250	1	16.96	190
Thalassometridae	69_148	9	luciferine	0.0282	300	0.0167	1	16.96	190
Thalassometridae	69_148	10	luciferine	0.0314	300	0.0167	1	16.96	190

Table S3. All samples for the luciferase assays come from the same thalassometrid 69_148. Weight is the sample's weight. Volume indicates the volume of Tris buffer used to crush the samples. Extract is the volume taken from the tissue mixture. Dilution corresponds to the extracted volume divided by the whole Tris buffer volume. Mean dilution is the mean between the three dilutions per sample. Filter indicates how much light comes through where 1 is the total light emitted. The value obtained measuring the tritium source that allows conversion from RLU to q is 16.96.

Family	Code IN2017_V03	Sample	Test	Weight (g)	Volume (µL)	Extract (µL)	Dilution	Mean dilution	Filter
Thalassometridae	69_148	1	luciferase	0.033	300	40	0.133	0.0778	0.002
						20	0.067		
						10	0.033		
Thalassometridae	69_148	5	luciferase	0.0207	200	40	0.200	0.1167	0.002
						20	0.100		
						10	0.050		
Thalassometridae	69_148	11	luciferase	0.0223	200	40	0.200	0.1167	0.002
						20	0.100		
						10	0.050		
Thalassometridae	69_148	12	luciferase	0.0231	200	40	0.200	0.1167	0.002
						20	0.100		
						10	0.050		
Thalassometridae	69_150	13	luciferase	0.0419	300	40	0.133	0.0778	0.002
						20	0.067		
						10	0.033		
Thalassometridae	69_153	14	luciferase	0.0335	300	40	0.133	0.0778	0.002
						20	0.067		
						10	0.033		
Thalassometridae	69_157	15	luciferase	0.0244	300	40	0.133	0.0778	0.002
						20	0.067		
						10	0.033		

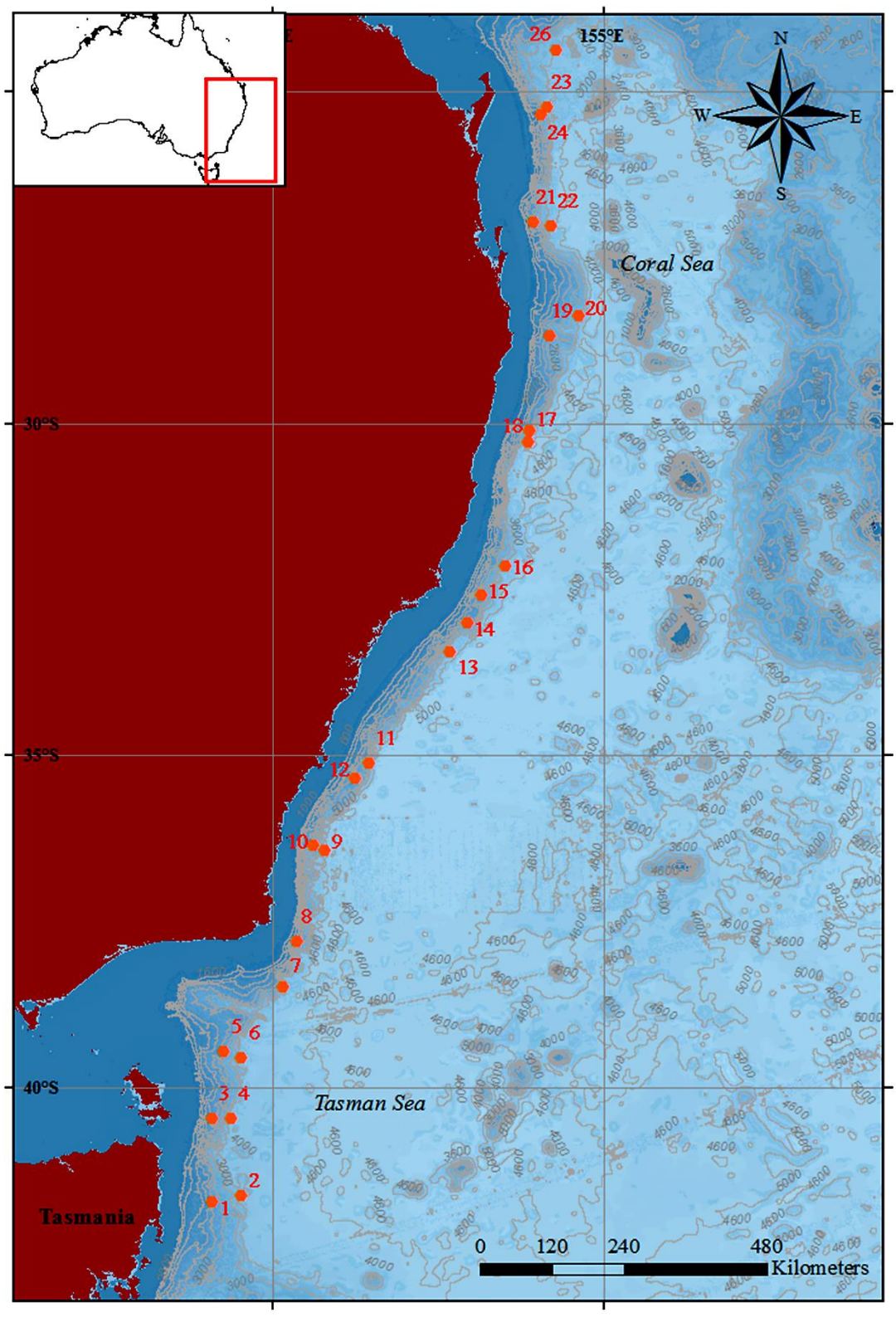

Figure S1. Supplementary map indicating sampling sites as red dots with their respective number. Red represents heights above sea level. Grey lines are bathymetric lines and associated numbers indicated the respective depth. The upper right corner presents a map of Australia with the red rectangle framing the relative position of the main map. By Constance Coubris.

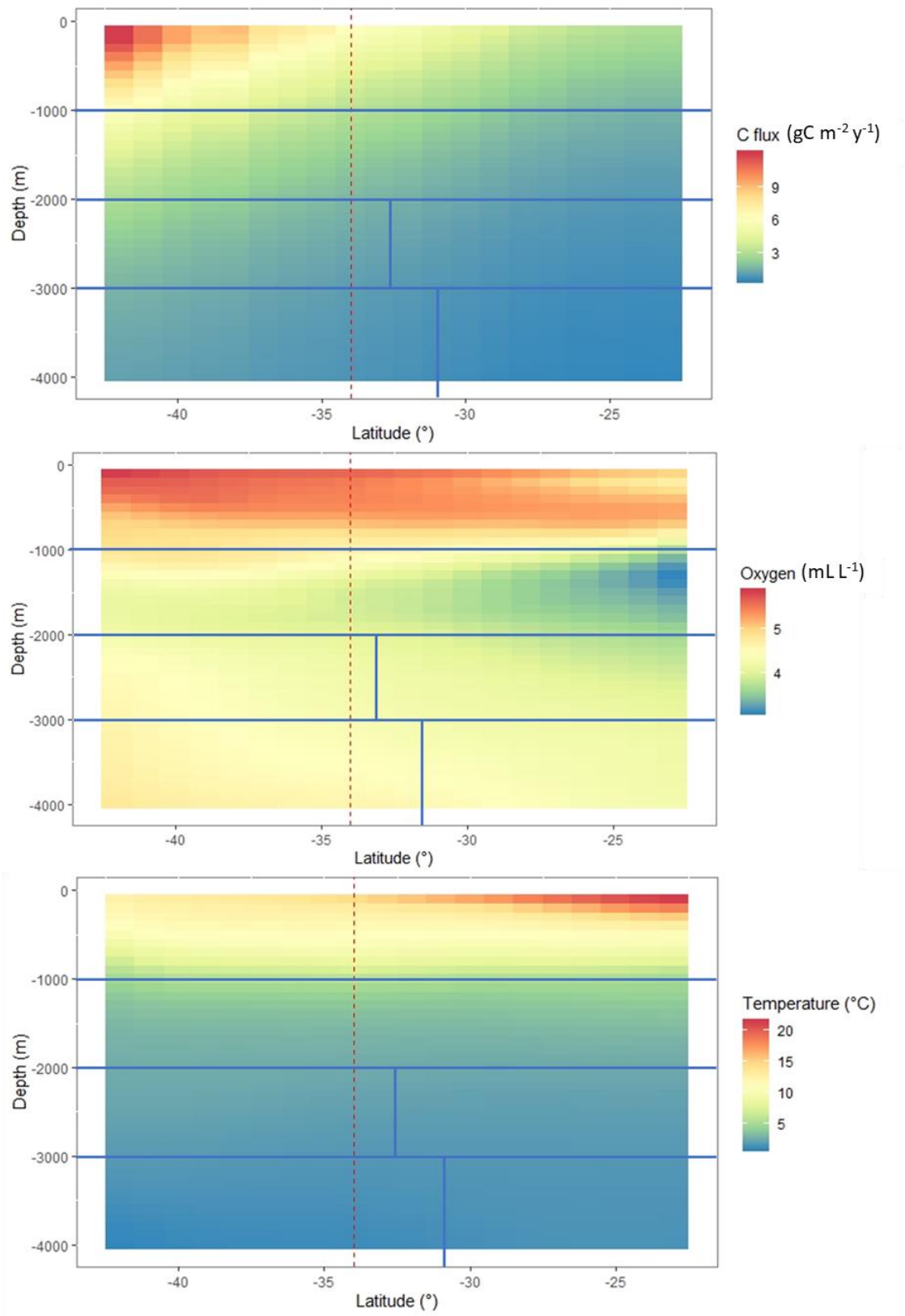

Figure S2 Tile graph showing mean annual A. carbon flux, B. oxygen, C. temperature between the latitudes 23° and 43° South and between 100 and 4000 m depth. Measurements are given at every 100 m depth at all latitudinal degree. The red dashed line indicates the tropical-temperate division made by O'Hara et al., 2019, at 34° South. Blue lines divide the graph horizontally into our three depth groups and vertically into tropical-temperate division according to our SIMPROF result Adapted from O'Hara et al., 2019.

Table S4. Output for the Spearman correlation matrix. Variables in yellow are the ones kept by the Escoufier method. Correlation coefficients are presented on the right side with font size proportional to the coefficient. Stars indicate significance following conventional criteria. Two by two crossed graphs present on the left. Script from David, 2017.S4

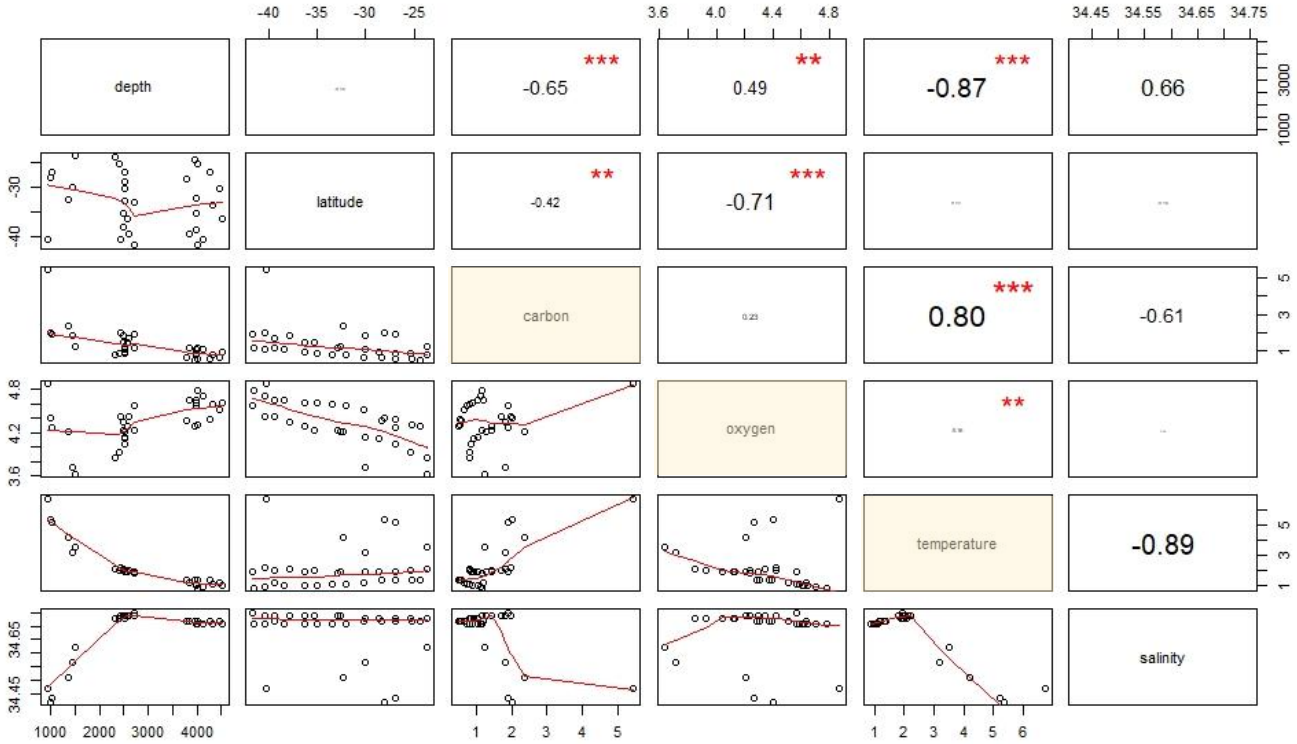

Table S5. Results from the different luminometry measurements done by Pr. Jérôme Mallefet presented in this work. Species indicates the species used. Code indicates the sample code given during the cruise. Body part indicates the part of the animal that was tested. Inducer indicates what was used to trigger light emission. L_{tot} indicates the Mq emitted in 180 s. L_{max} indicates the maximum peak intensity attained in that measurement (Mq s^{-1}). For detailed concentrations and arm sizes cf. to materials and methods.

Species	Code	Body part	Inducer	L_{tot} (Mq)	L_{max} (Mq s^{-1})
D. exilis	56_127	Arm distal	KCl	660.2	5.4
D. exilis	56_127	Arm distal	FW	105.5	3.2
D. exilis	56_127	Arm proximal	FW	317.5	8.9
D. exilis	56_127	Whole	FW	$2.7\ 10^4$	256.9
P. longicauda	56_111	Tail skin	FW	494.4	17.2
P. Longicauda	56_111	Tail skin	KCl	0.1	$8\ 10^{-3}$
P. longicauda	67_101	Tail skin	FW	$0.25\ 10^6$	$4\ 10^3$
P. longicauda	67_101	Tail skin	KCl	$4.5\ 10^3$	63.1
P. longicauda	90_111	Tail skin	KCl	75.1	0.5
O. rudis	103_106	Arm a distal	KCl	$3\ 10^6$	$2.2\ 10^4$
O. rudis	103_106	Arm a proximal	KCl	$1.2\ 10^6$	$1.1\ 10^4$
O. rudis	103_106	Arm b1 distal	KCl	$1.9\ 10^6$	$2.1\ 10^4$
O. rudis	103_106	Arm b1 median	KCl	$1.3\ 10^6$	$1.3\ 10^4$
O. rudis	103_106	Arm b1 proximal	KCl	$0.4\ 10^6$	$3.9\ 10^3$
O. rudis	103_106	Arm b2 distal	KCl	$3.8\ 10^6$	$2.1\ 10^4$
O. rudis	103_106	Arm b2 median	KCl	$0.5\ 10^6$	$5.4\ 10^3$
O. rudis	103_106	Arm b2 proximal	KCl	10^6	$9.3\ 10^3$
O. rudis	103_106	Arm c	ACh	49.1	2.6
O. rudis	103_106	Arm c	ACh	20.5	10
Thalassometridae	69_148	Arm a	Spo	426.9	4.7
Thalassometridae	69_148	Arm b	KCl	131.3	1.1
Thalassometridae	69_148	Arm c distal	FW	$1.6\ 10^3$	55
Thalassometridae	69_148	Arm c proximal	FW	784	14.9
Thalassometridae	69_148	Arm d distal	FW	361.4	21.4
Thalassometridae	69_148	Arm d proximal	FW	$1.7\ 10^3$	91.4
Thalassometridae	69_148	Arm e	Adre	217.6	2.9
Thalassometridae	69_148	Arm f	Adre	119.9	5.2
Thalassometridae	69_148	Arm g	Adre	338.4	3.2
Thalassometridae	69_148	Arm h	Adre	693.2	11.7
Thalassometridae	69_148	Calyx	FW	30.2	0.2
Thalassometridae	69_148	Cirri	FW	1.6	1.3

Table S6. Results from the luciferin assays on the thalassometrid 69_148. Sample number indicates the reference for table S2. Integral is the total emission during the measurement divided by the time the measurement lasted. Source is the value obtained measuring the tritium source that allows conversion from RLU to q. Time indicates the duration of the measurement. Integral without filter corrects the emission for the filter value (here the filter value is 1). Mq in 190 s indicates the total emission during the whole measurement. Weight x dilution gives the amount of arm tissue used for the test, both values are presented in table S2. L_{tot} gives the total amount of q emitted per gram of arm tissue. The first coelenterazine column gives the amount of coelenterazine per gram of arm tissue in ng and the second column in nmol.

Sample	Integral (RLU s^{-1})	Source (q RLU^{-1})	Time (s)	Integral without filter (q s^{-1})	Mq in 190 s	Weight x Dilution (g)	L_{tot} (Mq g^{-1})	Coelenterazine (ng g_{arm}^{-1})	Coelenterazine (nmol g_{arm}^{-1})
2	175586	16.96	190	2.98 10^6	565.8	0.75 10^{-3}	754.4 10^3	2.99	0.0070
4	178850	16.96	190	3.04 10^6	577.8	0.39 10^{-3}	1.49 10^6	5.92	0.0139
6	193128	16.96	190	3.28 10^6	622.3	0.57 10^{-3}	1.08 10^6	4.3	0.0102
9	94083	16.96	190	1.6 10^6	303.2	0.47 10^{-3}	645 10^3	2.56	0.0060
10	219263	16.96	190	3.72 10^6	706.6	0.52 10^{-3}	1.35 10^6	5.36	0.0127

Table S7. Results from the luciferase assays on the thalassometrid 69_148. Sample number indicates the reference for table S3. Extract is the volume taken from the tissue mixture. L_{max} indicates the maximal number of quanta emitted per second during the measurement given in RLU. A slash indicates that the measurement had a problem and thus the value was dropped for the assay as it was deemed unnecessary to redo the measurement. Mean L_{max} gives the mean of all the L_{max} obtained for a sample. Source is the value obtained measuring the tritium source that allows conversion from RLU to q. L_{max} gives the mean L_{max} for each sample in q s^{-1}. L_{max} without filter corrects the emission for the filter value (here the filter value is 0.002). Weight x dilution gives the amount of arm tissue in used for the test, both values are presented in table S3. The dilution value was adapted for the measurements with a slash. Activity presents the luciferase activity.

Sample	Extract (µL)	L_{max} (RLU s^{-1})	Mean L_{max} (RLU s^{-1})	Source (q RLU^{-1})	L_{max}(q s^{-1})	L_{max} without filter (q s^{-1})	Weight x Dilution (g)	Activity (q g^{-1} s^{-1})
1	40	/	0.86 10^6	16.96	14.65 10^6	7.3 10^9	1.65 10^{-3}	4.43 10^{12}
	20	1611585						
	10	116170						
5	40	870280	0.67 10^6	16.96	11.3 10^6	5.63 10^9	3.1 10^{-3}	1.81 10^{12}
	20	462105						
	10	/						
11	40	2476565	2.03 10^6	16.96	34.46 10^6	17.18 10^9	3.3 10^{-3}	5.13 10^{12}
	20	1484330						
	10	/						
12	40	1154380	0.68 10^6	16.96	11.50 10^6	5.73 10^9	2.7 10^{-3}	2.13 10^{12}
	20	593365						
	10	286520						
13	40	4316065	2.77 10^6	16.96	47.06 10^6	23.46 10^9	3.3 10^{-3}	7.2 10^{12}
	20	2753090						
	10	1255670						
14	40	2579860	1 83 10^6	16.96	31.11 10^6	15.51 10^9	2.6 10^{-3}	5.96 10^{12}
	20	1758185						
	10	1164445						
15	40	1703590	1.14 10^6	16.96	19.3 10^6	9.62 10^9	1.9 10^{-3}	5.07 10^{12}
	20	1078960						
	10	631140						

Table S8 Tables with revisited list of bioluminescent echinoderms: A. Asteroidea. B. Crinoidea. C. Holothuroidea. D. Ophiuroidea. Codes in the species column refer to the codes used during the cruise for the respective unidentified species. Author column indicates the author of the original description of the species. The IN2017_V03 column indicates if the species was observed during S*ampling the Abyss*. BL description refers to either the cruise during which the bioluminescence was supposedly first observed, the author of the publication first describing the light emission, List Mallefet indicates Mallefet personal communications that are probably already published.

A.

Class	Order	Family	Genus	Species	Author	IN20 17_V03	BL description
Asteroidea				40_128		Observed	IN2017_V03
Asteroidea	Brisingida	Brisingidae	*Brisinga*	*endecacnemos*	Asbjornsen 1856		Harvey 1952
Asteroidea	Brisingida	Brisingidae	*Hymenodiscus*	*coronata*	(Sars 1871)		Herring 1995 *Brisingella coronata*
Asteroidea	Brisingida	Brisingidae	*Novodinia*	*americana*	(Verrill 1880)		Birk et al. 2018
Asteroidea	Brisingida	Freyellidae	*Freyella*	78_103; 109_105; 109_107; 109_102		Observed	IN2017_V03
Asteroidea	Brisingida	Freyellidae	*Freyella*	*elegans*	(Verrill 1884)		Herring 1995 *Freyella spinosa*
Asteroidea	Brisingida	Freyellidae	*Freyella*	sp.			Herring 1995
Asteroidea	Forcipulatida	Asteriidae	*Coronaster*	*reticulatus*	(HL Clark 1916)	Observed	IN2017_V03
Asteroidea	Forcipulatida	Pedicellasteridae	*Hydrasterias*	*sexradiata*	(Perrier in Milne-Edwards 1882)		Herring 1974 *Hydrasterias ophidion*
Asteroidea	Forcipulatida	Zoroasteridae	*Zoroaster*	*fulgens*	Thomson 1873		Herring 1995
Asteroidea	Forcipulatida	Zoroasteridae	*Zoroaster*	*microporus*	Fisher 1916	Observed	IN2017_V03
Asteroidea	Notomyotida	Benthopectinidae	*Benthopecten*	14_115; 44_125		Observed	IN2017_V03
Asteroidea	Notomyotida	Benthopectinidae	*Benthopecten*	*simplex*	(Perrier 1881)		Herring 1995
Asteroidea	Notomyotida	Benthopectinidae	*Benthopecten*	*spinosus*	Verrill 1884		Herring 1983
Asteroidea	Notomyotida	Benthopectinidae	*Cheiraster*	69_144; 100_129; 128_109		Observed	IN2017_V03
Asteroidea	Notomyotida	Benthopectinidae	*Pectinaster*	*filholi*	Perrier 1885		Herring 1974 *Pectinaster forcipatus*
Asteroidea	Notomyotida	Benthopectinidae	*Pontaster*	*tenuispinus*	(Düben & Koren 1846)		Herring 1995
Asteroidea	Paxillosida	Astropectinidae		22_119; 35_128		Observed	IN2017_V03
Asteroidea	Paxillosida	Astropectinidae	*Dytaster*	*exilis*	Sladen 1889	Observed	IN2017_V03
Asteroidea	Paxillosida	Astropectinidae	*Dytaster*	*grandis*	(Verrill 1884)		Herring 1995
Asteroidea	Paxillosida	Astropectinidae	*Dytaster*	*insignis*	(Perrier 1884)		Herring 1995
Asteroidea	Paxillosida	Astropectinidae	*Dytaster*	*pedicellaris*	HES Clark & DG McKnight 2000	Observed	IN2017_V03
Asteroidea	Paxillosida	Astropectinidae	*Plutonaster*	56_159		Observed	IN2017_V03
Asteroidea	Paxillosida	Astropectinidae	*Plutonaster*	*agazissi notatus*	Sladen 1889		Herring 1974 *Plutonaster notatus*
Asteroidea	Paxillosida	Astropectinidae	*Plutonaster*	*bifrons*	(Wyville Thomson 1873)		SS10 Southern Surveyor 2005
Asteroidea	Paxillosida	Astropectinidae	*Plutonaster*	*complexus*	HES Clark & DG McKnight 2000	Observed	IN2017_V03
Asteroidea	Paxillosida	Astropectinidae	*Plutonaster*	*intermedius*	(Perrier 1881)		Herring 1995
Asteroidea	Paxillosida	Astropectinidae	*Plutonaster*	*knoxi*	Fell 1958	Observed	IN2017_V03
Asteroidea	Velatida	Pterasteridae	*Calyptraster*	35_171; 69_144; 100_127		Observed	IN2017_V03
Asteroidea	Velatida	Pterasteridae	*Calyptraster*	*gracilis*	Jangoux & Aziz 1988	Observed	IN2017_V03
Asteroidea	Velatida	Pterasteridae	*Diplopteraster*	*multipes*	(M Sars 1866)		Herring 1974 *Hymenaster membranaceus*
Asteroidea	Velatida	Pterasteridae	*Hymenaster*	*anomalus*	Sladen 1882		Herring 1995
Asteroidea	Velatida	Pterasteridae	*Hymenaster*	cf. *roseus*	Koehler 1907		Herring 1974
Asteroidea	Velatida	Pterasteridae	*Hymenaster*	*koehleri*	Fisher 1910		Martini et al. 2019
Asteroidea	Velatida	Pterasteridae	*Hymenaster*	*nobilis*	Wyville Thomson 1878	Observed	IN2017_V03
Asteroidea	Velatida	Pterasteridae	*Hymenaster*	*pellucidus*	Thomson 1873		Herring 1983
Asteroidea	Velatida	Pterasteridae	*Hymenaster*	*rex*	Perrier 1885		Herring 1995
Asteroidea	Velatida	Pterasteridae	*Pteraster*	*personatus*	Sladen 1881		Herring 1974 *Cryptasterias personatus*

B.

Class	Order	Family	Genus	Species	Author	IN20 17_V03	BL description
Crinoidea	Comatulida	Atelecrinidae	*Adelatelecrinus*	cf. *vallatus*	Messing 2013	Observed	IN2017_V03
Crinoidea	Comatulida	Bathycrinidae	*Monachocrinus*	cf. *aotearoa*	McKnight 1973	Observed	IN2017_V03
Crinoidea	Comatulida	Pentametrocrinidae	*Thaumatocrinus*	*jungerseni*	AH Clark 1915		Herring 1974
Crinoidea	Comatulida	Thalassometridae		69_148; 80_120		Observed	IN2017_V03 *Thalassometra cf gracilis*
Crinoidea	Comatulida	Thalassometridae	*Stiremetra*	cf. *breviradia*	(Carpenter 1888)		SS10 Southern Surveyor 2005
Crinoidea	Comatulida	Thalassometridae	*Thalassometra*	*lusitanica*	(Carpenter 18848)		Herring 1983
Crinoidea	Isocrinida	Isocrinidae	*Neocrinus*	*decorus*	(Thomson 1864)		Johnson et al. 2012
Crinoidea	Isocrinida	Isselicrinidae	*Endoxocrinus (Diplocrinus)*	*wyvilethomsoni*	(Thomson 1872)		Herring 1974 *Annacrinus wyvillethomsoni* (Jeffreys)

C.

Class	Order	Family	Genus	Species	Author	IN20 17_V03	BL description
Holothuroidea	Elasipodida	Elpidiidae	*Achlyonice*	*ecalcarea*	Théel 1879		IN2017_V03
Holothuroidea	Elasipodida	Elpidiidae	*Amperima*	*furcata*	(Hérouard 1899)	Observed	IN2017_V03
Holothuroidea	Elasipodida	Elpidiidae	*Amperima*	*rosea*	(E Perrier 1886)		Herring 1995
Holothuroidea	Elasipodida	Elpidiidae	*Ellipinion*	sp.			Herring 1974
Holothuroidea	Elasipodida	Elpidiidae	*Elpidia*	*glacialis*	Théel 1876		Herring 1995
Holothuroidea	Elasipodida	Elpidiidae	*Kolga*	*hyalina*	Danielssen & Koren 1879		Herring 1974
Holothuroidea	Elasipodida	Elpidiidae	*Peniagone*	*azorica*	von Marenzeller1892	Observed	IN2017_V03
Holothuroidea	Elasipodida	Elpidiidae	*Peniagone*	*diaphana*	(Théel 1882)		Herring 1995
Holothuroidea	Elasipodida	Elpidiidae	*Peniagone*	*ferruginea*	Grieg 1921		Herring 1995
Holothuroidea	Elasipodida	Elpidiidae	*Peniagone*	*théeli*	Ekman 1925		Herring 1974
Holothuroidea	Elasipodida	Elpidiidae	*Peniagone*	*vitrea*	Théel 1882	Observed	Herring 1995
Holothuroidea	Elasipodida	Elpidiidae	*Peniagone (Scotoanassa)*	*hollisi*	?		Widder et al. 1983
Holothuroidea	Elasipodida	Elpidiidae	*Penilpidia*	*ludwigi*	(von Marenzeller 1893)		Herring 1995 Irpa ludwigi
Holothuroidea	Elasipodida	Elpidiidae	*Scotoplanes*	*globosa*	(Théel 1879)	Observed	Widder et al. 1983
Holothuroidea	Elasipodida	Laetmogonidae	*Benthogone*	*rosea*	Koeler 1895		Herring 1974
Holothuroidea	Elasipodida	Laetmogonidae	*Laetmogone*	*maculata*	(Théel 1879)		
Holothuroidea	Elasipodida	Laetmogonidae	*Laetmogone*	*violacea*	Théel 1879		Herring 1974
Holothuroidea	Elasipodida	Laetmogonidae	*Pannychia*	*moseleyi*	Théel 1882		Widder et al. 1983
Holothuroidea	Elasipodida	Pelagothuriidae	*Enypniastes*	*eximia*	Théel 1882		Robison 1992
Holothuroidea	Elasipodida	Pelagothuriidae	*Pelagothuria*	*natatrix*	Ludwig 1893		Herring 1983
Holothuroidea	Elasipodida	Psychropotidae	*Benthodytes*	*lingua*	Perrier R 1896		Herring 1995
Holothuroidea	Elasipodida	Psychropotidae	*Benthodytes*	Mol new sp 1		Observed	IN2017_V03
Holothuroidea	Elasipodida	Psychropotidae	*Benthodytes*	Mol new sp 2		Observed	IN2017_V03
Holothuroidea	Elasipodida	Psychropotidae	*Benthodytes*	*typica*	Théel 1882		Herring 1983
Holothuroidea	Elasipodida	Psychropotidae	*Psychropotes*	*depressa*	(Théel 1882)	Observed	Herring 1974
Holothuroidea	Elasipodida	Psychropotidae	*Psychropotes*	*longicauda*	Théel 1882	Observed	IN2017_V03
Holothuroidea	Elasipodida	Psychropotidae	*Psychropotes*	*scotiae*	(Vaney 1908)	Observed	IN2017_V03
Holothuroidea	Elasipodida	Psychropotidae	*Psychropotes*	*semperiana*	Théel 1882		Herring 1995
Holothuroidea	Holothuriida	Mesothuriidae	*Mesothuria*	*maroccana*	Perrier R 1898		Herring 1995
Holothuroidea	Holothuriida	Mesothuriidae	*Zygothuria*	*lactea*	(Théel 1886)	Observed	Herring 1995 Mesothuria lactea
Holothuroidea	Molpadida	Molpadiidae	*Molpadia*	Probably new - similar to M. discors, liska, blakei		Observed	IN2017_V03
Holothuroidea	Persiculida		*Hansenothuria*	*benthi*	Miller & Pawson 1989		Johnsen et al. 2012
Holothuroidea	Persiculida	Gephyrothuriidae	*Paroriza*	*pallens*	(Koehler 1896)		Herring 1995
Holothuroidea	Persiculida	Gephyrothuriidae	*Paroriza*	sp.			Herring 1974
Holothuroidea	Persiculida	Molpadiodemidae	*Molpadiodemas*	*villosus*	(Théel 1886)		Herring 1983 Pseudostichopus villosus
Holothuroidea	Synallactida	Synallactidae	*Galatheathuria*	sp.			Herring 1974
Holothuroidea	Synallactida	Synallactidae	*Paelopatides*	*gigantea*	(Verrill 1884)		Herring 1995
Holothuroidea	Synallactida	Synallactidae	*Paelopatides*	*grisea*	Perrier R 1898		Herring 1995
Holothuroidea	Synallactida	Synallactidae	*Paelopatides*	sp.			Herring 1974
Holothuroidea	Synallactida	Synallactidae	*Scotothuria*	*herringi*	Hansen 1978		Herring 1974
Holothuroidea	Synallactida	Synallactidae	*Synallactes*	*cf crucifera*	Perrier R 1898	Observed	IN2017_V03

D.

Class	Order	Family	Genus	Species	Author	IN20 17_V03	BL description
Ophiuroidea	Amphilepidida	Amphiuridae		4			liste Mallefet
Ophiuroidea	Amphilepidida	Amphiuridae	*Amphipholis*	*squamata*	(Delle Chiaje 1828)		Harvey 1952
Ophiuroidea	Amphilepidida	Amphiuridae	*Amphiura*	13_112		Observed	IN2017_V03
Ophiuroidea	Amphilepidida	Amphiuridae	*Amphiura*	*arcystata*	HL Clark 1911		liste Mallefet
Ophiuroidea	Amphilepidida	Amphiuridae	*Amphiura*	*filiformis*	(OF Müller 1776)		Harvey 1952
Ophiuroidea	Amphilepidida	Amphiuridae	*Amphiura*	*kandai*	Murakami 1942		Harvey 1952
Ophiuroidea	Amphilepidida	Amphiuridae	*Amphiura*	*latisquama*	Mortensen 1924		liste Mallefet Amphioplus longirima
Ophiuroidea	Amphilepidida	Amphiuridae	*Amphiura*	sp.			liste Mallefet
Ophiuroidea	Amphilepidida	Amphiuridae	*Amphiura*	sp.'			liste Mallefet
Ophiuroidea	Amphilepidida	Amphiuridae	*Amphiura*	sp. MoV 3579			SS10 Southern Surveyor 2005
Ophiuroidea	Amphilepidida	Amphiuridae	*Amphiura*	sp. MoV 5516			SS10 Southern Surveyor 2005
Ophiuroidea	Amphilepidida	Amphiuridae	*Amphiura*	sp. MoV 5519			SS10 Southern Surveyor 2005
Ophiuroidea	Amphilepidida	Amphiuridae	*Amphiura (Amphiura)*	*constricta*	Lyman 1879		Mallefet et al. 2004
Ophiuroidea	Amphilepidida	Amphiuridae	*Amphiura (Amphiura)*	*duncani*	Lyman 1882		liste Mallefet
Ophiuroidea	Amphilepidida	Amphiuridae	*Amphiura (Amphiura)*	*grandisquama*	Lyman 1869		Herring 1983 Amphiura josephinae
Ophiuroidea	Amphilepidida	Amphiuridae	*Amphiura (Amphiura)*	*grandisquama*	Lyman 1869		Emson & Herring 1984
Ophiuroidea	Amphilepidida	Amphiuridae	*Amphiura (Amphiura)*	*magellanica*	Ljungman 1867		Mallefet et al. 2004
Ophiuroidea	Amphilepidida	Amphiuridae	*Amphiura (Amphiura)*	*trisacantha*	HL Clark 1928		liste Mallefet
Ophiuroidea	Amphilepidida	Amphiuridae	*Ophiocentrus*	*aspera*	Koehler 1905		liste Mallefet

Ophiuroidea	Amphilepidida	Aphilimnidae	Amphilimna	transacta	(Koehler 1930)		SS10 Southern Surveyor 2005
Ophiuroidea	Amphilepidida	Hemieuryalidae	Ophioplocus	bispinosus	HL Clark 1918		Mallefet et al. 2004
Ophiuroidea	Amphilepidida	Hemieuryalidae	Ophioplocus	bispinosus	HL Clark 1918		liste Mallefet
Ophiuroidea	Amphilepidida	Ophionereididae	Ophiochiton	ternispinus	Lyman 1883		Johnsen et al. 2012
Ophiuroidea	Amphilepidida	Ophionereididae	Ophiodoris	malignus	Koehler 1904		liste Mallefet
Ophiuroidea	Amphilepidida	Ophionereididae	Ophionereis	fasciata	Hutton 1872		Pentreath 1970
Ophiuroidea	Amphilepidida	Ophionereididae	Ophionereis	schayeri	(Müller & Troschel 1844)		Ball (unpublished)
Ophiuroidea	Amphilepidida	Ophionereididae	Ophionereis	semoni	(Döderlein 1896)		liste Mallefet
Ophiuroidea	Amphilepidida	Ophiopholidae	Ophiopholis	cf. longispina	HL Clark 1911		Widder et al. 1983
Ophiuroidea	Amphilepidida	Ophiopsilidae	Ophiopsila	annulosa	(M. Sars 1859)		Harvey 1952
Ophiuroidea	Amphilepidida	Ophiopsilidae	Ophiopsila	aranea	Forbes 1843		Harvey 1952
Ophiuroidea	Amphilepidida	Ophiopsilidae	Ophiopsila	californica	AH Clark 1921		Brehm 1975
Ophiuroidea	Amphilepidida	Ophiopsilidae	Ophiopsila	multipapilata	Guille & Jangoux 1978		liste Mallefet
Ophiuroidea	Amphilepidida	Ophiopsilidae	Ophiopsila	pantherina	Koehler 1898		liste Mallefet
Ophiuroidea	Amphilepidida	Ophiopsilidae	Ophiopsila	riisei	Lütken 1859		Emson & Herring 1984
Ophiuroidea	Amphilepidida	Ophiopsilidae	Ophiopsila	xmasilluminans	Okanishi, Oba & Fujita 2019		Okanishi et al. 2019
Ophiuroidea	Amphilepidida	Ophiotrichidae	Ophiothrix	fragilis	Abilgaard in OF Müller 1789)		Harvey 1952
Ophiuroidea	Amphilepidida	Ophiotrichidae	Ophiothrix (Acanthophiothrix)	armata	Koehler 1905		liste Mallefet
Ophiuroidea	Amphilepidida	Ophiotrichidae	Ophiothrix (Acantophiothrix)	purpurea	von Martens 1867		liste Mallefet
Ophiuroidea	Amphilepidida	Ophiotrichidae	Ophiothrix (Ophiothrix)	aristulata	Lyman 1879		liste Mallefet
Ophiuroidea	Ophiacanthida	Ophiacanthidae	Ophiacantha	abyssicola	GO Sars 1872		Emson & Herring 1984
Ophiuroidea	Ophiacanthida	Ophiacanthidae	Ophiacantha	aculeata	Verrill 1885		Herring 1974
Ophiuroidea	Ophiacanthida	Ophiacanthidae	Ophiacantha	alternata	AM Clark 1966		liste Mallefet
Ophiuroidea	Ophiacanthida	Ophiacanthidae	Ophiacantha	aristata	Koehler 1895		Herring 1983
Ophiuroidea	Ophiacanthida	Ophiacanthidae	Ophiacantha	bidentata	(Bruzelius 1805)		Harvey 1952
Ophiuroidea	Ophiacanthida	Ophiacanthidae	Ophiacantha	brachygnatha	AM Clark 1928	Observed	liste Mallefet
Ophiuroidea	Ophiacanthida	Ophiacanthidae	Ophiacantha	crassidens	Verrill 1885		Herring 1995
Ophiuroidea	Ophiacanthida	Ophiacanthidae	Ophiacantha	cuspidata	Lyman 1878		Herring 1983
Ophiuroidea	Ophiacanthida	Ophiacanthidae	Ophiacantha	densa	Farran 1913		Herring 1995
Ophiuroidea	Ophiacanthida	Ophiacanthidae	Ophiacantha	pacata	Koehler 1922		liste Mallefet
Ophiuroidea	Ophiacanthida	Ophiacanthidae	Ophiacantha	simulans	Koehler 1895		Herring 1983
Ophiuroidea	Ophiacanthida	Ophiacanthidae	Ophiacantha	simulans	Koehler 1895		Herring 1995
Ophiuroidea	Ophiacanthida	Ophiacanthidae	Ophiacantha	smitti	Ljungman 1872		Herring 1995
Ophiuroidea	Ophiacanthida	Ophiacanthidae	Ophiacantha	sollicita	Koehler 1922	Observed	IN2017_V03
Ophiuroidea	Ophiacanthida	Ophiacanthidae	Ophiacantha	sp. MoV 4537			SS10 Southern Surveyor 2005
Ophiuroidea	Ophiacanthida	Ophiacanthidae	Ophiolimna	antarctica	(Lyman 1879)		liste Mallefet
Ophiuroidea	Ophiacanthida	Ophiacanthidae	Ophiolimna	bairdi	(Lyman 1883)		Herring 1995 Ophiacantha bairdi
Ophiuroidea	Ophiacanthida	Ophiacanthidae	Ophiomitrella	sp.'			Herring 1995
Ophiuroidea	Ophiacanthida	Ophiacanthidae	Ophiophthalmus	relictus	(Koehler 1904)	Observed	IN2017_V03
Ophiuroidea	Ophiacanthida	Ophiacanthidae	Ophioplinthaca	chelys	(CW Thomson 1877)		liste Mallefet
Ophiuroidea	Ophiacanthida	Ophiacanthidae	Ophioplinthaca	plicata	(Lyman 1878)		liste Mallefet
Ophiuroidea	Ophiacanthida	Ophiacanthidae	Ophioplinthaca	rudis	(Koehler 1897)	Observed	liste Mallefet
Ophiuroidea	Ophiacanthida	Ophiacanthidae	Ophiurothamnus	clausa	(Lyman 1878)	Observed	liste Mallefet
Ophiuroidea	Ophiacanthida	Ophiocamacidae	Ophiocamax	sp nov.			Haddock pers. Comm. 2014
Ophiuroidea	Ophiacanthida	Ophiocomidae	Breviturma	pica	(Müller & Troschel 1842)		liste Mallefet
Ophiuroidea	Ophiacanthida	Ophiocomidae	Ophiomastyx	lymani	(de Loriol 1893)		liste Mallefet
Ophiuroidea	Ophiacanthida	Ophiodermatidae	Ophiarachnella	ramsayi	(Bell 1888)		Ball (unpublished)
Ophiuroidea	Ophiacanthida	Ophiotomidae	Ophiocomina	nigra	Abildgaard 1789		Jones & Mallefet 2012
Ophiuroidea	Ophiacanthida	Ophiotomidae	Ophiomitra	spinea	Verrill 1885		Herring 1995
Ophiuroidea	Ophiacanthida	Ophiotomidae	Ophiotoma	6_138		Observed	IN2017_V03
Ophiuroidea	Ophiacanthida	Ophiotomidae	Ophiotoma	paucispina	(Lütken & Mortensen 1899)	Observed	IN2017_V03
Ophiuroidea	Ophiacanthida	Ophiotomidae	Ophiotoma	sp. MoV 5504			SS10 Southern Surveyor 2005
Ophiuroidea	Ophioleucida	Ophiernidae	Ophiernus	vallincola	Lyman 1878	Observed	liste Mallefet
Ophiuroidea	Ophioleucida	Ophioleucidae	Ophioleuce	seminudum	Koehler 1904		SS10 Southern Surveyor 2005
Ophiuroidea	Ophioscolecida	Ophioscolecidae	Ophiolycus	sp.			liste Mallefet
Ophiuroidea	Ophioscolecida	Ophioscolecidae	Ophiolycus	sp. MoV 5489			SS10 Southern Surveyor 2005
Ophiuroidea	Ophioscolecida	Ophioscolecidae	Ophioscolex	glacialis	Müller & Troschel 1842		Millot 1966
Ophiuroidea	Ophioscolecida	Ophioscolecidae	Ophioscolex	sp. MoV 2721			SS10 Southern Surveyor 2005
Ophiuroidea	Ophiurida	Astrophiuridae	Ophiomisidium	irene	Fell 1952		liste Mallefet
Ophiuroidea	Ophiurida	Ophiomusaidae	Ophiomusa	lymani	(Wyville Thomson 1873)	Observed	Herring 1995 Ophiomusium lymani
Ophiuroidea	Ophiurida	Ophiopyrgidae	Amphiophiura	distincta	(Koehler 1904)		liste Mallefet
Ophiuroidea	Ophiurida	Ophiopyrgidae	Amphiophiura	urbana	(Koeler 1904)		liste Mallefet
Ophiuroidea	Ophiurida	Ophiopyrgidae	Aspidophiura	100_126		Observed	IN2017_V03
Ophiuroidea	Ophiurida	Ophiopyrgidae	Ophioplinthus	tessellata	(Verrill 1894)		Herring 1995 Homalophiura tesselata
Ophiuroidea	Ophiurida	Ophiosphalmidae	Ophiosphalma	glabrum	(Lütken & Mortensen 1899)	Observed	Ophiosphalma fimbriatum
Ophiuroidea	Ophiurida	Ophiuridae	Ophiura	ooplax	(HL Clark 1911		liste Mallefet
Ophiuroidea	Ophiurida	Ophiuridae	Ophiura	sp. MoV 2734			SS10 Southern Surveyor 2005
Ophiuroidea	Ophiurida	Ophiuridae	Ophiura (Ophiura)	mundata	(Koeler 1606)		Herring 1995 Ophiura mundata
Ophiuroidea	Ophiurida	Ophiuridae	Ophiura (Ophiuroglypha)	irrorata concreta	(Koeler 1901)		Herring 1995 Ophiura concreta an actual species complex
Ophiuroidea	Ophiurida	Ophiuridae	Ophiura (Ophiuroglypha)	rugosa	(Lyman 1878)	Observed	liste Mallefet

UNIVERSITÉ CATHOLIQUE DE LOUVAIN
Faculté des sciences
Place des sciences, 2 bte L6.06.01, 1348 Louvain-la-Neuve, Belgique | **www.uclouvain.be/sc**